Prediction of forest soil trafficability by topography-based algorithms and in-situ test procedures

Dissertation

to attain the doctoral degree (Dr. rer. forest.)

of the Faculty of Forest Sciences and Forest Ecology

Georg-August-Universität Göttingen

submitted by

Marian J. Schönauer

born on the 27th of March 1992 in Kufstein, Österreich

Göttingen, March 2022

1st Referee: Prof. Dr. Dirk Jaeger

2nd Referee: Ao.Univ.Prof. Dipl.-Ing. Dr.nat.techn. Klaus Katzensteiner

Date of oral examination: 18th of February 2022

“Es ist das Abenteuer im Kopf, das mich reizt.”

Harald Berger (* 1972, † 2006)

Table of Contents

Summary

Modern forest management entails the utilization of harvesting machinery, which enables safe and efficient forest operations. Still, such machines are frequently resulting in severe soil damage, such as compaction and displacement. To maintain or even increase year-round timber mobilization with minimal negative impacts on forest soils is a challenging task, especially in times of changing climatic conditions. One solution to address this issue is the prediction of trafficability, aiming at the reduction of traffic-induced damages.

Through multiple investigations, this thesis reports on methods to predict trafficability: (1) values of the depth-to-water (DTW) index and the topographic wetness index (TWI) were related to rut depths observed during a field trial in a broad-leaved forest stand. In addition, different terramechanical test procedures were performed and related to rut depth following the fully mechanized harvesting operation. A modified Cone Index was shown to be successful in the prediction of occurring ruts. Therefore, this parameter was chosen for use in further validations. (2) Time-series data of soil strength, quantified by the modified Cone Index, and soil moisture were captured on six study sites across Europe. The measuring results were validated against DTW-derived predictions, resulting in a prediction accuracy of 76% for soil strength, and 82% for values of soil moisture. Yet, a high share of measurements indicating soft or wet soils deviated from the predictions made. Apparently, the conjectured season-adapted representation of overall levels of soil moisture by DTW map-scenarios could not be confirmed, probably owing to site-specific effects, non-linear behaviour of water accumulation across landscapes and the omission of reliable estimations of current levels of soil moisture. (3) Such effects were considered by machine learning approaches. Tree-based machine learning models were trained on merged data, containing daily retrievals of remotely-sensed soil moisture (Soil Moisture Active Passive mission), values of DTW, TWI and openly available soil maps. This procedure significantly improved the accuracy of predictions and reduced the class error for wet soil states. With this improved trafficability prediction, mitigating measures could sufficiently be implemented in forest management, potentially leading to environmentally sound forest management and lower costs for forest operations. The required in-put data for creating DTW maps is commonly available among governmental institutions of Central and Northern Europe, and in some countries already further processed to have topography-derived trafficability maps and respective enabling technologies at hand. It is hoped that a broader adoption of these information by forest managers throughout Europe will take place to enhance sustainable forest operations. (4) The application of a mitigating technology, namely a traction-assist winch, was surveyed on a flat site where the application of such technology has not yet been investigated.

In this dissertation, particular focus was placed on the spatio-temporal patterns of soil moisture and strength on several study sites, indicating the limitation of the basic DTW concept. A method to remedy existing constraints and promote adequate implementation of openly available data, particularly soil moisture retrievals, to further improve predictive tools applicable in forest operations was demonstrated.

Zusammenfassung

Vorhersage von Bodenbefahrbarkeit durch topografische Modellierung und Felderhebungen

Moderne Waldbewirtschaftung bedingt den Einsatz von Forstmaschinen, da diese sichere und effiziente Erntemaßnahmen ermöglichen. Dennoch führen solche Maschinen häufig zu schwerwiegenden Bodenschäden, beispielsweise Verdichtung und Bodenumlagerung. In Zeiten sich ändernder klimatischer Bedingungen stellt die Sicherstellung einer ganzjährigen Nutzung mit minimalen negativen Auswirkungen auf den Waldboden eine anspruchsvolle Aufgabe dar. Eine Lösung für dieses Problem besteht in der Vorhersage der Bodenbefahrbarkeit durch kartographische Indizes.

Diese Dissertation zeigt Möglichkeiten zur Vorhersage der Befahrbarkeit und beinhaltet mehrere Untersuchungen: (1) Werte von *Depth-To-Water* (DTW) und Werte des *Topographic Wetness Index* wurden mit Fahrspurtiefen korreliert, die während einer Spätdurchforstung in einem Laubholzbestand gemessen wurden. Zusätzlich wurden verschiedene terramechanische Testverfahren vor der Befahrung durchgeführt und mit der auftretenden Fahrspurtiefe verglichen. Der gemessene Cone-Index konnte nach einer Modifizierung zur Vorhersage auftretenden Spurtiefen verwendet werden. Daher wurde dieser Parameter für weiteren Validierungen ausgewählt. (2) Zeitreihen von Bodentragfähigkeit, quantifiziert mit dem modifizierten Cone-Index, und Bodenfeuchte wurden an sechs Untersuchungsstandorten in Europa erfasst. Die Messergebnisse wurden mit DTW-Vorhersagen validiert, was in 76 % (Cone-Index) bzw. 82 % (Bodenfeuchte) akkuraten Vorhersagen resultierte. Allerdings wich ein hoher Anteil der Messungen, die nasse oder weiche Böden anzeigten, von den Vorhersagen ab. Die von DTW angenommene jahreszeitliche Anpassung an Feuchteverhältnisse konnte nicht bestätigt werden, wahrscheinlich aufgrund von Standortseffekten, nicht-linearen hydrologischen Prozessen und dem Fehlen zuverlässiger Schätzungen der aktuellen Feuchteverhältnisse. (3) Solche Effekte und deren Interaktionen können durch leistungsfähige Methoden Maschinellen Lernens berücksichtigt werden. Ein Random-Forest-Modell sowie ein Gradienten-Boosting wurden mit zusammengeführten Daten trainiert. Dieser Datensatz enthielt dreistündliche Mittelwerte von fernerkundlich geschätzter Bodenfeuchte (Soil Moisture Active Passive Mission), Werte von DTW und TWI, sowie frei verfügbaren Bodenkarten. Das vorgeschlagene Verfahren verbesserte die Genauigkeit der Vorhersagen erheblich und reduzierte insbesondere den Klassenfehler für nasse Messungen. Mit diesem verbesserten Vorhersagemodell könnten Bodenschutzmaßnahmen umgesetzt werden, die eine umweltschonende Forstwirtschaft ermöglichen würden. Die benötigten Input-Daten sind über weite Gebiete Europas verfügbar, und wurden teilweise bereits zu Befahrungsrisikokarten verarbeitet. Eine Ausweitung der Anwendung solcher Karten in der forstlichen Praxis kann erwartet werden. (4) Die Anwendung einer bodenschonenden Technik, nämlich die Anwendung einer Traktionshilfswinde, wurde auf einem flachen Standort untersucht, wo eine solche Technologie bisher kaum untersucht wurde.

Diese Arbeit untersuchte vor allem das raum-zeitlichen Verhalten der Bodenfeuchte und -tragfähigkeit an mehreren Untersuchungsstandorten und zeigte die Grenzen des DTW-Konzepts auf. Es wurde gezeigt, wie maschinelles Lernen eingesetzt werden kann, um bestehende Einschränkungen zu beheben und wie eine adäquate Einbindung offen verfügbarer Daten praxistaugliche Vorhersagewerkzeuge verbessern kann.

1. General introduction

1.1. Background and relevance

The European Green Deal promoted and prioritized sustainable resource management, aiming towards an efficient use of natural resources (European Commission - Joint Research Centre, 2019). Focus was given to the protection of the natural environment, including biodiversity and the multifunctional role of forest ecosystems. In particular by means of the forestry strategy, enhanced resilience of forests through adequate and sustainable forest management was envisaged (European Commission - Joint Research Centre, 2021a). In addition, the strategy foresees an intensified utilization of forest resources, to be used as construction timber, as a carbon sequestrating and renewable resource for substituting other materials (European Commission - Joint Research Centre, 2021a). To mobilize the forest timber resource and to be able to react to forest damages, such as fire, floods and insect pests, year-round access into forest stands is key. In Germany, 88% of the forested area is trafficable by ground-based machinery (Thünen-Institut, 2012), which translates to improved safety and working conditions (Albizu-Urionabarrenetxea et al., 2013), as well as increased productivity compared to manual harvesting operations (Rickenbach and Steele, 2005). These advantages have led to an intensified utilization of ground-based machines in forest management (Marchi et al., 2018; Brown et al., 2020).

In contrast to the advantages associated with the ongoing mechanization of forest operations, machine traffic usually leads to unavoidable impacts on the structure and integrity of soil, since the high mass of forest machines inevitably exceeds the precompression stress of soils trafficked (Vossbrink and Horn, 2004; Ampoorter et al., 2011; Cambi et al., 2015; Crawford et al., 2021). Factors like traffic frequency, carried loads, wheel slippage, machine specifications and the relationship between soil bearing capacity and the machine's ground pressure determine the impact on physical soil properties (Labelle and Jaeger, 2019), which leads to lasting consequences, such as soil compaction (Rab, 2004). Soil compaction occurs when the experienced pressure at the contact area between machine and soil exceeds the intrinsic mechanical resistance of the soil. Ampoorter et al. (2012) reviewed an average increase of soil bulk density of 15% after traffic in forests. In addition to the characteristics of the various forestry machines employed and the traffic intensity experienced, two soil-related factors highly influence the susceptibility of soils towards compaction (Cambi et al., 2015): (I) initial soil bulk density, with lower values making the soil more prone to compaction (Hillel, 1998; Williamson and Neilsen, 2000) and (II) soil moisture content, since bearing capacity and thus trafficability decreases on wet soils (Poltorak et al., 2018; D'Acqui et al., 2020; Uusitalo et al., 2020).

When exceeding a specific soil bulk density, negative effects on plant available water (Arvidsson et al., 2003) and plant growth (Daddow and Warrington, 1983) can occur. In addition to changed physical soil characteristics, effects on soil's fauna and biota are driven by compaction. Due to the reduced macropore volume and the altered hydrological conditions, negative effects on various soil faunal groups were reported in the review by Beylich et al. (2010). Although Beylich et al. could not attribute a distinct site-specific critical level for soil bulk density, only negative effects on microbial biomass were observed above an effective value of 1.7 g cm^{-3}. In contrast to the absolute quantitative increase of soil bulk density due to compaction, a relative bulk density metric provides a qualitative assessment of impacts experienced across sites, while accounting for site-specific effects on the soil's functions. The relative bulk density is defined by the ratio between field bulk density and maximum bulk density (Labelle and Jaeger, 2011), obtained by a standardized Proctor compaction test (DIN 18127:2012-09). Labelle and Kammermeier (2019) promoted the use of this relative bulk density in order to assess traffic induced impacts and showed that a relative bulk density of 0.77 or above led to significantly decreased growth of Spruce (*Picea abies* [L.] Karst) seedlings.

In addition to soil compaction, machine traffic can result in vertical and horizontal soil displacement. Due to the decreased frictional resistance and the consequent shear failure when load is applied on a wet soil, soil displacement in the form of ruts along the trafficked machine trails can occur (Crawford et al., 2021). In turn, the combination of compacted soil within the deep track (Sakai et al., 2008) and the morphological formations per se can lead to the accumulation of precipitation and surface-near water flow. Thus, ruts were reported to act as flow channels, fortifying soil erosion (Jourgholami and Labelle, 2020), which can foster further deepening of existing ruts (Edlund et al., 2013).

The occurrence of deep ruts interferes with the sustainable development goals for forest management (UNFCCC, 2015) and has been addressed by several policies (e.g. Owende et al., 2002; Niedersächsische Landesforsten, 2017) and contracts made with forest entrepreneurs. Some forest companies introduced penalties for entrepreneurs incurring soil damages (Flisberg et al., 2021). As intended by such regulations, a low site impact is essential for cost-efficient forest operations, since the energy required to overcome a high rolling resistance, i.e. when the machine creates deep ruts, reflects on the fuel consumption and machine wear (Suvinen, 2006; Ala-Ilomäki et al., 2020; Melander et al., 2020). Moreover, forest operations must be oriented towards mitigating site impacts since societal acceptance of forestry operations in general depends upon it.

1.2. Status quo of soil protection in forest operations

1.2.1. *Constructive and operational concepts to mitigate soil disturbance*

Common cut-to-length operations are defined by the utilization of single grip harvesters for felling and processing of trees into logs, followed by driving forwarders which extract the processed logs. Driven by economic interests, these machines were developed towards higher pay load capacities and improved technical capability. These developments can be related to increases in machine mass (Nordfjell et al., 2010). In Sweden, the mass of unloaded forwarders significantly increased to an average of 14.5 Mg in 2010, with an average loaded mass of 31.8 Mg (Nordfjell et al., 2019). Yet, since the early development of “forwarders” in the middle of the 20th century, the ground pressure (kPa) of forwarders has decreased due to improvements in construction, such as an increased number of axles, wider tires and bogie axles, all designed to mitigate the machine-induced soil impact (Nordfjell et al., 2019). However, the reduction of ground pressure through additional axles can be seen as critical. Since total impact on the soil is increased through a higher number of axle-passes, the ongoing trend of forest machines towards higher total mass and loading capacity remains questionable.

Along with the developments of forestry machines, several operational and technical solutions have been introduced for use in mechanized forest operations to support the day-to-day work of machine operators:

(i) To increase traction and enhance machine-soil contact area, bogie tracks are commonly used for forest operations on sensitive sites, to mitigate negative site impacts (Bygdén et al., 2003; Sakai et al., 2008; Labelle and Jaeger, 2019).

(ii) Through lower tire inflation pressure, the contact area between machine and soil increases, reducing the contact pressure and extent of occurring impacts (Arvidsson and Keller, 2007).

(iii) The use of rubber tracked machines can lead to notable improvements regarding soil impact, fuel consumption, and operator comfort when operating on sensitive sites (Gelin and Björheden, 2020).

(iv) The traction of an operating machine can be supported by additional winching to reduce wheel slippage and the formation of deep ruts, especially in steep terrain (Cavalli and Amishev, 2019; Garren et al., 2019).

(v) The soil surface can be fortified through the deposition of brush material (Labelle and Jaeger, 2018; Labelle et al., 2019). Smaller piles of brush material deposited on machine trails can achieve a similar effect.

(vi) Innovative machine concepts are envisaged to reduce site impact, for example by means of intelligent machine steering (Andersson et al., 2021), which could also support the machine to adapt to complex terrain conditions (Li and Kang, 2020).

The majority of measures invented to reduce site impacts are designed to further reduce the ground pressure of operating machines. Still, the utilization of such measures (in particular i-iv) for actual operations relies upon the knowledge of expected site conditions. This information enables appropriate planning for given operations, for example, forest machines can be equipped with floating tracks when operating on wet and therefore soft soil. In addition, operational adjustments and appropriate instructions for machine operators (e.g. v) can be implemented during ongoing operations to reduce occurring soil compaction and displacement.

1.2.2. *Methods to assess and predict trafficability*

Information about operational conditions is vital for appropriate planning of forest operations, especially for scheduling mitigating measures to be applied (i-v). Moreover, the spatial estimation of trafficability across forest sites is a key factor to be considered during machine traffic, making the provision of such information inevitable for sustainable forest management (Vega-Nieva et al., 2009; Kuglerová et al., 2017; Sirén et al., 2019b; Uusitalo et al., 2019). Only if the spatial risk for severe soil damage is known, can areas and sites currently possessing a high susceptibility to soil deformations be avoided – during off-road traffic, as common in Northern countries, as well as in Central Europe, where machine traffic is usually restricted to permanently used machine operating trails. There, the technical functionality, and consequent permanent accessibility into forest stands can be maintained if machine operators know which segments of a machine operating trail to avoid. Therefore, it is fundamental to know *when* and *where* machine traffic is feasible to ensure environmentally sound operations. In the following section, methods to clarify both uncertainties are shown, including cartographic solutions and in-situ test procedures.

In-situ measurements to assess trafficability

A practical decision system was introduced by Bavarian State Institute of Forestry (2012), where the assessment of current trafficability was made according to the shape of a soil probe, manually thrown against a blank surface. Another approach for individual assessment of trafficability was based on the analysis of disturbed soil probe collected with a regular spade. There, the content of coarse fraction, soil texture, content of humus and soil hydrology were considered to evaluate trafficability by the in-field method described by Lüscher et al. (2019). A higher level of detail was reached when this in-field analysis was combined with early modelling approaches by Ziesak (2004). Also, terramechanical test procedures can be applied to evaluate the current soil strength along machine operating trails to be trafficked. A handheld penetrologger has frequently been used for scientific purposes to assess trafficability (Farzaneh et al., 2012; Kumar et al., 2012; Sirén et al., 2019b), potentially applicable to forest operations. Measurements with a vane meter led to adequate assessments of current soil strength (Heubaum, 2015a). Although in-situ measurements are supposed to reveal valid estimations of current trafficability, the application of such tools for practical purposes is lacking due to high time demands and associated costs.

Trafficability predictions based on maps and cartographic indices

Trafficability maps are assumed to bear great potential for improving forest management and forest operations by reducing site impacts (Sirén et al., 2019b; Uusitalo et al., 2019; Tuomasjukka et al., 2020) at low costs. Cartographic predictions of trafficability were used by the forest state agency in Lower Saxony, Germany (Niedersächsische Landesforsten, 2017). These maps were based on a detailed soil mapping, soil hydrological properties and terrain characteristics, which were used to derive four risk classes for soil damage, ranging from “low” to “very high”. The information was made accessible via an internal geographic information system. Similar approaches were developed by other German state agencies (e.g. Grüll, 2011; Heubaum, 2015b). Yet, a common disadvantage of such solutions is the low spatial resolution of the risk assessment and the lack of consideration for seasonal changes in soil moisture.

Topographical modelling of wet areas has been suggested as a solution to this problem (Murphy et al., 2009; Ågren et al., 2014). To take advantage of the increasing availability of high resolution digital elevation models, the depth-to-water (DTW) concept was conceived, developed and tested at the University of New Brunswick (Faculty of Forestry and Environmental Management), by Fan-Rui Meng, Jae Ogilvie and Paul Arp, as described by Murphy et al. (2007; 2009; 2011). This concept was reported as a robust tool for the prediction of perennial streams, wet or water saturated areas, and sensitive areas for ground-based trafficking (Murphy et al., 2011; Ågren et al., 2014; Ågren et al., 2015; Mohtashami et al., 2017), where low soil strength and the occurrence of deep ruts are assumed (McNabb et al., 2001; Poltorak et al., 2018; Uusitalo et al., 2020). DTW aims to represent different levels of soil moisture by providing several map-scenarios (A detailed description of the DTW concept can be found in **Appendix III** (2019) and **Appendix IV** (2021)). Although experienced users might choose the most reliable scenario for a given operation, the concept lacks an evidence-based selection of map-scenarios and omits hydrological information. Adequate incorporation of soil moisture into trafficability assessments was pointed out by forestry stakeholders to be of high importance (Danielsson) and is additionally reflected by the presence of recent research projects, such as TECH4EFFECT (2020, European Union’s Horizon 2020, grant agreement No 720757), SmartForest (NIBIO, 2021), TRAM (Natural Resources Institute Finland, 2020), EFFORTE (2018, European Union’s Horizon 2020, grant agreement No 720712) and BefahrGut (University of Göttingen, 2021, funded by the State of North Rhine-Westphalia, Germany).

Solutions to include current soil moisture estimates into trafficability predictions were developed already. Salmivaara et al. (2020) used statistical models to merge daily estimates of soil moisture, derived from a spatial hydrological model (Launiainen et al., 2019) with open spatial data and traffic-derived data to predict the occurring rut depth on a testing trail in Southern Finland. It is possible to develop and validate models using machine-mounted sensors, which were reported to reveal reliable and cost-efficient measurements of rut depth (Talbot et al., 2017; Salmivaara et al., 2018; Jones and Arp, 2019). Moreover, weather forecasts could be integrated, aiming towards an improved planning and timing of forest operations, and near-instantaneous assistance to forest machine operators in the field. Lidberg et al. (2020) argued that existing trafficability maps or predictions are highly site-specific, hampering the large-scale applicability of such methods. Therefore, it was intended to use available spatial data, namely information on local topography, topography-derived indices (DTW and TWI), bedrock, and wetland-mapping and seasonal water runoff, to delineate wet areas across a variety of landscapes. It was possible to increase the accuracy of predictions of wet and dry occurrences by 5%, when compared to basic DTW-predictions, which correctly assessed 79% of points.

Improvements in trafficability predictions were repeatedly reached through the application of machine learning approaches (Pohjankukka et al., 2016; Bont et al., 2020; Lidberg et al., 2020). The increasing capability of such modelling was used to successfully integrate the local variability in soil characteristics

and terrain topography. A fundamental reason for the promising application of machine learning is the consideration of non-linear and site-specific effects (Lidberg et al., 2020; Melander et al., 2020), allowing for successful predictions of trafficability on heterogeneous landscapes. Tree-based machine learning algorithms are probably the most common approaches chosen to make predictions of trafficability and soil state (Heung et al., 2016; Hengl et al., 2018). In general, such models combine tree predictors, which are built of leaves and nodes. Models of this kind split the data under the premise of maximized within-node homogeneity and between-node heterogeneity, and can be used to include data derived from different resources.

1.3. Problem statement and objectives

Forest management is currently facing less favourable conditions owing to milder winters and extended wetter periods in spring and autumn with increased levels of soil moisture (Max-Planck-Institute for Meteorology, 2009), limiting the time available for carrying out forest operations with a low traffic-induced impact during periods of high soil bearing capacity (Mattila and Tokola, 2019; Uusitalo et al., 2020). Thus, forest operations are frequently resulting in unsightly soil damages with associated ecological drawbacks and increased costs caused by necessary machine relocations and holdups. Moreover, increasing public awareness, has promoted intensified soil protection in forest management (Jacke et al., 2015; Bethmann and Wurster, 2016), to ensure environmentally sound, efficient and socially acceptable wood mobilization.

The spatial prediction of trafficability is essential for efficient and sustainable forest management – to successfully schedule the location of upcoming forest operations, to specify the equipment used and to give useful instruction to drivers for reducing the impacts of forest machine traffic. Although different predictive tools have already been developed for use in Central Europe, high degrees of rutting continue to occur during forest operations, threatening the lasting technical functionality of permanent machine operating trails. The DTW concept was reported as a renowned tool to predict wet soils with low trafficability, but thus far validations of DTW-derived predictions are confined to Northern countries, such as Canada (Murphy et al., 2009) and Sweden (Ågren et al., 2014; Väätäinen et al., 2019). An application of DTW in temperate forests is still lacking.

An adequate predictive tool demands the appropriate integration of operational conditions in terms of current site-specific moisture levels. DTW aims at the representation of soil moisture levels, but this concept lacks empirical evidence.

Motivated by both a scientific need and potential practical application, the objective of this thesis was to answer five research questions:

(I) Are terramechanical test procedures reliable tools to predict rut depth?
(II) Is the DTW concept successful in predicting soil moisture and soil strength in temperate forests?
(III) Can the intended representation of soil moisture levels through DTW map-scenarios be statistically confirmed?
(IV) How is the status of current applications of trafficability maps and data availability in European forestry?
(V) Is it possible to include reliable soil moisture estimates into trafficability predictions?
(VI) Can winch-assist technology be used to mitigate machine-induced soil damage on flat terrain?

1.4. Thesis structure and outline of the studies

In this thesis, the **Chapters 2** to **6** comprise of answers to the posed research questions (I-VI) in the form of articles already published or submitted to peer-reviewed journals as part of a cumulative dissertation. The published versions might show small differences compared to the respective chapters. Therefore, I encourage the reader of this thesis to consider the openly available publications. Links are provided at the header of each chapter.

Rationales for the **Chapters 2** to **6** and summaries of applied methods and findings are given below:

Chapter 2: Several tools are available for the assessment of current trafficability, including in-situ analysis and cartographic indices, such as DTW or TWI. Yet, a holistic comparison among these approaches has not been facilitated so far, leaving the question of the most appropriate test procedure. We compared occurring rut depth with DTW- and TWI-derived predictions, and different in-situ measurements gathered through terramechanical test procedures.

> *Material and methods*: Field measurements were performed in two stands, predominantly stocked with *Fagus sylvatica*, in Lower Saxony, Germany, where a regular cut-to-length thinning operation was scheduled. Prior to the operation, terramechanical test procedures were applied at 90 measuring positions on untrafficked ground, along marked machine operating trails which were trafficked afterwards. Variables measured included volumetric soil moisture content, soil penetration resistance by means of both a hand-held penetrologger and a dual-mass dynamic cone penetrometer, and soil shear strength (vane tester). In addition, two cartographic indices, namely DTW and TWI were calculated for the respective area. After completing the field measurements, a thinning operation was conducted. The occurring rut depth was captured and related to the previously estimated parameters. The coefficients of individually fitted linear models were compared to assess the quality of derived rut depth predictions. *Results*: Under the rather dry soil conditions (29±9 vol%), total rut depth ranged between 2.2 and 11.6 cm, and was clearly predicted from the rut depth after a single pass of the harvester, which was used for further validations. The results indicated the easy to measure penetration depth metric as the most accurate approach to predict total rut depth, considering coefficients of correlation (r_P=0.44). Also, dual-mass cone penetration (penetrometer) provided reliable results (r_P=0.34). Surprisingly, no response between rut depth and Cone Index (handheld penetrologger) was observed, although Cone Index is commonly used to assess trafficability. The relatively low moisture conditions probably inhibited a correlation between rutting and moisture content. Consistently, cartographic indices could not be used to predict rutting. *Conclusions:* Rut depth after the harvester passed was a reliable predictor for total rut depth (r_P=0.50). Rarely used parameters, such as cone penetration or shear strength, performed better than the highly reputed Cone Index to predict rut depth, emphasizing further investigations of the applied tools.

Chapter 3. The representation of moisture conditions by DTW map-scenarios lacks empirical evidence. This chapter shows a comparison between time-series data of in-situ measured soil state to season-specific soil state predictions derived from DTW map-scenarios. Limitations of the concept were also investigated.

> *Material and methods*: As part of the Horizon 2020 project “TECH4EFFECT”, six study sites, known to show temporarily unfavourable operating conditions due to sensitive soils were selected in Finland, Germany and Poland. Different DTW map-scenarios were produced for these areas and used to perpendicularly position measuring transects across indicated wet areas. Along these transects, time-series data of soil moisture (impedance measuring technique) and soil penetration resistance (handheld penetrologger) were captured through repeated field

campaigns, covering the time span of approximately one year. The measuring campaigns conducted on each site were asserted to three moisture classes, with respect to mean values of in-field soil moisture for a given campaign and site. Thresholds between the classes were deduced from texture-specific water retention curves, resulting in *wet* (pF < 1.9), *moist* (pF between 1.9 and 3.05) and *dry* (pF > 3.05) levels. In-field values of soil moisture content measured during a *wet* campaign were compared to DTW maps created using a flow initiation area (FIA) of 0.25 ha. When the campaign was classified as *moist*, a FIA of 1.00 ha was used to create a DTW map-scenario, while a FIA of 4.00 ha was used for *dry* campaigns. Consequently, a confusion matrix could be defined, summarizing the occurrence of low values of soil penetration resistance or high values of soil moisture within or outside of an area with a DTW index ranging from 0 - 1 m. The overall accuracy and Matthews correlation coefficients, derived from the confusion matrix, were considered to assess the performance of prediction of wet soils via the DTW map-scenarios. Differences between the map-scenarios used were tested using permutation tests for linear models. *Results and conclusions*: 82% of moisture measurements were predicted correctly by the map-scenario for overall dry conditions, with 44% of wet measurements deviating from the predictions made. The prediction of soil strength was less successful, with 66% of low values occurring on areas where DTW indicated dryer soils and subsequently a sufficient trafficability. The condition-specific usage of different map-scenarios did not improve the accuracy of predictions, as compared to static map-scenarios, chosen for each site. We assume that site-specific and non-linear hydrological processes compromise the generalized assumptions of simulating overall moisture conditions by different FIAs.

Chapter 4: One main advantage of topographic indices for trafficability predictions is the low demand of input data. However, the utilization of such indices did not penetrate entirely into forest operations. To assess the current status of application as well as the availability of necessary input data, we executed a review, as part of a joint TECH4EFFECT research.

Material and methods: This review on the DTW concept in the context of trafficability mapping, follows the snowball approach, where the bibliography of a known recent key publication on that topic was used as a starting point to identify further publications. Subsequently, selected publications were reviewed and those' bibliographies used to identify additional publications until no more new references of relevance appeared. This approach was selected since in contrast to a purely keyword focussed data base search, the snowball system considers all relevant references, including non-peer reviewed early-stage research, as well as institutional and industry reports. Moreover, the authoring team consists of experts on the topic, being involved in the two multiyear EU projects TECH4EFFECT [grant number 720757] and EFFORTE [grant number 720712], which conducted intensive research in the field of trafficability prediction. *Results and conclusions:* The required in-put data is commonly available among governmental institutions, and in some countries already further processed to have topography-derived trafficability maps and respective enabling technologies at hand. Particularly the Nordic countries are ahead within this process and currently pave the way to further transfer static trafficability maps into dynamic ones, including additional site-specific information received from detailed forest inventories. Yet, it is hoped that a broader adoption of this information by forest managers throughout Europe will take place to enhance sustainable forest operations.

Chapter 5: Current research suggests the promising potential of machine learning approaches when applied to predictions of soil state (e.g. Ågren et al., 2021; Baltensweiler et al., 2021). Several machine learning algorithms were trained on the data captured during the time-series (**Chapter 3**), to improve the overall accuracy of predictions of wet soils with low strength.

> *Materials and methods.* The work presented looks at methods to model field measured spatio-temporal variations of soil moisture content (SMC, [%vol]) – a crucial factor for soil strength and thus trafficability. We incorporated large-scaled maps of soil characteristics, high-resolution topographic information - depth-to-water (DTW) and topographic wetness index - and openly available temporal soil moisture retrievals provided by the NASA Soil Moisture Active Passive mission. Time-series measurements of SMC were captured at six study sites across Europe. This data was then used to develop linear models, a generalized additive model, and the machine learning algorithms Random Forest (RF) and eXtreme Gradient Boosting (XGB). The models were trained on a randomly selected 10% subset of the dataset. *Results.* Predictions of SMC made with RF and XGB attained the highest R^2 values of 0.49 and 0.51, respectively, calculated on the remaining 90% test set. This corresponds to a major increase in predictive performance, compared to basic DTW maps (R^2=0.02). Accordingly, the quality for predicting wet soils was increased by 49% when XGB was applied (Matthews correlation coefficient=0.45). *Conclusions.* We demonstrated how open access data can be used to clearly improve the prediction of SMC and enable adequate trafficability mappings. Spatio-temporal modelling could contribute to sustainable forest management.

Chapter 6: An accurate prediction of trafficability enables adequate planning of forest operations, for instance by supporting the choice of equipment used. The chapter shows the application of winch-assist technology, usually used in steep terrain, to reduce site impact in a flat forest stand, where the application of such technology was not investigated so far. A comprehensive investigation of traffic-induced impacts, including rutting, soil compaction and wheel slippage was conducted to compare the impact of the machine when driving unassisted to driving under assistance of the traction-assist winch.

> *Material and methods*: A scientific setting was chosen for the estimation of the effect of a traction-assist winch on wheel slippage and machine induced soil disturbance. A loaded forwarder with an integrated traction-assist was monitored during six consecutive machine passes on a permanent machine operating trail in a coniferous forest stand in Rhineland-Palatinate, Germany. The first section of the machine operating trail was passed without traction-assist, while the remaining section was passed with traction-assist, resulting in two treatment groups. To assess soil impacts, three test plots were positioned per treatment group. Within these plots, pre- and post-operational soil bulk density, soil displacement and rutting depth were determined. Additionally, wheel slippage and cable tensile force were examined using incremental rotary encoders and a flexible tensile force measurement kit, respectively. *Results and conclusions*: It was observed, that wheel slippage responded inversely with tensile force. Traction-assist technology reduced wheel slippage from 5.3±11.9% to 0.37±10.19% along the section of the machine operating trail, as compared to results from the unassisted section. Although wheel slippage was significantly reduced, no mitigating effect by the usage of traction-assist technology on soil disturbance could be observed, probably due to the low volumetric water content of 27%.

An overall discussion and concluding remarks of the findings revealed through the pursued investigations will be given in the **Chapters 7** and **8**, respectively.

2. Prediction of rutting through terramechanical test procedures and cartographic indices

This chapter was published under the title “Comparison of selected terramechanical test procedures and cartographic indices to predict rutting caused by machine traffic during a cut-to-length thinning-operation“ in Forests, January 2021a, and is available at: https://doi.org/10.3390/f12020113

Full author list: Marian Schönauer [1,*], Stephan Hoffmann [1,2], Joachim Maack [1], Martin Jansen [3] and Dirk Jaeger [1]
* Corresponding author

[1] Department of Forest Engineering and Work Science, Georg-August-Universität Göttingen, Büsgenweg 4, 37077 Göttingen, Germany
[2] School of Forestry, University of Canterbury, Kirkwood Avenue, 8041 Christchurch, New Zealand
[3] Department of Soil Science of Temperate Ecosystems, Georg-August-Universität Göttingen, Büsgenweg 2, 37077 Göttingen, Germany

Author's contributions: M.S. and S.H. conceived and designed the experiments; M.S. and S.H. performed the experiments, with the acknowledged help of two associates; J.M. and M.S. calculated the cartographic maps; data preparation, M.S.; data analysis and interpretation, M.S. and S.H.; writing – original draft preparation, M.S., J.M. and S.H.; writing – review and editing, M.J., S.H., D.J., J.M. and M.S.; supervision, D.J. and M.J.; project administration, D.J.

Abstract

Introduction: Timber harvesting operations using heavy forest machinery frequently result in severe soil compaction and displacement, threatening sustainable forest management. An accurate prediction of trafficability, considering actual operating conditions, minimizes these impacts and can be facilitated by various predictive tools. Within this study, we validated the accuracy of four terramechanical parameters, including Cone Index (MPa, Penetrologger), penetration depth (cm, Penetrologger), cone penetration (cm $blow^{-1}$, dual-mass dynamic cone penetrometer) and shear strength (kPa, vane meter), and additionally two cartographic indices (topographic wetness index and depth-to-water). *Material and methods:* Measurements applying the four terramechanical approaches were performed at 47 transects along newly assigned machine operating trails in two broadleaved dominated mixed stands. After the CTL thinning-operation was completed, measurement results and cartographic indices were correlated against rut depth. *Results:* Under the rather dry soil conditions (29±9 vol%), total rut depth ranged between 2.2 and 11.6 cm, and was clearly predicted by rut depth after a single pass of the harvester, which was used for further validations. The results indicated the easy to measure penetration depth as the most accurate approach to predict rut depth, considering coefficients of correlation (r_P=0.44). Also cone penetration (r_P=0.34) provided reliable results. Surprisingly, no response between rut depth and Cone Index was observed, although commonly used to assess trafficability. The relatively low moisture conditions probably inhibited a correlation between rutting and moisture content. Consistently, cartographic indices could not be used to predict rutting. *Conclusions:* Rut depth after the harvester pass was a reliable predictor for total rut depth (r_P=0.50). Rarely used parameters, such as cone penetration or shear strength, outcompeted the highly reputed Cone Index, emphasizing further investigations of applied tools.

Keywords: Cone Index; Penetrologger; dual-mass dynamic cone penetrometer; soil penetration resistance; shear strength; soil moisture; trafficability; forest operations; depth-to-water; topographic wetness index.

2.1. Introduction

Currently, the forest in Germany and other countries suffer from several climate change induced stressors like drought, fires and other extreme weather conditions (Overpeck et al., 1990; Seidl et al., 2011). One consequence of these weather phenomena is an ongoing large scale bark beetle infestation (Schelhaas et al., 2003). Thus, prompt salvaging of infected trees is necessary for forest protection (Jenkins et al., 2008; Adams et al., 2010; Simard et al., 2011) and to limit economic losses for forest owners. In some regions, the required machine operating trails for off-road traffic still have to be established to ensure the necessary year-round access to the affected stands. Despite, off-road traffic is currently a general matter of debate, since it causes multiple adverse impacts to soil characteristics (Eliasson, 2005; Sakai et al., 2008; Botta et al., 2009; Beylich et al., 2010; Labelle and Jaeger, 2011), and thus the stand growth (e. g. Kozlowski, 1999). Negative impacts like compaction (e. g. Ampoorter et al., 2009) and soil displacement (e. g. Owende et al., 2002) are the consequence of heavy machine traffic on forest soils. Following Horn et al. (Horn et al., 2007), soil displacements, caused by shearing forces and soil compression under wet conditions, lead to ruts. Soil moisture content, terrain slope, soil properties and the operating vehicle, are decisive for the creation of ruts (e. g. Bygdén et al., 2003). Additionally, the cumulative weight associated with the number of passes is linked to rut formation (Botta et al., 2009; Sirén et al., 2019b; Starke et al., 2020). Since ruts show a strong relationship to decreased forest productivity in the affected areas (Lacey and Ryan, 2000), it is a priority of sustainable operation management to keep their formation to a minimum.

Estimating soil trafficability is a key aspect for preserving soils integrity and thus the forest as an ecosystem on the one hand, and for optimizing timber harvest and efficient machine utilization on the other. In theory, soil trafficability can be derived from terrain characteristic, machine configurations, and weather conditions. An accurate prediction of rutting is necessary for sustainable, low-impact harvesting operations, since it supports the mitigation and avoidance of impacts (Jones and Arp, 2017; Sirén et al., 2019b; Uusitalo et al., 2019) on machine operating trails, which are established without pavement or any other fixation. The assessment of forest sites' trafficability continues to be commonly based on the appraisal of the forester in charge (e. g. Flisberg et al., 2021), mainly requiring a long-year experience to enable a sufficient estimation of current harvesting condition, in a designated area. However, because of varying weather conditions, considerably affecting the trafficability, the assessment of current conditions and subsequently the timing of operations is a challenging task. In many cases, the machine operator himself is faced with this task, when arriving at the site of operation. Usually, the machine operator starts the operation, until the occurring ruts are individually judged as too severe. Consequently, the operation has to be stopped, requiring a cost-intensive relocation of the machine to alternative stands with better trafficability. Hence, lacking knowledge of current trafficability on stand level may result in manifold drawbacks – financial shortcuts and, even worse, ecological damages with long lasting, severe impacts on tree growth, water infiltration, soil organisms and soil erosion (Cambi et al., 2015).

A prediction of such damages can be facilitated by terramechanical test procedures (e. g. Farzaneh et al., 2012) or by trafficability maps **Appendix III**. Recent approaches show the possibility to incorporate information of trafficability, measured during the first machine pass, in such maps (Salmivaara et al., 2018; Sirén et al., 2019b; Ala-Ilomäki et al., 2020). Both, terramechanical tests and trafficability maps, can sufficiently support the operational flexibility of company management and entrepreneurs as well as machine operators, in order to avoid and reduce disturbances to forest soils, with associated high costs. Some of the equipment used for assessing soil's bearing capacity has already been validated towards the predictability of ruts. For example, Sirén et al. (2019b; 2019a) reported a correlation between rut depth after harvest and Cone Index (CI). Same index has been frequently used for validations of accessibility maps, whereas CI was used, instead of assessing actual machine traffic (e. g.

Jones and Arp, 2019). Less commonly used, but already reported by Heubaum et al. (2015a), a vane meter can be used to assess soil trafficability through the determination of shear strength. Especially if measured in a mineral soil depth between 10 and 15 cm, this rather simple instrument is reported as promising, regarding the accuracy of prediction. Besides, the relatively unknown dual-mass dynamic cone penetrometer has been used in the estimation of pavements moduli (Siekmeier et al., 2000; David Suits et al., 2005). But, as far as we know, it was not validated at forest soils up to now. Certainly, numerous studies revealed the link between soil moisture content and rutting (Cambi et al., 2015; Poltorak et al., 2018), giving this parameter a high relevance for the prediction of rutting.

Subsequently, two pivotal approaches of remote analyses for the simulation of soil moisture content were chosen in addition. The calculated indices topographic wetness index (TWI, Pei et al., 2010; Waga et al., 2020) and depth-to-water (DTW) index (Murphy et al., 2009; 2011; Campbell et al., 2013) link the terrain characteristics with the soil wetness by the simulation of accumulating water runoff. In principal, both indices quantify the contributing area to a distinct cell within a grid, and calculate the likelihood for cells to be water saturated or moist. Especially in dense stands, with a lacking network of machine operating trails, visibility is restricted for machine operators. The cartographic knowledge of moist and therefore sensitive areas, in particular when available through geo-referenced digital maps on the forest machine's on-board computer screen, can highly contribute to the avoidance of deep ruts and other soil impacts (Tuomasjukka et al., 2020).

Still, the above-mentioned approaches for the prediction of rutting differ in regard of accuracy, financial efforts, handling and applicability, leading to specific advantages and drawbacks. Nevertheless, comparative studies between different approaches are lacking. In order to fill this knowledge gap, we conducted a study which aimed to assess relevant terramechanical testing procedures and cartographic indices, all assumed to predict rutting during forest operations. In particular, the following questions were addressed:

1. Can rut depth after a cut-to-length (CTL) thinning-operation be predicted by the two used cartographic indices (i.e. depth-to-water and topographic wetness index)?
2. Which of the applied terramechanical testing procedures show a reliable response with occurring rut depth, in terms of a high Pearson coefficient of correlation?
3. Is rut depth formation after the first machine pass (i.e. facilitated by a harvester) a reliable figure to predict total rutting of a consecutive CTL thinning-operation?

To answer these questions, a field trial was conducted at newly assigned machine operating trails. There, cartographic indices were calculated and in-situ measurements were performed in advance to a regularly planned CTL thinning-operation. Rut depth was estimated after the first and final machine pass and analysed in relation to cartographic indices and previously conducted field measurements.

2.2. Material and methods

2.2.1. *Stand Characteristics*

The study was performed in two stands, both located near the town of Uslar in Lower Saxony, Germany. The larger stand B (**Figure 2-1B**, area: 7.7 ha, x: 9.61, y: 51.71, WGS 84) was characterized by 95-year-old beech (*Fagus sylvatica*), showing a mean diameter at breast height of 28 cm. This stand was intermixed with grouped Norway Spruce (*Picea abies*, age: 75 years). The smaller stand A (**Figure 2-1A**, area: 1.9 ha, x: 9.60, y: 51.70, WGS 84) was stocked by 40-year-old beech, scattered with European larch (*Larix decidua*) and Norway Spruce. The stands were growing on Cambisol (IUSS Working Group WRB, 2015), based on a silicate bedrock. The terrain was smooth with a slight slope,

less than 30%. The long-term mean of annual precipitation amounts 892 mm (WetterKontor GmbH, 2020). Yet, overall dry conditions were present during the field campaigns, caused by a low precipitation of 345 mm between March and August (WetterKontor GmbH, 2020).

2.2.2. *Harvesting Operation*

A CTL thinning operation was performed at the study sites. Felling and processing were executed by a single grip harvester (see **Table 2-1** for machine specifications) on 4 August 2020 (**Table 2-2**). In the days between felling and forwarding (**Table 2-1**, 17–21 August), 45 mm of precipitation occurred at the site. On average, 36 m^3 ha^{-1} were harvested at the study area by clearing the machine-operating trails and thinning the forest stands.

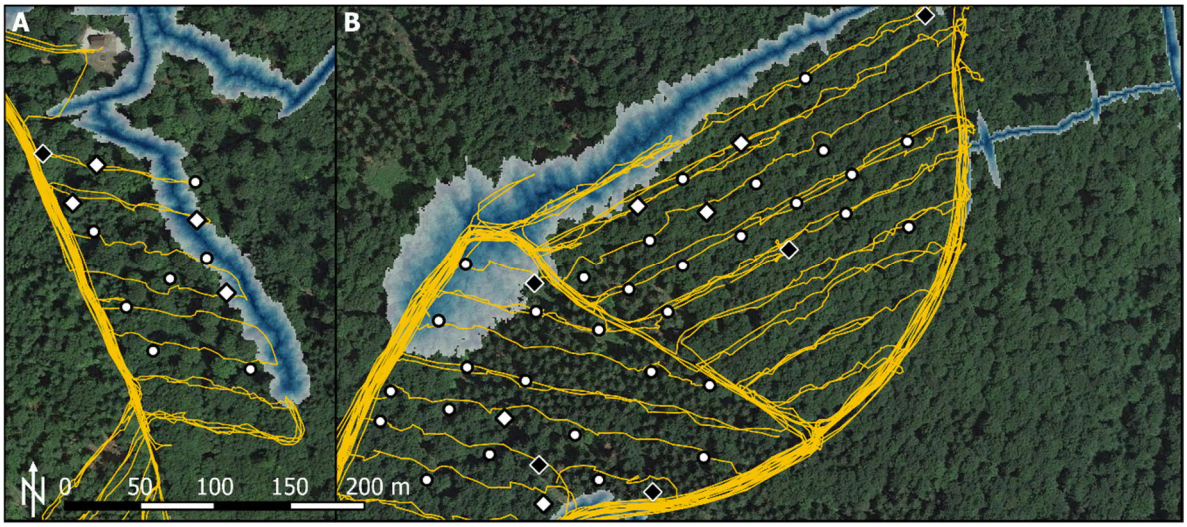

Figure 2-1. Study area of the field trial, conducted in two broadleaved dominated mixed stands (**A**, **B**). White symbols represent 47 remaining cross-sectional measuring transects from initial 90 transects in total (**section 2.2.3**) with four meters of width, located at newly assigned machine-operating trails. Terramechanical parameters and rutting process were quantified there (**section 2.2.3**). On nine of these transects, soil samples were collected (white rhombs). Additional soil samples were taken on six transects (black rhombs), where terramechanical parameters were captured, but rutting could not be measured. Lines show forwarder tracks. Blue colouring indicates predicted wet areas, according to the depth-to-water (DTW) index ranging from 0 to 1 m (**section 2.2.4**).

Table 2-1. Machine specifications of the used 8-wheel machines, a harvester (Ponsse Bear) and a forwarder (Ponsse Buffalo), conducting the investigated CTL thinning operation.

Character	Unit	Ponsse Bear	Ponsse Buffalo
power	kW	260	210
typical mass	Mg	24.5	19.8
loading capacity	Mg	-	15.0
tire type		Nokian Forest King TRS 2	Alliance Forestar 344, 20 PR
tire size (width, diameter)	mm	750, 1485	710, 1340
inflation pressure	kPa	600	500

The operating harvester resulted in a single machine pass on the machine operating trails (number of machine pass = 1). The subsequently operating forwarder was equipped with a GNSS device, constantly tracking the machine position during timber extraction. Thus, the number of passes, as illustrated in **Figure 2-1**, was assigned to all 47 measuring transects.

2.2.3. *Field Measurements*

Rutting on Machine-Operating Trails

Following the concept of permanent machine operating trails, a new system of parallel running machine-operating trails, with a spacing of 24 m from the centre line, was established in both stands to make the area of 9.6 ha in total accessible for forest machines. Therefore, the projected machine operating trails were marked in the stands. On a total of 19 newly planned machine operating trails, 90 perpendicularly positioned transects with a length of 4 m each, were created. At both ends, wooden pegs were placed, in order to mark each transect and to position a reference beam (**Figure 2-2**), used to measure the rutting process during the conducted harvesting operation. For that purpose, the initial profiles along each transect were measured using a yardstick at 20 cm spacing.

Figure 2-2. Example of a cross-sectional measuring transect on a machine operating trail. In-situ measurements were performed in advance of the regularly planned CTL thinning operation, using a Penetrologger (squares), vane tester (circles), a dual-mass dynamic cone penetrometer (cross) and a TDR probe (asterisks) as described in **section 2.2.3**. The levelled reference beam, positioned on wooden pegs and a yardstick were used to determine rut depth (**Figure 2-3**), as it occurred during the given operation.

This initial profile or reference surface was defined by the distance between the beam (levelled at the wooden pegs) and the surface, giving Dz_{init} (**Figure 2-3**). This (1.) measurement was done after loose humus material had been removed. Profiles along each transect were repeatedly measured: (2.) after the harvester passed, giving Dz_H (**Figure 2-3**) and (3.) after the timber extraction via forwarder was accomplished, giving Dz_F (**Figure 2-3**). Several wooden pegs, used to position the reference beam, were severely displaced during the harvesting operation, reducing the initial 90 measuring transects to the remaining 47 (**Figure 2-1**), since the rut depth could not be quantified anymore. When Dz_H and Dz_F were measured, the position of the tracks on the transect was captured as a dummy variable (t, where a visually detectable track was defined as "L" (left machine track) or "R" (right machine track, **Appendix I**), used for the calculation of occurring rutting (**Appendix II**). Consequently, where t equals "L" or "R", the maximum difference between Dz_H and Dz_{init} (**Figure 2-3**) of the left and right track were used to calculate the rut depth after the operating harvester, rut_H (cm), according to equation (1):

$$\mathrm{rut_H} = \sum^{n=2} \frac{Dz_{H,i} - Dz_{init,H,i}}{n} \tag{1}$$

Used variables for equations (1)–(3) are illustrated in **Figure 2-3**, where i represents "L" or "R"; the applied R-grammar is shown in **Appendix II**. Following the same approach, rutting after forwarding (rut_F, cm) was calculated according to equation (2), whereas the differences between Dz_F and Dz_H were used to quantify rut_F, describing the additional rutting after the harvester has passed already:

$$\mathrm{rut_F} = \sum^{n=2} \frac{Dz_{F,i} - Dz_{H,F,i}}{n} \tag{2}$$

Since total rut depth (rut_T, cm) cannot be calculated as the sum of rut_H and rut_F, as both machines might not drive exactly in the same machine track, the same procedure was applied to quantify rut_T. Differences between either Dz_F or Dz_H, and Dz_{init} were analysed on tracks, after the CTL thinning-operation was accomplished, as illustrated **Figure 2-3**, according to equation (3):

$$\mathrm{rut_T} = \sum^{n=2} \frac{Dz_{F|H,i} - Dz_{init,F,i}}{n} \tag{3}$$

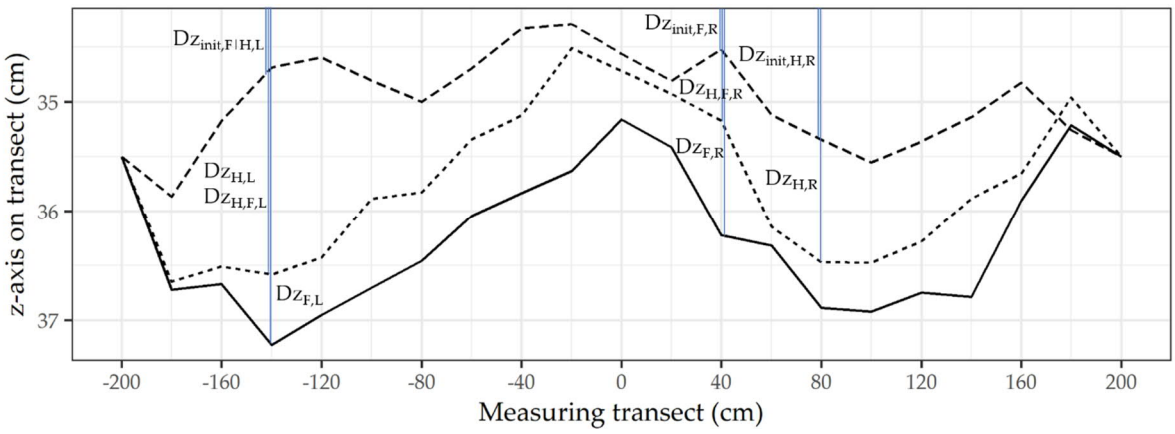

Figure 2-3. Scheme of recording rut depth during a CTL thinning-operation, applied on an exemplary measuring transect: The initial surface along the measuring transect (dashed line) was scaled by Dz_{init}. After the harvester passed (dotted line), Dz_H was measured. Coherently, Dz_F was measured after the timber was extracted (solid line) by a forwarder (**Table 2-1**). Each of the Dz-values were used to calculate rut_H, rut_F and rut_T, according to equations (1), (2) and (3), respectively. The maximum difference of the left and right machine track (i = 'R' or 'L') were averaged therefore.

Soil Samples

Along the newly assigned and still uncleared machine operating trails, soil samples were collected at randomly chosen measuring transects. Pre- and post-operational sampling was done at 15 measuring transects (**Figure 2-1**, rhombs), out of the 90 initial transects. Samples collected at nine of these 15 transects could be used to correlate parameters derived from soil samples with occurring rut depth, due to the above-mentioned reduction of measuring transects to 47 remaining ones (**section 2.2.3**). Still, the six remaining sampling positions (**Figure 2-1**, black rhombs) were used for correlations with terramechanical test procedures only.

The soil samples were either collected at the potential right or left machine track (position was assumed during the initial sampling), using 100 cm^3 sampling rings. Pre- and post-operational samples were taken in a depth between 10 and 15 cm of the mineral soil. Subsequently, initial soil bulk density (SBD_{INIT}, g cm^{-3}), as well as post-operational soil bulk density (SBD_{POST}, g cm^{-3}) were used to calculate compaction (comp, %), according to equation (4):

$$comp = \frac{SBD_{POST} - SBD_{INIT}}{SBD_{INIT}} * 100 \tag{4}$$

The fresh samples were weighed, giving an initial mass (M_{FRESH}, g), then dried in an oven (105 °C) until mass constancy was reached. Afterwards, samples were weighed again, giving M_{DRY} (g), used to calculate gravimetric soil moisture content (SMC_{GRAV}, %), according to equation (5). Additionally, soil texture was analysed on three mixture probes, containing all soil samples, according to the approach of Durner et al. (2017).

$$SWC_{GRAV} = \frac{M_{FRESH} - M_{DRY}}{M_{DRY}} * 100 \tag{5}$$

Terramechanical Test Procedures

Despite SBD_J and M_J, both being measured before and after the CTL thinning operation, the remaining soil parameters were measured in advance of the operation only (**Table 2-2**), describing initial conditions. These initial conditions were further used to address the posed research question concerning

the comparison among the included terramechanical test procedures. For that, initial measurement results were associated with rut_H. Soil moisture content, penetration resistance, depth and shear strength were measured on the 90 initial measuring transects, but only 47 of them could be used to be correlated with rut_H. The measurements by the used instruments (**Figure 2-4**) were spaced by 10 cm to each other, with a spacing of 50 cm along each transect (**Figure 2-2**):

- Moisture meter: Volumetric soil moisture content (SMCVOL, vol%) was quantified in the mineral topsoil, where a 57 mm long TDR probe (HH2-moisture meter, Delta-T-Devices, Cambridge, UK) was inserted from above, after the removal of humus. This moisture meter measures volumetric moisture content, θv, by responding to changes in the apparent dielectric constant of moist soil, resulting in a ratio between the volume of water and the total volume of the soil sample (Eijkelkamp Agrisearch Equipment, 2013). Seven measurements on each transect were averaged, giving SMCVOL.
- Penetrologger: Penetration resistance was measured, using a handheld Penetrologger (1.0 cm2, 60° cone, Eijkelkamp Soil and Water, Giesbeek, The Netherlands). This device captures the soil penetration resistance for each centimetre by means of a load cell, whereas values of the upmost 15 cm of mineral soil were averaged giving a Cone Index (CI, MPa), as mean value for seven penetrations on each transect. Based on my previous experience, a modified Cone Index (CIMOD, MPa) was calculated in addition. In contrast to the estimation of CI, soil penetration values between 10 and 20 cm were considered to quantify CIMOD, due to the high variance of penetration resistance in the upmost centimetres. Besides, the total penetration depth, captured by the Penetrologger, was averaged for each measuring transect, giving PD (cm).
- Dual-mass dynamic cone penetrometer: Since we decided to keep the time demand for measurements approximately similar between the compared methods, the number of samples was reduced for this instrument. Consequently, one measurement, consisting of six hammer blows, was done in the middle of each transect. The incremental penetration depth was captured and used to calculate the corresponding parameter, derived by the dual-mass dynamic cone penetrometer, DCP (cm blow−1), defined as the average of penetration depth per hammer blow, until it exceeded 15 cm penetration depth.
- Vane tester: The used Eijkelkamp (Eijkelkamp Soil and Water, Giesbeek, The Netherlands) field inspection vane tester is an instrument for in-situ measurements of shear strength through vanes of different sizes. Measurements are conducted through a spiral spring, detecting the torque, which needs to be applied to a handle in order to displace the soil through the vane. The used (and smallest, 16 mm × 32 mm sized) vane allows to cover readings up to 260 kPa, by an accuracy within 10% (Eijkelkamp Agrisearch Equipment, 2020). The current measurements were done in a mineral soil depth of 10 to 15 cm, as recommended by Heubaum (2015a), giving shear strength (τ, kPa) as mean value for each measuring transect.

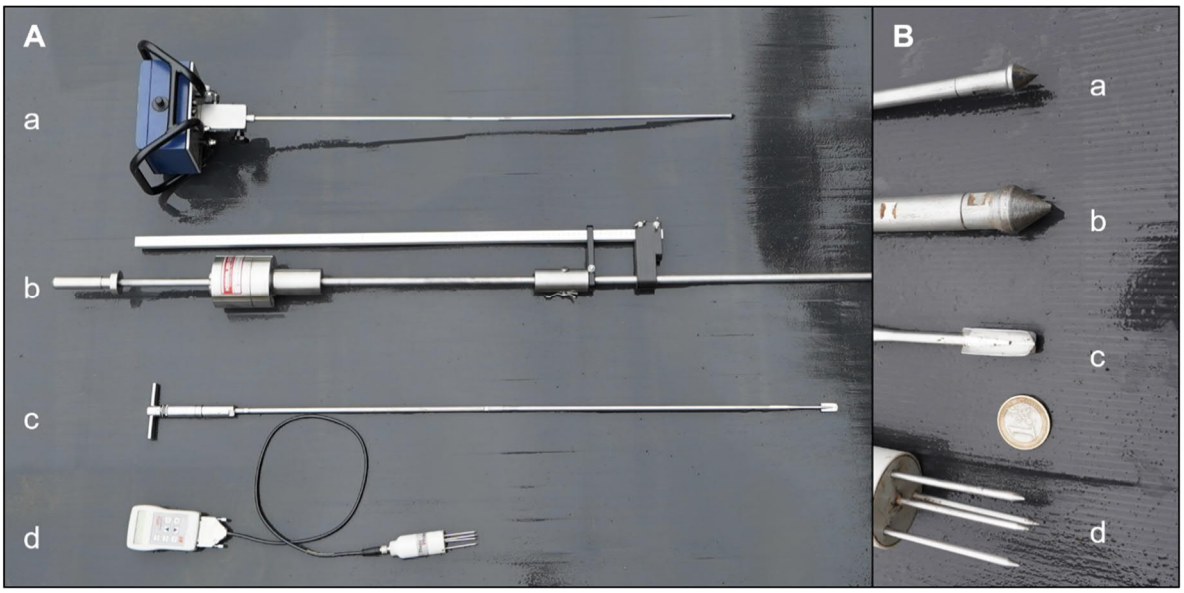

Figure 2-4. Selected terramechanical instruments to assess trafficability and to predict rutting caused by machine traffic during a CTL thinning operation. (**A**) shows a Penetrologger (**a**), dual-mass dynamic cone penetrometer (**b**), a vane tester (**c**) and the used moisture meter (**d**). Tips are shown in (**B**), respectively.

Table 2-2. Overview and date of performed in-situ measurements. For the study, volumetric and gravimetric soil moisture content (SMC_{VOL}, vol%; SMC_{GRAV}, % (M_{FRESH} and M_{DRY}, equation (5)), respectively), commonly used and a modified Cone Index (CI, CI_{MOD}, respectively, MPa), penetration depth (PD, cm), penetration resistance by means of dual-mass dynamic cone penetrometer (DCP, cm $blow^{-1}$) shear strength (τ, kPa) initial and post-operational soil bulk density (SBD_{INIT}, SBD_{POST}, respectively, g cm^{-3}) were measured. For the estimation of rut depth increments, transect profiles were measured (Dz_{init}, Dz_H, Dz_F, **Figure 2-3**, cm).

Date (2020)		Objective	Measurement
15 July	initial measurements of 90 transects	reference profile to estimate rut depth increment and	Dzinit
		terramechanical parameters	SMCVOL, CI, CIMOD, PD, DCP, τ, SBDINIT, SMCGRAV
4 August	**harvester performed the felling and processing**		
10 August	measurement of profiles rut depth after harvester		DzH
17–21 August	**forwarder excavated timber**		
1 September	post-operational measurements	rut depth after forwarder, total rut depth and	DzF
	on the remaining 47 transects	post-operational soil bulk density and moisture content	SBDPOST, SMCGRAV

2.2.4. *Trafficability Maps*

During the field campaigns, multiple positioning measurements were conducted using a handheld GPS device (Oregon 700, Garmin Ltd., Olathe, KS, USA). Later, these waypoints were averaged to get the nearest approximation of the transects' position. From the 90 initial measuring transects, 47 were used for the correlation between measured rut depth and calculated indices. These point positions were used to join field measured data with remote processed data using QGIS (version 3.10.10, Open Source Geospatial Foundation Project (QGIS.org, 2020)). Two trafficability indices for the identification of wet and therefore sensitive areas within forest stands were calculated using QGIS.

Depth-to-Water Index

Digital terrain models (DTM) are the only prerequisite input data to calculate depth-to-water (DTW) maps. Within this study, a DTM with a grid size of 1 m has been used, originally collected by the State Office for Geoinformation of Lower Saxony (LGLN, 2020). Based on this model, DTW maps were created according to Murphy et al. (2009), as extensively described already (Jones; Murphy et al., 2011; White et al., 2012; Ågren et al., 2014; Mohtashami et al., 2017; Bartels et al., 2018). In short, a flow accumulation model of the DTM is generated using the D8 flow algorithm. When the flow accumulation of a cell reaches a certain value, the very cell is defined as the starting point of a flow line, which continues the flow downhill until leaving the mapped area. The required area to start a flow line is defined as "Flow Initiation Area" and herein was set to 4 ha, as suggested by Jones and Arp (2019) for likewise conditions. Subsequently, a least-cost function calculates the least slope path from each cell within the grid towards the nearest flow line (Murphy et al., 2009; Murphy et al., 2011). Hence, low values of the metric DTW index indicates a spatial proximity (in a vertical direction) to the nearest flow line, with assumed wet or poorly to imperfectly drained areas. A DTW index of up to 1 m is usually assumed to show areas with water-saturation, which are associated with a high susceptibility towards rutting. Contrarily, high values of the index generally indicate dryer and therefore accessible areas.

Topographic Wetness Index

In addition, the topographic wetness index (TWI), commonly used to quantify topographic control on hydrological processes was calculated according to Sørensen et al. (2006). This index combines the local upslope contributing area (a) and slope (β), given by equation (6):

$$TWI = \ln \frac{a}{\tan \beta} \tag{6}$$

Within this study, we aggregated the grid size of 1 m to receive a grid of 5 m resolution (Ågren et al., 2014). The procedure Zevenberg Thorne was chosen within a GDAL algorithm to calculate the slope grid, since the terrain was smooth. To generate the required flow accumulation grid, a SAGA algorithm was applied, which filled occurring sinks during reprocessing. Subsequently, having slope and contributing area given by the flow accumulation, TWI could be calculated according to equation (6).

2.2.5. *Data Analysis*

All data were merged and analysed using R core (version 4.0.2, R Foundation for Statistical Computing, Vienna, Austria (R Core Team, 2020)), interfaced with R studio (version 1.3.959, PBC, Boston, USA). Normal distribution of CI, CI_{MOD}, DCP, τ, rut_H and rut_F was assessed and approved via QQ-plots. Both cartographic indices were adjusted, DTW was transformed into a dummy-variable, with a margin of 1 m, TWI was log-transformed. Individual linear models were fitted between parameters. Coherently, Pearson coefficients of correlation (r_P) were used to evaluate the quality of the given models, and were depicted applying a modified correlation matrix (Peterson and Carl, 2020). Residuals of linear models were visually assessed to identify outliers. In addition, values from transects with exceptionally high traffic were identified. Accordingly, four observations were removed. Afterwards, normal distribution of residuals was tested and confirmed by Shapiro–Wilk tests. Initial gravimetric soil moisture content was compared with post-operational, by means of a one-sided paired t-test. An unpaired t-test was applied to test for differences of rut_H measured within predicted sensitive areas (DTW) and remaining ones. Analyses were usually performed on 47 observations (90 initial transects, 43 of them unusable, since rut depth could not be measured, or seemed unreliable according to the outlier analysis), or 15 observations for variables derived from soil samples. The correlation between soil bulk density and rut_H was performed on nine remaining observations. All tests were done using a significance level of 0.05,

tendencies were reported up to a significance level of 0.10. Values within the text are usually given as mean ± standard deviation.

2.3. Results

2.3.1. *Soil Properties*

The Cambisol (IUSS Working Group WRB, 2015) at the study area, composed of 33±5% sand, 35±10% silt and 32±7% clay, showed a mean penetration depth of 31±15 cm, derived from measurements using the Penetrologger. Across the study site, the initial volumetric moisture content averaged at 29±9 vol% (spatial distribution is depicted in **Figure 2-5**), before the operation had been started. Initial gravimetric soil moisture content (SMC_{GRAV}), estimated on 15 gathered soil samples, described similar values, with an average of 31±6%. Due to 45 mm of rainfall, occurring between the time of felling (harvester) and forwarding (**Table 2-1** and **Table 2-2**), SMC_{GRAV} slightly increased to 34±7% (p = 0.046). Apparently, the increase of SMC_{GRAV} was higher on measuring transects with low initial SMC_{GRAV} (**Figure 2-6**A), compared to rather moist initial conditions. Soil bulk density across the study site was quantified with 1.2±0.1 g cm^{-3}. Through the harvesting operation, this initial density increased by 10% (p = 0.017), up to 1.3±0.1 g cm^{-3}. It was observed that measured compaction showed higher extents on measuring transects with lower initial soil bulk density (**Figure 2-6**B).

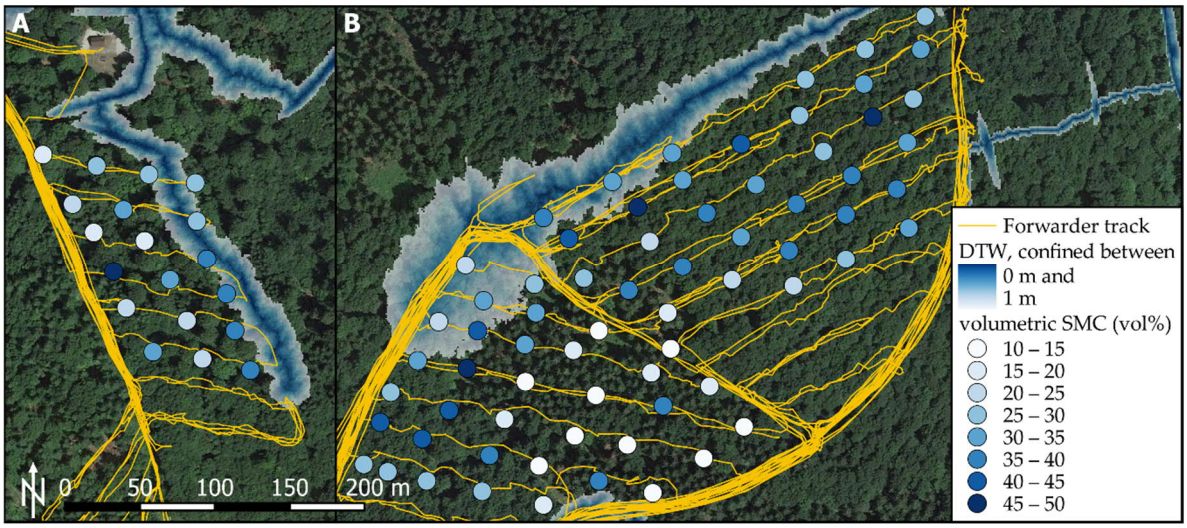

Figure 2-5. Sites of study (**A**, **B**). Initial volumetric soil moisture content (SMC_{VOL}) was measured at 90 transects and is indicated by blue points. Blue colouring indicates predicted wet areas, according to the depth-to-water (DTW) index ranging from 0 to 1 m, as described in **section 2.2.4**.

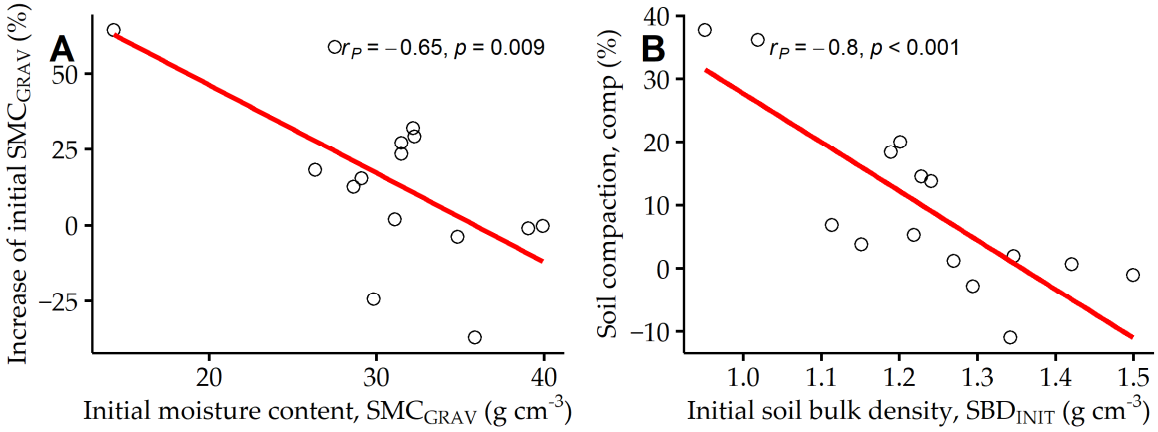

Figure 2-6. Scatterplot and regression line (**A**) between the increase from initial to post-operational gravimetric soil moisture content, related to initial values and (**B**), describing soil compaction after 2–5 machine passes, according to equation (4), depending on initial soil bulk density. With Pearson coefficients of correlation (r_P) and *p*-value for 15 observations.

2.3.2. *Rutting*

The clearing of the 19 machine operating trails and the thinning of the adjacent stand area (**Figure 2-1**) was conducted by the 24.5 Mg heavy harvester (**Table 2-1**), resulting in on average 3.6±1.7 cm deep ruts (rut_H), ranging from −0.4 to 7.0 cm. The subsequently driving forwarder, trafficking the same machine operating trails, resulted in additional average rut_F of 3.8±2.1 cm, ranging from 0.0 to 9.9 cm. Although differences between rut_H and rut_F were low, rut_F clearly explained more variance of total rut depth (rut_T), with r^2 of 0.63, compared to r^2 of 0.25, when rut_H was correlated with rut_T. Still, rut_T responded to rut_H, given as rut depth after the first machine pass ($p < 0.001$), as can be seen in **Figure 2-7**A. Thereby, rut_T could be quantified with 6.3±2.1 cm (2.2 to 11.6 cm). Under the given operational conditions of the current study, rut_T showed no dependency of traffic frequency (2–5 passes, **Figure 2-7**B).

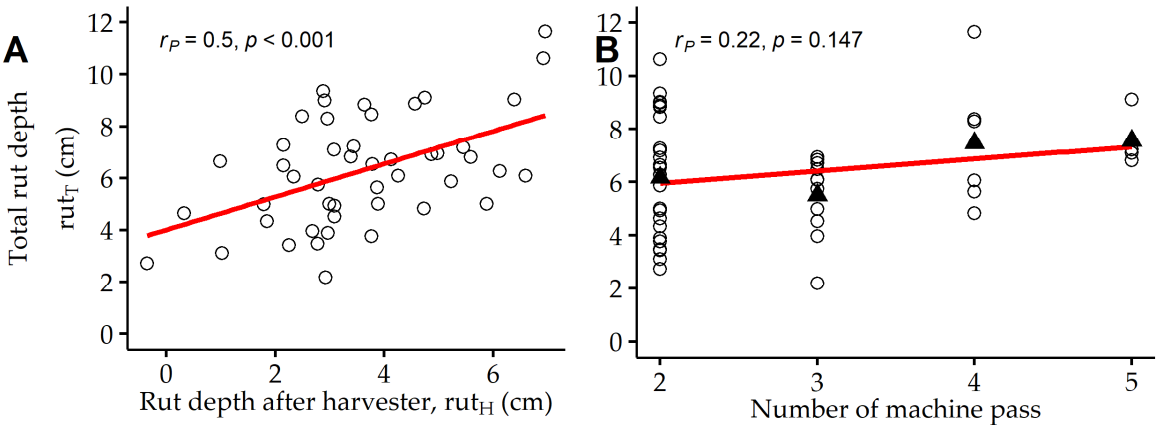

Figure 2-7. Scatterplot and regression line between total rut depth after completion of a CTL thinning operation (2–5 passes) and (**A**) rut depth after a single pass of the operating harvester (rut_H, **Table 2-1**), as well as (**B**) number of machine passes. Note, that total rut depth was quantified after completion of forwarding at various locations (**Figure 2-1**), containing a different number of forwarder passes. Average values of rut_H for each traffic frequency are represented by filled triangles. With Pearson coefficients of correlation (r_P) and *p*-value for 47 observations.

2.3.3. *Correlations with Terramechanical Tests*

Terramechanical tests were applied on every measuring transect along the previously marked machine operating trails, to capture initial conditions. Descriptive statistics for these tests are given in **Table 2-3**.

Table 2-3. Descriptive statistics of terramechanical parameters, measured prior to harvesting operation. Parameters are regular and modified Cone Index (CI, CI_{MOD}, respectively) and penetration depth (PD), measured by Penetrologger, DCP (cm $blow^{-1}$, dual-mass cone penetrometer) and shear strength (τ, kPa, vane tester). With the number of observations, mean value, standard deviation, extreme values, first and third quantiles.

Parameter	n	Mean	SD	Min.	0.25	0.75	Max.
CI (MPa)	47	1.52	0.31	1.01	1.29	1.70	2.53
CI_{MOD} (MPa)	47	2.24	0.61	1.25	1.78	2.51	3.61
PD (cm)	47	30.86	14.78	10.29	18.00	41.00	62.86
DCP (cm $blow^{-1}$)	47	4.18	4.22	0.00	1.77	4.94	21.60
τ (kPa)	47	214.02	69.63	127.43	150.14	265.57	365.14

Due to high uncertainties regarding the load mass of the forwarder, we decided to use rut_H to validate the surveyed cartographic indices, and terramechanical test procedures. Three of the contained parameters, CI, CI_{MOD} and shear strength (τ), are capturing forces, required to overcome a given resistance within the soil. Analogously, these parameters showed inverse responses to rut_H, as can be seen in **Figure 2-8** and **section 2.4.2**. Whereas a correlation can be assumed for τ (p = 0.088), an unreliable response was observed for CI (p = 0.415). Regardless of a standard definition of CI, given as the mean penetration resistance of the upmost 15 cm soil, we also generated a modified CI. For this, penetration resistance of a soil depth between 10 and 20 cm was averaged, giving CI_{MOD}, which was significantly linked with rut_H (r_P = −0.30, p = 0.040, Section 2.4.2). In addition to CI and CI_{MOD}, penetration depth (PD) was also derived from measurements by the Penetrologger. Whereas CI possessed an insufficient prediction of rut_H, the latter showed a significant correlation to PD (p = 0.001) with a high r_P of 0.44. As indicated in **Figure 2-8**, DCP, measured by means of the dual-mass cone penetrometer, correlated with rut_H (p = 0.020), resulting in the second highest value of r_P (0.34).

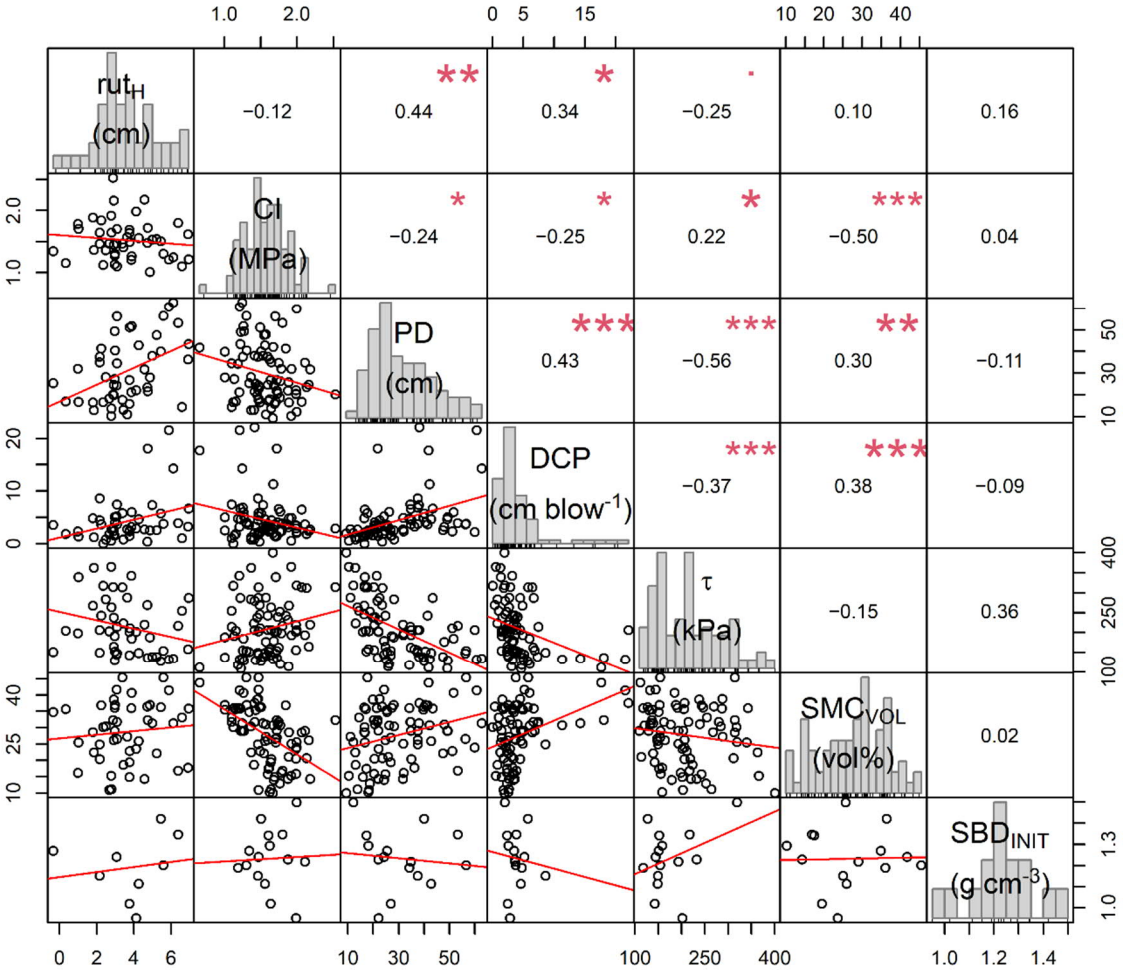

Figure 2-8. Correlation plot between field measured parameters, with labelled Pearson coefficients of correlation. Red asterisks indicate significance codes (*** 0.001 ** 0.01 * 0.05 ˙ 0.10), regression lines are shown by red lines. Histograms are showing data distributions. Parameters are rut depth after harvester (rut_H), Cone Index (CI), penetration depth (PD), DCP (measured by dual-mass cone penetrometer), shear strength (τ), volumetric soil moisture content (SMC_{VOL}) and initial soil bulk density (SBD_{INIT}), as described in **section 2.2.3**.

2.3.4. *Correlations with Cartographic Indices*

A DTW map with a flow initiation area of 4 ha was calculated for the study area. There, the values of DTW ranged between 0 and 8.7 m. The overall mean at the analysed transects was 3.6±2.3 m. Out of those, four measuring transects exhibited a DTW index below 1 m (**Table 2-4** and **Figure 2-1**), usually assumed to indicate areas with a low bearing capacity and high susceptibility to soil displacement. Within this study, rut_H measured on these transects averaged at 2.65 cm. Besides, beneficial operational conditions were predicted for 43 measuring transects, where a similar extent of rut depth was estimated (**Table 2-4**). The relatively dry conditions, from the perspective of forest operations, might have caused a missing relationship between rut_H and DTW values (**Figure 2-9**A). In addition, it might impede a correlation between values of SMC_{VOL} and DTW values (p = 0.336, r_P = −0.14).

Table 2-4. Mean values and standard deviations (SD) of rut depth after the harvester (rut_H, **Table 2-1**) and after a CTL thinning operation was accomplished (rut_T) on newly assigned machine operating trails (**Figure 2-1**). An unequal variance t-test was used to compare between 4 values of rut_H within predicted sensitive areas, where the depth-to-water (DTW) index was below 1 m and 43 values, measured within areas with predicted high trafficability (see **section 2.2.3**).

		rut_H (cm)		rut_T (cm)		Test Statistics for rut_H	
DTW	n	Mean	SD	Mean	SD	t-Value	*p*-Value
<1 m	4	2.65	2.50	5.17	1.54		
>1 m	43	3.71	1.56	6.43	2.14	1.35	0.18

Similar to the observations made regarding DTW, the TWI was also not able to predict occurring rutting, since no correlation between log-transformed TWI and rut_H could be approved (**Figure 2-9**B).

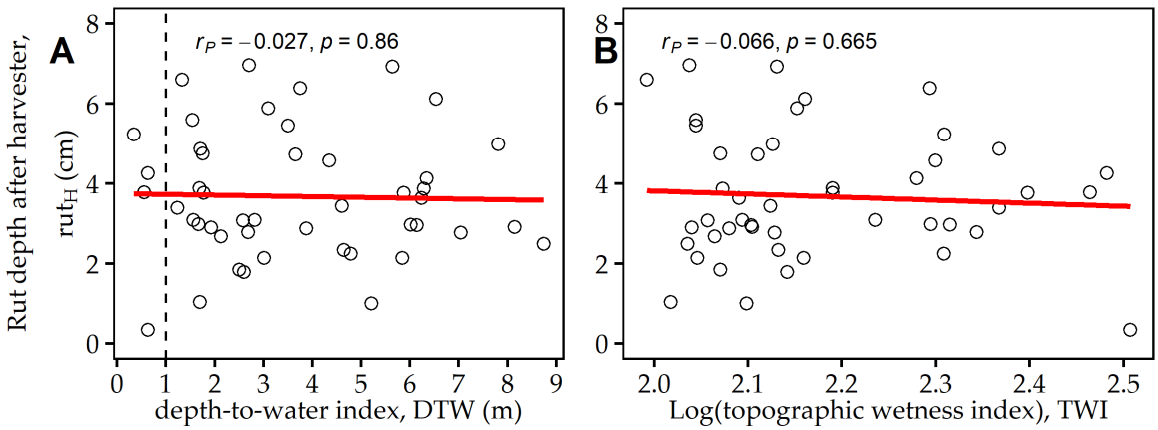

Figure 2-9. Scatterplot and regression line between rut depth after a harvester performed a CTL thinning operation (single pass), and values of two accessibility maps, (**A**) depth-to-water and (**B**) topographic wetness index (**section 2.2.4**). (**A**): The dashed line indicates the threshold at 1 m, whereas sensitive conditions are assumed in the range between 0 and 1 m of DTW. With Pearson coefficients of correlation (r_P) and *p*-value for 47 observations.

2.4. Discussion

Within this study, a regularly scheduled forest operation was analysed in two broadleaved dominated mixed stands, with machine traffic on 19 newly established permanent machine operating trails. Prior to the operation, measuring transects have been established along the machine operating trails. On each of these, terramechanical parameters were quantified in advance to the operation, using different equipment. Additionally, two cartographic indices were calculated. In order to validate the compiled parameters and indices, correlations with occurring rut depth, measured after the first and final machine, were performed.

2.4.1. *Soil impact*

Numerous factors, like wheel slippage, high traffic and the relationship between soil bearing capacity and a machine's ground pressure can lead to severe soil impacts, harming physical soil properties (Labelle and Jaeger, 2019). The long lasting (Rab, 2004) impacts, disturbing the integrity of the soil, can be caused by all vehicles. Due to a compression stress and plastic deformation (Vossbrink and Horn, 2004), soil impacts and displacement emerge.

After the off-road traffic by heavy forest machines (**Table 2-1**), values of *soil compaction* within this study averaged at 10%, related to the initial soil bulk density of 1.2 g cm^{-3}. This is in line with results reported in the meta-analysis by Ampoorter et al. (2009), revealing an average increase of soil bulk density of 15% under similar operational conditions. Kozlowski (1999) reported a critical soil bulk density of 1.4 – 1.6 g cm^{-3} to hamper root penetration into fine-textured soil (Daddow and Warrington, 1983). It can be assumed, that in particular the first machine passes prevailingly lead to soil compaction (Han et al., 2006; Ampoorter et al., 2009; Agherkakli et al., 2010). Consequently, additional machine passes result in a lower increase of soil bulk density, since preceding passes pre-compacted the soil already. In agreement, we have clear evidence for a higher soil compaction on measuring transects with low initial soil bulk density (**Figure 2-6**B). Although soil compaction by forest machines might decrease with additional traffic frequency, rut depth increment can be enhanced after a certain compaction has been reached (McNabb et al., 2001; Jamshidi et al., 2008). Soils are susceptible to compression, especially under moist and wet soil conditions (Arvidsson et al., 2003; Horn et al., 2007), since the particle to particle bonding is low then (Hillel, 1998). The measured initial soil moisture content in the study area of only 29 vol% can be associated with an smaller extent of soil displacement (Froehlich et al., 1980; Cambi et al., 2015) and might have impeded a vast soil displacement (McNabb et al., 2001). In this respect, Poltorak et al. (2018) resumed deep ruts and high soil compaction more likely to occur at soils with a moisture content of more than 50 vol%, way higher as our measured 29 vol%.

Subsequently, *ruts* measured within this study appeared at a moderate extent, averaging at 6.3±2.1 cm, with a maximum depth of 11.6 cm. Overall, only on two out of 47 measuring transects, ruts deeper than 10 cm could be observed. These results are in line with findings from other studies, reporting moderate rut depths between 3 cm (**Chapter 6)**, over 9-12 cm (Eliasson, 2005; Agherkakli et al., 2010; Haas et al., 2016), and up to 20 cm (Horn et al., 2007; Naghdi et al., 2009; Labelle and Jaeger, 2011), when measured on designated machine operating trails. In general, appearing rutting within this study is in agreement with the recommendations of Owende et al. (2002), who proposes to limit rut depths to a maximum of 10 cm to ensure an eco-efficient wood harvesting in Europe. Considering, that the presented field study was conducted on newly assigned machine operating trails, the experienced rut formation was further below the internal guidelines of the state forest enterprise of Lower Saxony, stating a maximum tolerance value of 15 cm rut depth on 90% of length of the machine operating trail (Niedersächsische Landesforsten, 2017). These guidelines are set to ensure the technical trafficability of permanent machine operating trails for future operations, rather than actively protecting forest soils. Yet, since maintaining the technical trafficability is inevitable to avoid the conversion of further stand areas to new machine operating trails, counteracting the soil conservation thoughts behind the permanent machine operating trail concept, it is fundamental to keep rut formation there as low as possible, too (Vossbrink and Horn, 2004; Ampoorter et al., 2009). But, it should be noted, that the moderate extent of ruts experienced in this study after the crossing of a 24.5 Mg harvester, and subsequent timber extraction by a forwarder, is most likely supported by the relatively low logging volume of just 36 m^3 ha^{-1}. This, in return, led to a low traffic frequency (**Figure 2-1** and **Figure 2-7**B) with limited loads. It should be mentioned, that rutting at the measuring transects was favoured due to the conductance of this study, since operators were advised not to create brush mats in the transect areas, contrary to common recommendation to reduce rut formation (Labelle et al., 2019).

2.4.2. *Validation of surveyed tools*

In general, observed rutting and soil compaction are in line with earlier findings (Ampoorter et al., 2009; Cambi et al., 2015). Still, rut formations arising after forwarding possess an unfortunate nuisance within the current study, also reflected by the relatively weak correlation between rut_H and rut_F. The latter mentioned was probably deranged: (i) by changing moisture conditions, as rain fall occurred in the time

gap between harvester and forwarder trafficked the study site, (ii) through the study's arrangement within a real harvesting operation, where numerous measuring transects became unusable, since the wooden pegs, used to position the reference beam, were displaced, reducing our number of observations to 47 (from initial 90), and (iii) because loads and consequently total mass of the machine could not be captured during forwarding, reducing the potential independent variables in the linear models. Hence, linear models of parameters to be validated were fitted with rut_H, created by the harvester, in order to account for the uncertainties (i-iii) within the validation of the surveyed approaches. Deviations from a standardized study design were assumed to be lower when using rut_H, compared to rut_T. Although, we assumed one machine pass by the harvester (driving without GNSS-tracking), short back and forth movements of the harvester may have led to multiple crossings on a measuring transect during the felling and processing, difficult to quantify at a given transect.

Although Sirén et al. (2019b; 2019a) reported *Cone Index* (CI), measured by means of a handheld Penetrologger, to be correlated with rut depth after a harvester pass (r_P=-0.27 (Sirén et al., 2019b) or r_P=-0.24 (Sirén et al., 2019a)), we were not able to statistically confirm this relationship within the current study (r_P=-0.12, p=0.415). This instrument possesses a pivotal nuisance, as the measured values are highly depending on users handling (Jones and Arp, 2017), what might have perturbed the correlation within this study. In addition, patterns of the upmost few centimetres of soil might not be associated with actual bearing capacity, as organic matter content (Uusitalo et al., 2020) or divergent soil moisture conditions there can highly affect measured penetration resistance. To avoid these uncertainties, we calculated a *modified Cone Index*, CI_{MOD}, which includes penetration resistance between 10 cm and 20 cm soil depth, as compared to CI, considering values measured in a depth between 0 and 15 cm. As shown in **Figure 2-10**, CI_{MOD} inversely responded to rut_H. Contrarily, common CI turned out to be the least accurate terramechanical parameter to predict rut_H, as summarized in **Figure 2-8**. Interestingly, the much easier to measure *penetration depth* (PD), herein also derived from the Penetrologger, turned out to be in clear response with rut_H. A lower PD might be driven by increased coarse fraction (Niemi et al., 2017) or more intense root network within the soil, which both can be considered to impede rutting.

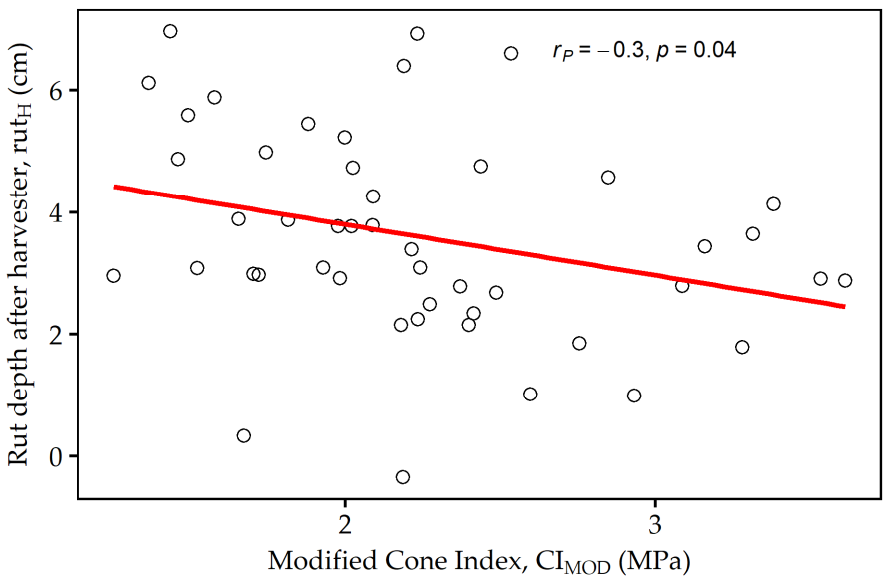

Figure 2-10. Scatterplot and regression line between modified Cone Index, given as mean of penetration resistance between 10 cm and 20 cm soil depth, and rut depth after first machine pass (harvester). With Pearson coefficients of correlation (r_P) and p-value for 47 observations.

Besides penetration depth, also the *dual-mass dynamic cone penetrometer* uses a metric scale (DCP). Measurements of this relatively simple mechanical device appeared to show robust predictions of rut_H and resulted in a more reliable r_P (0.11) with total rut depth, rut_T, compared to CI. The latter mentioned, curiously, showed a positive trend to rut_T, meaning that deeper ruts tended to occur, where high values of CI were captured (p=0.15). During the application of the dual-mass dynamic cone penetrometer, the hammer is raised carefully without lifting the cone before it is allowed to drop (Webster et al., 1992). By doing so, an artificial bias during handling can be avoided almost certainly. We assume, that this, in combination with a larger cone resulted in a better prediction of rut_H, compared to the Penetrologger. However, it should be noted that the penetrometer is an instrument with a weight of 12.8 kg, limiting its application for individual users at extended stand levels.

Although seldomly used in research, *shear strength* (τ), measured by use of a vane meter led to rather reliable results, regarding the correlation of τ and rut_H. Thereby, r_P of -0.25 exceeded the coefficients achieved by CI. This correlation is in close agreement to the findings from Jacke et al. (2011), who promoted the usage of a vane meter to measure shear strength and to assess temporal soil trafficability, as already verified (Heubaum, 2015a).

In summary, the surveyed terramechanical parameters PD, DCP and τ (in decreasing order according to revealed r_P) bear a high potential towards prediction of rutting.

2.4.3. *Correlations with cartographic indices and soil moisture*

Nonetheless, these measurements are time consuming and might not be doable in day-to-day work by harvesting operators and entrepreneurs. Subsequently, remotely analysed trafficability maps, covering the whole area of operation could match the demands of practitioners, presuming, that those maps show a valid prediction of expectable rutting. Both used cartographic indices simulate water saturation or soil wetness, as it would accumulate in depressions, sinks or if a sufficiently sized area drains into a spot. However, measured spatial distribution of soil moisture content (SMC_{VOL}) could not be reflected by *depth-to-water* (DTW) maps within the present study, as shown in **Figure 2-5**. This might have also caused the contradictory response between DTW index and observed rut_H, which occurred completely independent of DTW (**Figure 2-9**A). The analysed DTW maps, which were calculated with an flow initiation area of 4 ha (Murphy et al., 2009; 2011), would represent a low overall moisture (Jones and Arp, 2019). The created index is usually converted to a dummy variable, with a threshold of 1 m (White et al., 2012), were values below this threshold are assumed to predict wet and sensitive areas. By doing so, four measuring transects would have been assessed to have inferior bearing capacity, due to the assumed water saturation. Measured rut_H and rut_T at these four transects showed low means of 2.7 cm or 5.2 cm, respectively, similar to values measured on the remaining transects (**Table 2-4**). However, considering the generally acceptable extents of rut_T (Owende et al., 2002; Niedersächsische Landesforsten, 2017), the DTW index reasonably assessed actual operational conditions for 43 out of 47 transects, as favourable trafficability was predicted there. In addition, the occurring precipitation between felling and forwarding may limit the meaningfulness of the made observations. The validity of this approach could be restricted, since soil moisture increased particularly at dryer transects (**Figure 2-6**A), thereby smoothing the spatial distribution of moisture. Hence, the prediction of wet or water saturated areas might be jeopardized. Along with the DTW, also the second surveyed cartographic index, *topographic wetness index*, revealed no reasonable correlation with rut_H (**Figure 2-9**B).

The inferior performance of both surveyed indices might be driven by two main aspects: (i) Due to the systematic allocation of measuring transects, some of these were positioned at former machine operating trails, which could be observed at both forest stands, although assumed to be un-trafficked. Whereas terramechanical testing procedures capture the divergent soil conditions there, trafficability maps are

not able to include these effects. (ii) The influence of soil moisture on rutting has been reported extensively (Cambi et al., 2015; Poltorak et al., 2018), with inevitable influence on soil displacement. But, within this study, measured rutting turned out to be independent of *soil moisture content* (SMC_{VOL}), which is simulated by DTW and TWI in the first place. The relatively low SMC_{VOL} (from the perspective of forest operations) during the field trials, with only six observations above 40 vol%, could have limited the effect of SMC_{VOL} (Uusitalo et al., 2020) on appearing rut formation and consequently the predictability of rut depth by means of both cartographic indices.

2.4.4. *Prediction of rutting*

As none of the surveyed tools was able to predict final rutting to a satisfying level at the given conditions, alternative approaches are requested to match the desired prediction of soil impact (Jones and Arp, 2017; Uusitalo et al., 2019). Findings of Sirén et al. (2019b; 2019a) approved the rut formation of the first machine pass, there and in our case by the harvester (rut_H), to predict further rutting caused by the consecutive passes of the forwarder. In agreement to these findings, rut_H of the present study turned out to be the best indicator for total rut depth after 2 to 5 machine passes, possessing a highly significant correlation among both variables (**Figure 2-7**A). Under the given conditions, higher traffic frequency did not lead to additional rut depth increments (**Figure 2-7**B), what supports the overall assumptions of this survey. The results give a further impetus to use rut_H within regard to the prediction of rutting. In the modelling of Sirén et al. (2019b), variables like SMC, CI did not further increase accuracy, when rut_H has been included already. In agreement to this, rut_H acted as pivotal influence, explaining the highest share of deviations in the present study, where additional variables did not increase model's quality (not shown). Consequently, rut_H should be considered to design the extraction trail network. This exchange of knowledge between both operating machines could contribute to the optimal routing of the subsequently driving forwarder and thereby support an eco-efficient forestry through the avoidance of areas with a high susceptibility for rut formation. Making it useful for operational purposes, Lidar-based sensors could detect actual rutting, created by an operating harvester, evolving the real-time generation of trafficability maps as a part of normal forestry operations (Salmivaara et al., 2018). Another sensor-based solution aims at rolling resistance, which has been recently assumed to be able to assess machine operating trails trafficability (Ala-Ilomäki et al., 2020). In line, Salmivaara et al. (2020) reported the high potential of CAN-bus derived rolling resistance to be used for predictions of trafficability across complex landscapes and changing conditions.

These more operation-based monitoring approaches, in particular have potential to support the management of extraction activities, consecutive to the harvesters felling and processing, in order to prevent further soil impact whilst forwarding. Such technologies could support harvesting operations without fixed machine operating trails, as conducted in many plantations of the tropics or boreal forests. If the harvester detected areas with low bearing capacity, timber extraction could be conducted on alternative routes, in order to avoid severe soil impact. However, it does not solve the problem of the impact caused by the first machine pass, which requires a reliable pre-operation assessment of the trafficability situation at both, permanent machine operating trails with pre-compaction, and previously non-trafficked areas.

2.5. Conclusion

The findings of the current study can be used to answer the posed research questions. One of these questions addressed the potential prediction of total rut depth after CTL operations, based on rutting after an initial machine pass. The results give clear evidence, that rut depth caused by the first machine pass of the harvester remains a reliable indicator of further rut formation through up to four consecutive machine passes at current site conditions, and should therefore be cautiously monitored during the felling.

However, for operational planning purposes, assessment of the logging site prior machine traffic is mandatory to ensure efficient machine utilization and to avoid negative impacts on soils or the technical trafficability of permanent machine operating trails in first way. In this respect, the auspicious remote sensing based cartographic indices DTW and TWI seem promising towards an operational usage, presuming a high accuracy of rut prediction. However, both used indices did not proof to be reliable alternatives compared to conventional terramechanical in-situ measurements of actual site conditions, at least during the experienced situation with already long-lasting precipitation deficits. The surveyed terramechanical testing procedures possess specific advantages and drawbacks, but have not been compared with another so far. This begs the question of the tool-specific ability to assess operational conditions in terms of trafficability, and in turn the ability to predict ruts. Surprisingly, the frequently used site assessment indicator CI showed a low certainty of rut depth prediction, compared to the less commonly applied dual-mass dynamic cone penetrometer and vane tester. Finally, none of the investigated methods can be fully approved or disapproved due to the limited scale of observations and intensity of monitored machine traffic in this study. However, the results clearly revealed, that the various approaches, already available for operational planning, would lead to a different assessment of the situation. Thus, state-of-the-art applications like cartographic indices need further adaptation to increase the predictive power on the one hand, but also parameters measured by more simple instruments such as the DCP, should be further considered as an alternative, or at least as supplementary aid to determine current site conditions and risks of trafficability.

Acknowledgements: The authors acknowledge the opportunity for conducting this survey, as well as the contribution during the field work, both provided by “Niedersächsische Landesforsten” (State Forest Enterprise), “Forstamt Dassel”, in particular supported by Jendrik Niebel, BSc. Further we acknowledge the help of Thilo Habert and Christopher Pohle for performing the measurements with the dual-mass dynamic cone penetrometer. We acknowledge the help of Heike Strutz, Soil Science Department, accomplishing soil analyses.

3. Prediction of soil moisture content and strength by depth-to-water maps

This chapter has been published under the same title in the International Journal of Applied Earth Observation and Geoinformation, November 2021c. It is available at: https://doi.org/10.1016/j.jag.2021.102614

Full author list: Marian Schönauer [1,*], Kari Väätäinen [3], Robert Prinz [3], Harri Lindeman [3], Dariusz Pszenny [4], Martin Jansen [5], Joachim Maack [1], Bruce Talbot [2], Rasmus Astrup [2], Dirk Jaeger [1]
* Corresponding author

[1] Department of Forest Work Science and Engineering, Georg-August-Universität Göttingen, Göttingen, Germany

[2] Norwegian Institute of Bioeconomy Research (NIBIO), Ås, Norway

[3] Szkoła Główna Gospodarstwa Wiejskiego w Warszawie SGGW, Warszawa, Poland

[4] Natural Resources Institute Finland (Luke), Helsinki, Finland

[5] Soil Science of Temperate Ecosystems, University of Göttingen, Göttingen, Germany

Author's contributions: Marian Schönauer: Conceptualization, Methodology, Formal analysis and Visualization, Investigation and Resources, Writing – Original Draft, Writing – Review and Editing. **Kari Väätäinen:** Investigation and Resources, Writing – Review and Editing. **Robert Prinz:** Investigation and Resources, Writing – Review and Editing. **Harri Lindeman:** Investigation and Resources. **Dariusz Pszenny:** Investigation and Resources, Writing – Review and Editing. **Martin Jansen:** Investigation and Resources, Writing – Review and Editing, Supervision. **Joachim Maack:** Writing – Original Draft, Writing – Review and Editing. **Bruce Talbot:** Writing – Review and Editing. **Rasmus Astrup:** Writing – Review and Editing, Project administration, Funding acquisition. **Dirk Jaeger:** Conceptualization, Methodology, Writing – Review and Editing, Supervision, Project administration, Funding acquisition.

Abstract

Introduction: The utilization of detailed digital terrain models entails an enhanced basis for supporting sustainable forest management, including the reduction of soil impacts through predictions of site trafficability during mechanized harvesting operations. Since wet soils are prone to traffic-induced damages, soil moisture is incorporated into several systems for spatial predictions of trafficability. Yet, only few systems consider temporal dynamics of soil moisture, impeding the accuracy and practical value of predictions. The depth-to-water (DTW) concept calculates a cartographic index which indicates wet areas. Temporal dynamics of soil moisture are simulated by different DTW map-scenarios derived from set flow initiation areas (FIA). However, the concept of simulating seasonal moisture conditions by DTW map-scenarios was not analysed so far. *Material and methods:* Therefore, we conducted field campaigns at six study sites across Europe, capturing time-series of soil moisture and soil strength along several transects which crossed predicted wet areas. Assuming overall dry conditions (FIA=4.00 ha), DTW predicted 20% of measuring points to be wet. When a FIA of 1.00 ha (moist conditions) or 0.25 ha (wet conditions) were applied, DTW predicted 29% or 58% of points to be wet, respectively. *Results and conclusions:* De facto, 82% of moisture measurements were predicted correctly by the map-scenario for overall dry conditions – with 44% of wet measurements deviating from predictions made. The prediction of soil strength was less successful, with 66% of low values occurring on areas where DTW indicated dryer soils and subsequently a sufficient trafficability. The condition-specific usage of different map-scenarios did not improve the accuracy of predictions, as compared to static map-scenarios, chosen for each site. We assume that site-specific and non-linear hydrological processes compromise the generalized assumptions of simulating overall moisture conditions by different FIA.

Keywords: depth-to-water, soil moisture content, precision forestry, trafficability prediction, forest operations, soil bearing capacity.

3.1. Introduction

High resolution digital elevation models (DEM) have become state-of-the-art in supporting sustainable forest management. One of many applications of such models is given through cartographic indices, which are used for predicting trafficability across forest sites. Current site trafficability is an important factor to consider during forest operations with heavy machines. As a result of this, such operations used to be executed during winter, when ground was frozen. Soil impacts are commonly low then, since frozen mineral soils possess a high soil strength. However, a change of weather regime across large parts of Europe made it difficult to conduct the entirety of annual harvesting operations in periods of favourable conditions. Intensive precipitations during summer and a lack of winter frosts (Max-Planck-Institute for Meteorology, 2009) will shorten such periods. Especially when soils plasticity limit is reached during periods of high moisture, traffic can result in severe soil displacement (Horn et al., 2007; Poltorak et al., 2018; Labelle and Jaeger, 2019; Uusitalo et al., 2020), with long-lasting (Rab, 2004; Sohrabi et al., 2021) consequences towards forest growth and microbiological activity (Beylich et al., 2010).

To enable eco-efficient and therefore sustainable forest management, numerous approaches were established for predicting trafficability, including the creation of maps showing sensitive areas. The high spatial resolution of DEMs available is supposed to embrace highest possible accuracy for such maps (Vega-Nieva et al., 2009; White et al., 2012; Jones and Arp, 2017). However, commonly applied systems provide static information about trafficability but do not consider temporarily changing site conditions. Changing site conditions are driven by temporal and spatial variations of soil moisture, known to have an effect on soil strength and correlate with the extent and degree of soil-impacts like deep ruts (McNabb et al., 2001; Cambi et al., 2015; Poltorak et al., 2018; Uusitalo et al., 2020).

The depth-to-water (DTW) concept was conceived, developed and tested at the University of New Brunswick (Faculty of Forestry and Environmental Management), by Fan-Rui Meng, Jae Ogilvie and Paul Arp, as described by Murphy et al. (2007; 2009; 2011). DTW is based on the utilization of geo-spatial data and is renowned as a robust tool for the prediction of perennial streams, wet or water saturated areas, and sensitive areas for ground-based trafficking (Murphy et al., 2011; Ågren et al., 2014; Ågren et al., 2015; Mohtashami et al., 2017; Väätäinen et al., 2019). When calculating DTW maps, in a first step, local depressions are removed by using a fill-function (e.g. Tarboton, 1997). Afterward, a flow accumulation tool (D8, O'Callaghan and Mark, 1984) is applied and the resultant accumulation is further used to define starting points. The starting points are set by an adjustable value of the upstream contributing areas' size and used to initiate flow paths. Afterward, the DEM is used to delineate the shortest vertical difference between each surface grid cell and adjacent flow paths: The vertical difference is minimized by the use of a least-cost function, applied onto least cumulative slopes between each grid cell and adjacent flow paths. The process ensures the assignment of each surface grid cell to the nearest downslope flow path with the most likely hydrological connection. Accordingly, low values of DTW indicate moist or water saturated conditions, while high values indicate well drained areas. This concept is numerically robust and can be applied to DEMs of different spatial resolutions (Ågren et al., 2014). Yet, the resolution of the used input data should not exceed 5-10 m, to guarantee a practical value of the created maps for forest operations.

When applying the DTW concept, temporal variations of trafficability are simulated by means of several scenarios of created maps, each representing a different overall moisture regime at the site. This is facilitated by condensing and extending upstream contribution areas for initiating flow lines across the landscape. Subsequently, Higher extents of such areas represent a high soil moisture at a site, whereas a small extent would represent dryer conditions. The map-scenarios cover moisture conditions reaching

from “very dry or frozen” to “wet” (Jones and Arp, 2019). Accordingly, the user of such DTW maps can individually choose the most reliable scenario for a given time and site of harvesting operation.

In large Canadian forestry companies, high-resolution accessibility maps based on wet-areas mapping (Murphy et al., 2009) are being used in combination with DTW to minimize traffic damage to forest soil through improved resource road planning (Vega-Nieva et al., 2009; Campbell et al., 2013). In addition, DTW maps were recently related with species abundance and used for ecological monitoring (Oltean et al., 2016b; Bartels et al., 2018). In Sweden, DTW-maps or DTW-like systems have been utilized for roughly six years in planning of loggings and during logging operations (Ågren et al., 2014; Väätäinen et al., 2019). In Finland, soil moisture was derived from digital terrain models and the risk of damage from traffic on rural roads was estimated (Niemi et al., 2017). Recent research reveals potential improvements of such topographic soil wetness indices through a merge with open spatial data and different machine learning approaches (Lidberg et al., 2020; Salmivaara et al., 2020).

Although DTW maps and possible applications have been evaluated extensively, we identified two research gaps: (I.) While numerous implementations of the DTW concept were performed and studied in boreal forests of Scandinavia and Northern America, such measures are lacking in temperate forests of large areas across Europe. (II.) The scenarios of DTW maps, as made through specific settings of the FIA, are envisaged to represent seasonal variations of moisture and therefore soil strength in forest stands. Prior research conjectured the ability to capture such varying conditions by these scenarios, but the concept lacks strong empirical evidence. Consequently, we formulated two research questions:

1. Can differences in the quality of DTW-predictions of soil moisture and strength be observed between the study sites and attributed to site characteristics?

2. Can spatio-temporal variations of soil moisture and strength be predicted by the DTW map-scenarios?

To answer these questions, different DTW scenarios were compared to time-series of in-situ measurements, conducted on six study sites in three European countries. We captured temporal and spatial variations of soil moisture content and soil strength by repeated measurements across 24 transects.

3.2. Material and methods

3.2.1. *Study sites*

Field measurements were conducted in three countries: Finland, Germany and Poland (**Figure 3-1**, **Table 3-1**). In each of the three countries, two study sites were established in mature forest stands, under closed, homogeneous canopy. Together with local experts, approximately 1,000 ha large study sites, known to be temporarily inaccessible because of low soil strength, were selected on flat or moderately sloped terrain (<35%).

Figure 3-1. Locations of the study areas, where time-series of soil strength and moisture measurements were performed and compared to different scenarios of depth-to-water maps.

Table 3-1. Characteristics of the study sites, where a validation of depth-to-water maps was conducted.

		Country		
	Site	**[1] Finland**	**[2] Germany**	**[3] Poland**
Region		North-Karelia	Sauerland, North-Rhine-Westphalia	South Poland, Border of Silesian and Lodz Voivodeship
Coordinates (X/Y)	A	29.625486	8.01625	19.492248
	A	62.653529	51.47680	50.954030
EPSG: 4326	B	30.16780	8.03922	19.535888
	B	62.775407	51.40679	50.903021
Elevation [m]	A	110	270	217
	B	110	260	220
Geology		Migmatitic tonalite, biotite paragneiss and granite	Claystone and Sandstone from Devon and Carbon	Sands and gravels and tills as well as glacial sands and gravels
Soil types		Haplic Podzol, Histosol	Cambisol, Stagnosol	Haplic Podzol
Texture class		loamy sand	silty loam	sand
Soil bulk density [g cm^{-3}]		1.20	1.20	1.60
[4] Humus form	A	Dysmoder	Mull	Dysmoder
	B	Humimor	Mesomull	Dysmoder
Mean Temp.		[5] 2.5°C	[6] 8.9°C	[7] 7.9°C
Mean annual precipitation		[5] 600 mm	[6] 790 mm	[7] 580 mm
Tree species		*Pinus sylvestris, Picea abies, Betula pubescens*	*Fagus sylvatica, Picea abies, Pinus sylvestris*	*Pinus sylvestris, Larix decidua, Picea abies*

[1] Site A: Onttola, Site B: Eno
[2] Site A: Neheim, Site B: Obereimer
[3] Site A: North, Site B: South
[4] According to Zanella et al. (2011).
[5] Finnish Meteorological Institute (2021).
[6] DWD (2019a).
[7] IMGW-PIB (2021).

3.2.2. *Depth-to-water maps*

A DEM with a sufficiently high spatial resolution is the only necessary input data to calculate DTW maps. Within this study, DEMs derived from airborne laser scanning campaigns (Figure 3-2), provided by respective governmental authorities (**Table 3-2**), were used to create DTW maps covering the selected sites.

Table 3-2. Data sources of digital elevation models used to calculate depth-to-water maps.

Country	Data provider	Cell size [m]	Point density [points m^{-2}]	Accuracy [m]	Year of flight
Finland	National Land Survey of Finland	2.0	≥0.5	±0.3	2019
Germany	Bezirksregierung Köln	1.0	4-10	±0.2	2019
[8] Poland	Polish Main Office of Geodesy and Cartography	1.0	4-12	±0.10 to ±0.15	2020

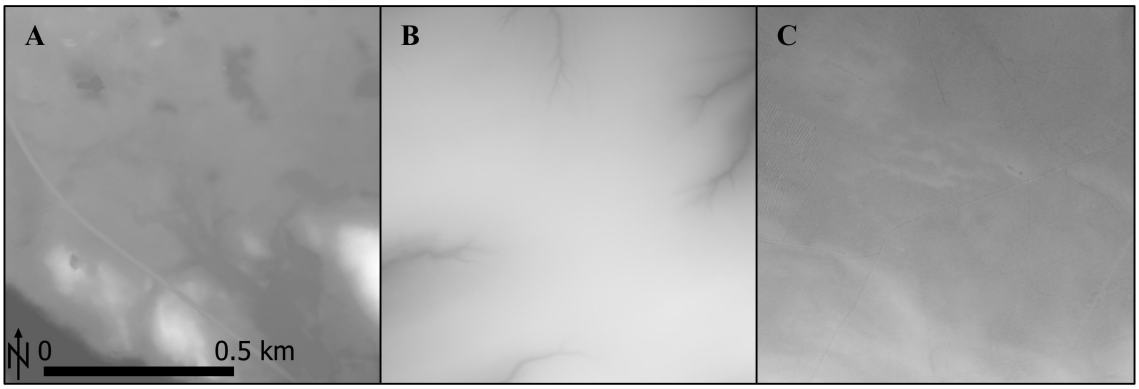

Figure 3-2. The topography-based depth-to-water index was calculated based on digital elevation models, derived from airborne laser scannings, on sites in Finland (A), Germany (B) and Poland (C).

The maps generated for each flow initiation area (FIA) are given as grids of the metric DTW index (e.g. $DTW_{0.25}$ for FIA=0.25 ha, [m]), with a grid size equal to the input layer. To create DTW maps, the already described procedure, e.g., Murphy et al. (2009; 2011), was recreated in the programming environment R (R Core Team, 2020), using the package “rgrass7” (Bivand, 2021), which provides an interface to run commands from the free toolbox GRASS GIS (Awaida and Westervelt, 2020) in R. To spread the DTW concept for improved soil protection, we added the commented R-script in **Appendix IV**.

For the present study, three scenarios of DTW maps were created, using FIA according to Jones and Arp (2019), who stated likely upslope flow-channel initiation areas for different seasons and moisture conditions. This were 4.00 ha, 1.00 ha and 0.25 ha, simulating generally *dry*, *moist* or *wet* soil conditions, respectively (**Figure 3-3**).

[8] Kurczyński and Bakuła (2013).

3.2.3. *Field measurements*

Transects

Each study site contained four transects. Three of these transects were centered perpendicularly across mapped sensitive areas, according to the DTW maps. The transect "4.00" crossed a delineated wet area ($DTW_{4.0}$<1 m), calculated using a FIA of 4.00 ha (**Figure 3-3** A). Accordingly, transects "1.00" and "0.25" crossed wet areas, generated when the concept was run with 1.00 ha or 0.25 ha FIA, respectively (**Figure 3-3**B, C). The fourth transect was located apart from mapped sensitive areas, to serve as control ("exp", **Figure 3-3**). Each transect had a length of 40 m (resulting in 21 transect points, **Figure 3-3**c) and was permanently marked with wooden pegs, at its starting and end points. The position of starting and end points were captured by means of a handheld GNSS-device with the post-correction of position data, for later analyses within a geographic information system.

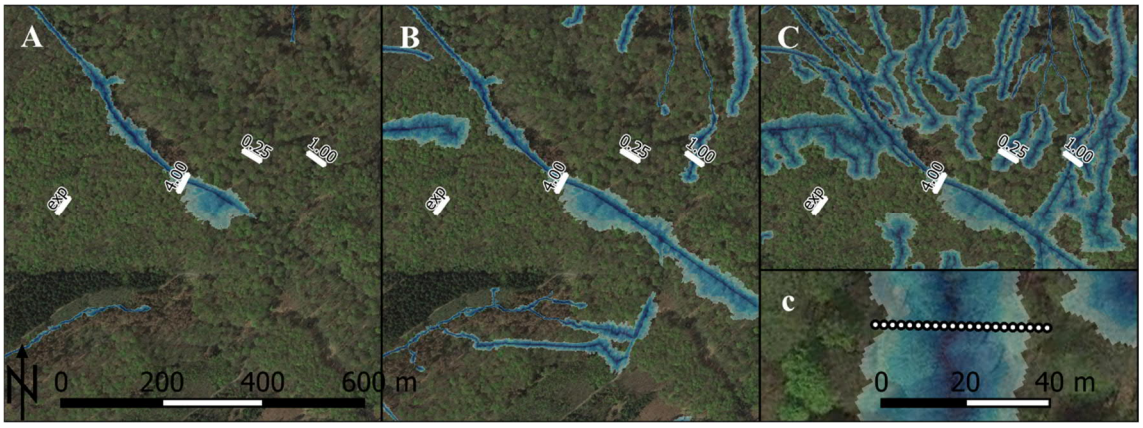

Figure 3-3. Three scenarios of depth-to-water (DTW) maps, according to different flow initiation areas (FIA) of 4.00 ha (A), 1.00 ha (B) and 0.25 ha (C). The FIA is defined as required contributing upstream area to start a flow line, with subsequently low values of DTW-index in vertical proximity of those lines (coloured blue areas). The Figure shows site A in Germany (**Table 3-1**).

Measuring campaigns

In each of the three participating countries, repeated field measuring campaigns were conducted once a month. To reveal seasonal and spatial variations, eleven campaigns were captured in Germany, ten campaigns in Poland, and six campaigns were captured in Finland, between September 2019 and February 2021. At the in total 27 measuring campaigns, soil strength and moisture were measured at all transect points. Period-to-period measurements were shifted with an interval of 0.2 m along the transect, to probe undisturbed soil.

Soil penetration resistance

After the removal of coarse litter at the points along the transect (**Figure 3-3**c), penetration resistance was measured threefold at each point at randomly selected spots within the area of 0.2 m x 0.2 m, using a handheld Penetrologger (1.0 cm², 60° cone, Eijkelkamp, Netherlands). This device captures the soil penetration resistance [MPa] for each centimetre by means of a load cell. Values measured between a depth of 10 and 20 cm of mineral soil (**Chapter 2**), were averaged for each of the three pseudo replications. Subsequently, these three mean values were averaged giving the cone index (CI). The consecutive measurements for the following measuring campaigns were carried out next to the previous 0.2 x 0.2 m area.

Soil moisture content

At the same time and position of CI-measurements, volumetric soil moisture content (SMC, [%vol]) was quantified in the topsoil below the litter layer with a TDR probe (HH2-moisture meter, Delta-T-Devices, England). The 57 mm long probes were inserted into the soil from above to measure SMC, which is estimated by the ratio between the volume of water and the total volume of the soil sample (Eijkelkamp Agrisearch Equipment, 2013).

Moisture conditions and assigned DTW indices

The conducted measurement campaigns were asserted to three condition classes (*wet*, *moist* and *dry*), with respect to mean values of SMC, grouped by site and campaign. Thresholds between classes of condition were deduced from texture-specific water retention curves (model: 'van Genuchten', Seki, 2007) and are shown in **Figure 3-4**. Therefore, soil probes were taken along the transects and the prevailing texture was estimated according to DIN 19682-2:2007-11. In addition, each measurement of SMC was transformed into binary values, with **wet** values when soils were close to water saturation (<1.5 pF, **Figure 3-4**), and **not-wet** values when the matrix potential was higher than 1.5 pF. In order to give clarity about the used terms, we write '*wet*' when referring to the three classes of condition, and '**wet**' (binary) when measured SMC on a given transect point and campaign indicated water saturation.

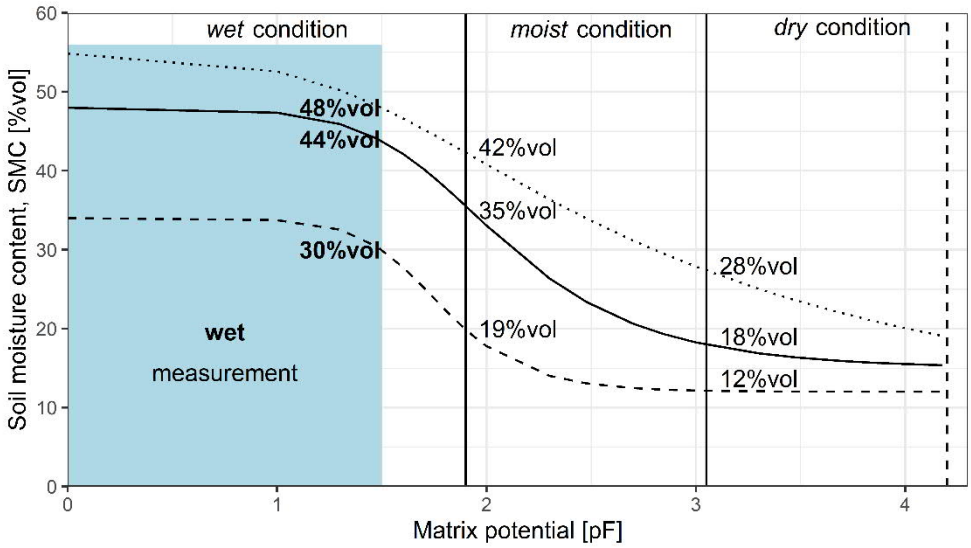

Figure 3-4. Texture-specific water retention curves for the study sites in Germany (pointed), Finland (solid) and Poland (dashed). Thresholds (vertical lines, labelled) were applied to mean values of soil moisture content (SMC), grouped by site and campaign. Values of SMC above field capacity (1.9 pF) were used to identify *wet* conditions. Centered between field capacity and the permanent wilting point (4.2 pF), the threshold distinguishing between *moist* and *dry* conditions was set (3.05 pF). Each field-measured value was assessed as **wet**, when SMC indicated a low matrix potential (<1.5 pF), as shown by blue colouring (applied thresholds are given in bold).

In-field values measured during *dry* conditions were related to $DTW_{4.00}$ maps. When measurements were conducted under *moist* conditions, the resulting values were compared to $DTW_{1.00}$ maps, and values measured during *wet* conditions with $DTW_{0.25}$ maps. Subsequently, the respective index for each moisture condition, was saved as a new variable, DTW_{FIA} (**Figure 3-5**).

3.2.4. *Data analysis*

The transects' end- and starting GNSS-positions were transferred to a geographical information system, QGIS, version 3.10.7-A Coruña (QGIS.org, 2020). The points along the transects were added,

considering the spacing of 2 m between points. Since DTW maps are given as raster grids, cell values could be extracted to the measuring points along the transects. The resultant table of attributes, containing the point ID and associated DTW-indices, was exported and merged with data from field measurements and subsequently used for further analyses (**Figure 3-5**). Calculations were performed with the free programming language R (version 4.0.2, R Core Team, 2020), linked with RStudio (version 1.4.1103, RStudio, PBC, Boston, MA). Normal distribution of CI and SMC was assessed and approved via QQ-plots. A linear model was used to correlate CI and SMC, with contrasts set to sums for the factors 'Country' and 'condition', followed by a type-III ANOVA (Fox and Weisberg, 2019). In addition, a full-factorial linear model was fit to SMC values, followed by a Tukey post-hoc test (Lenth et al., 2019) to compare means between levels of DTW.

Confusion matrix and performance of predictions

The prediction of low soil strength and **wet** soils by means of each DTW index, and by means of a season-adjusted DTW index was assessed, as illustrated in **Figure 3-5**.

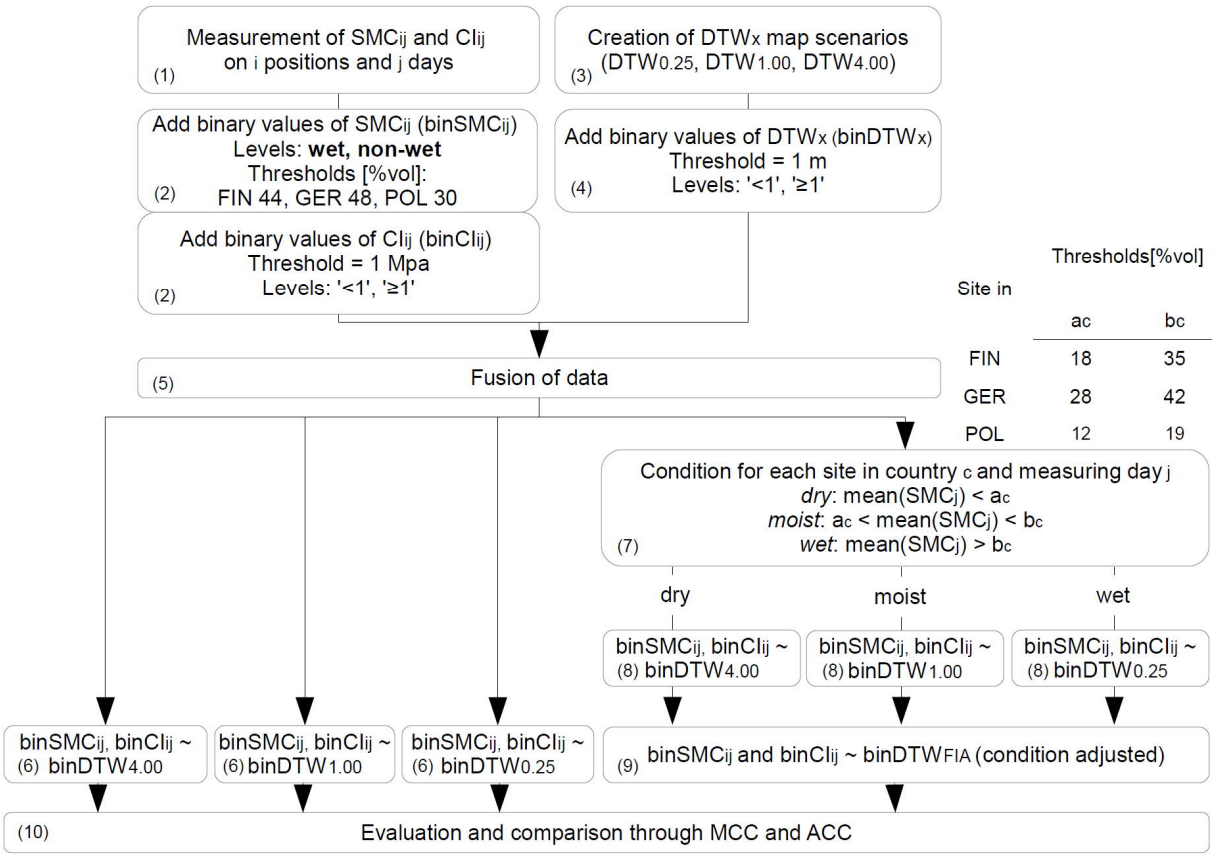

Figure 3-5. For assessing the performance of predictions, the following process was pursued: (1) In-field measurements of soil moisture content (SMC_{ij}) and soil strength (CI_{ij}) were conducted on i positions (along several transects on sites in FINland, GERmany and POLand) during a time-series of j measuring days. (2) Values of SMC_{ij} and CI_{ij} were transformed into binaries ($binSMC_{ij}$ and $binCI_{ij}$, respectively). (3) Depth-to-water (DTW_x) maps were created with different flow initiation areas (x=0.25 ha, 1.00 ha and 4.00 ha), and (4) transformed into binary values ($binDTW_x$). (5) The data was fused and used for further validations: (6) all values of $binSMC_{ij}$ and $binCI_{ij}$ were compared to $binDTW_x$; in addition, (7) the data was split by moisture conditions – for that mean values of SMC_j of each site and day j were compared with texture-specific moisture thresholds (**Figure 3-4**). This allowed for (8, 9) a condition-adjusted comparison between $binSMC_{ij}$ or $binCI_{ij}$ and $binDTW_{FIA}$. Finally, (10) a confusion matrix was created and ACC (equation (7) and MCC (equation (8)) were calculated.

The performance of made predictions was assessed via a confusion matrix, with the classes defined in **Table 3-3**.

Table 3-3. Used confusion matrix to summarize depth-to-water predictions of soil moisture content (binary values of SMC, **Figure 3-4** and **Figure 3-5**) and binary values of soil strength (CI, **Figure 3-5**). Counts in the matrix, true positives (TP), false positives (FP), true negatives (TN) and false negatives (FN) (Kuhn, 2020) were used for the equations (7) and (8).

	binary SMC		binary CI	
DTW	**wet**	**not-wet**	<1 MPa	≥1 MPa
<1 m	TP	FN	TP	FN
≥ 1 m	FP	TN	FP	TN

This classification was used to calculate accuracy of prediction (ACC, [%]) and Matthews (1975) correlation coefficient (MCC), according to equation (7) and (8), respectively:

$$\mathrm{ACC} = \frac{\mathrm{TP} + \mathrm{TN}}{\mathrm{TP} + \mathrm{TN} + \mathrm{FP} + \mathrm{FN}} \tag{7}$$

$$\mathrm{MCC} = \frac{\mathrm{TP} * \mathrm{TN} - \mathrm{FP} * \mathrm{FN}}{\sqrt{(TP + FP)(TP + FN)(TN + FP)(TN + FN)}} \tag{8}$$

Linear models using permutation tests (Wheeler et al., 2016) were used to compare ACC and MCC between the usage of static FIA and those, where FIA was adjusted to the current condition.

The significance level used for all tests was α=0.05. Mean values are given as least squares mean ± standard error.

3.3. Results

3.3.1. *Soil moisture and strength*

Overall soil moisture content (SMC) varied moderately among participating countries between 14.4±0.61%vol, measured at Polish, and 31.8±0.31%vol at German study sites (**Figure 3-6**A). The differences of SMC between measuring campaigns were considerable in Germany and Poland. Less variation was observed in Finland, where average values of SMC were between 21.9±1.12%vol (“Onttola”) and 38.40±1.12%vol (“Eno”) only. The entirety of 2,954 observations, measured on 371 points in total, was assigned to the three defined classes of condition, grouped by site and campaign. This resulted in 614 (*dry*), 1840 (*moist*), or 500 (*wet*) values being related to $DTW_{4.00}$, $DTW_{1.00}$ or $DTW_{0.25}$ respectively (**Figure 3-6**).

The occurrence of **wet** values (close to water saturation), related to the entirety of cases, peaked with 35.7% under *wet* conditions on Finnish sites. The low of **wet** measurements was observed on Polish study sites, under *dry* conditions (**Figure 3-6**).

Soil strength, quantified by CI averaged at 1.82±0.02 MPa on German study sites, and 2.02±0.03 MPa on Finnish ones. In Poland, higher values of CI were measured, averaging at 2.24±0.05 MPa (**Figure 3-6**B). A threshold of 1 MPa was set for CI, with values below this threshold assumed to represent highly traffic-sensitive soils. The proportion of such occurrences did not differ from the frequency of **wet** measurements (p=0.212, unequal variance t-test).

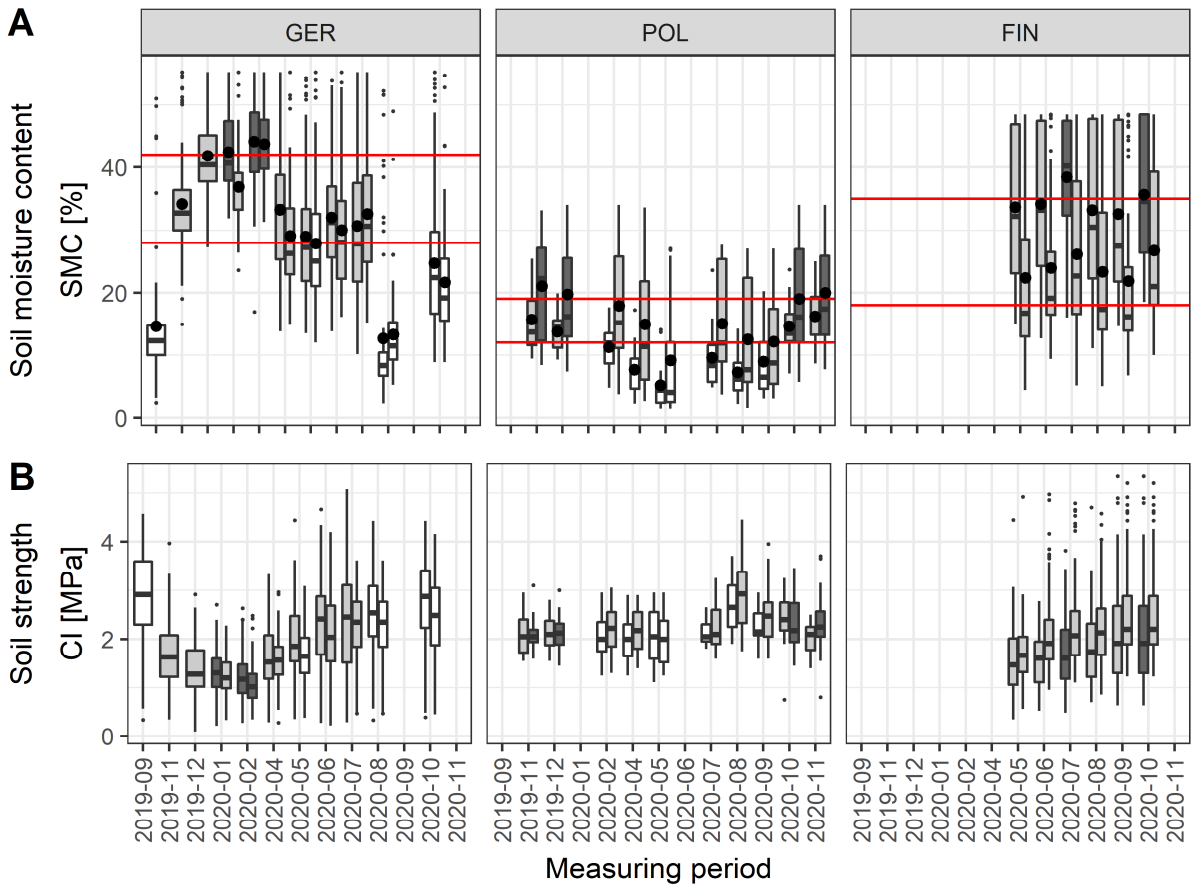

Figure 3-6. Monthly repeated measurements of (A) volumetric soil moisture content and (B) soil strength in three countries, grouped by the study site. Defined thresholds (horizontal lines) were applied on mean values of soil moisture (large points) to assign each group to overall moisture conditions (i.e., *dry* - white, *moist* - light grey and *wet* - dark grey, **Figure 3-4**).

Including all data, a response between CI and SMC could be observed ($p<0.001$), with significant interactions between SMC and Country as well as condition, indicating site- and season-specific patterns.

Table 3-4. Type-III ANOVA for the linear model, fitted to values of soil strength (MPa).

	Sum of Squares	Df	F value	Pr(>F)
(Intercept)	1349	1	2257	0
SMC	91	1	152	<0.001
country	96	2	80	<0.001
condition	1.9	2	1.5	0.213
SMC:country	136	2	114	<0.001
SMC:condition	5.4	2	4.5	0.011
Residuals	1726	2887	-	-

3.3.2. *Depth-to-water and soil moisture*

Overall, DTW detected 47% of the covered area across all study sites as sensitive for soil disturbances, classified when $DTW_{1.00}$ was less than 1 m (**Table 3-5**).

Table 3-5. The table shows an overview of the average terrain slope, the partial area with a depth-to-water index between 0 m and 1 m (calculated with different flow initiation areas) compared to total area of the study sites. In each country, two sites, each 1000 ha in size, were analysed.

		partial area with DTW less than 1 m [%]		
Country	Terrain slope [%]	$DTW_{4.00}$	$DTW_{1.00}$	$DTW_{0.25}$
FIN	4.7±6.5	40.4	58.9	77.6
GER	15.5±15.1	10.7	19.9	37.9
POL	1.8±1.9	35.9	62.3	88.8

These areas predicted to be wet or water saturated are derived from a stream network, with low DTW values nearby. When overall moisture condition is classified as *wet*, all three transects cross areas with DTW<1 m (**Figure 3-3**), whereas under *dry* conditions, only the transect '4.00' crosses an area predicted to be **wet**. This resulted in the behaviour shown in **Figure 3-7**.

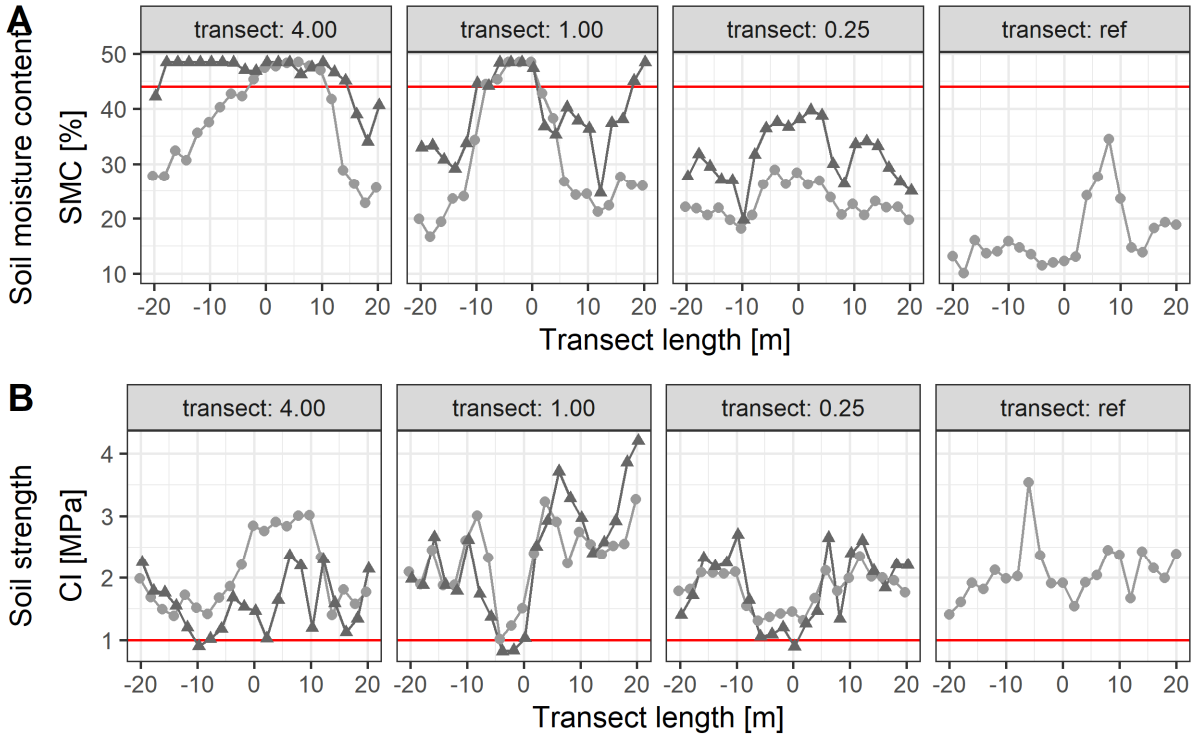

Figure 3-7. Values of (A) soil moisture and (B) soil strength along transects, perpendicularly positioned on flow lines (transect length=0) derived from the depth-to-water concept. The examples show data from Finnish study sites, where **wet** soil with low soil strength occurred in proximity to the flow line, during *moist* (filled circle) and *wet* (triangle) conditions on the transect '1.00'. Horizontal lines indicate set thresholds to assess **wet** (**Figure 3-4**) or sensitive soils.

Subsequently, **wet** values should predominantly occur in areas with DTW_{FIA}<1 m. In fact, up to 100% (Figure 7) of **wet** values were measured within a DTW range between 0 and 1 m on the Polish study sites, under given *moist* or *wet* conditions. Similar to the results revealed in Poland, high shares of **wet** values could be associated with low DTW indices in Finland, too. There, 88% of **wet** values were measured at $DTW_{1.00}$<1 m or $DTW_{0.25}$<1 m, when soils were *moist* or *wet*, respectively.

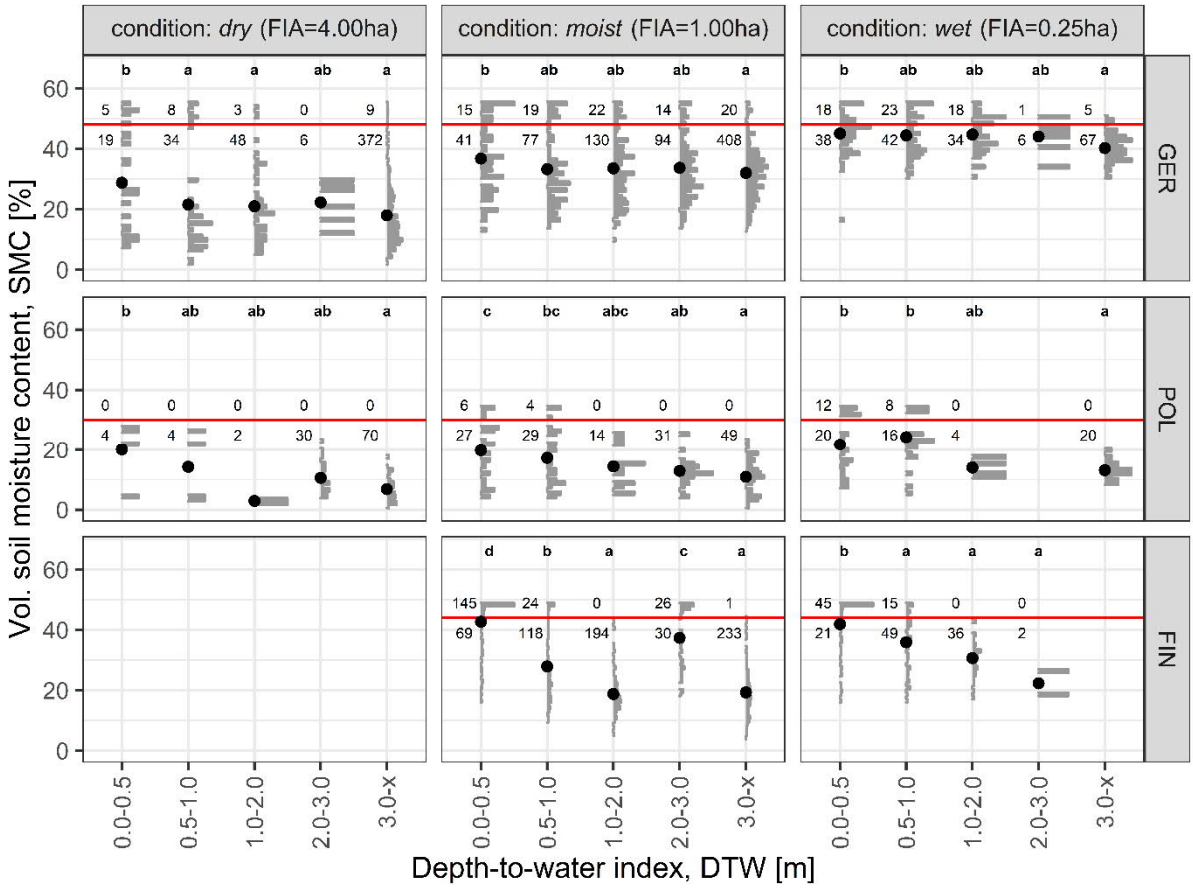

Figure 3-8. Values of soil moisture content (SMC) in respect to related depth-to-water (DTW) maps, calculated with different flow initiation areas (FIA), to represent classes of overall soil moisture condition (**Figure 3-4**). Density of SMC for levels of DTW is shown by histograms. From that, number of SMC-measurements indicating water saturation (**Figure 3-4**) are labelled above the horizontal line. The number of remaining values is given below this line. Mean values are given by points - significant differences between group means are shown by letters according to a Tukey post-hoc test.

3.3.3. *Prediction of soil moisture and strength*

The fact that the extent of areas with DTW<1 m increases with decreasing FIA or rather *wet* (or *moist*) conditions (**Table 3-5**) is considered when accuracy (ACC) and Matthews correlation coefficient (MCC) is used to assess the performance of DTW. Overall, ACC for SMC-predictions via DTW_{FIA} averaged at 72%, with corresponding mean MCC of 0.31. When in-situ measurements are related to DTW maps, calculated with FIA set fixed, different assessments of performance were made (**Figure 3-9**), with averages of ACC for each DTW scenario between 51% and 82% and MCC between 0.25 and 0.38. For example, when SMC was predicted by $DTW_{4.00}$ maps, best performance was reached on the study sites "Obereimer" in Germany and "South" in Poland, regardless of the prevalent moisture condition. On the Finnish study site "Eno", FIA of 1.00 ha led to successful prediction of SMC, with MCC of 0.58 and corresponding ACC of 80% under *wet* conditions. During *moist* conditions on the same site, highest values of performance were retrieved when SMC was compared to $DTW_{1.00}$ too, with 0.51 MCC and 77% ACC.

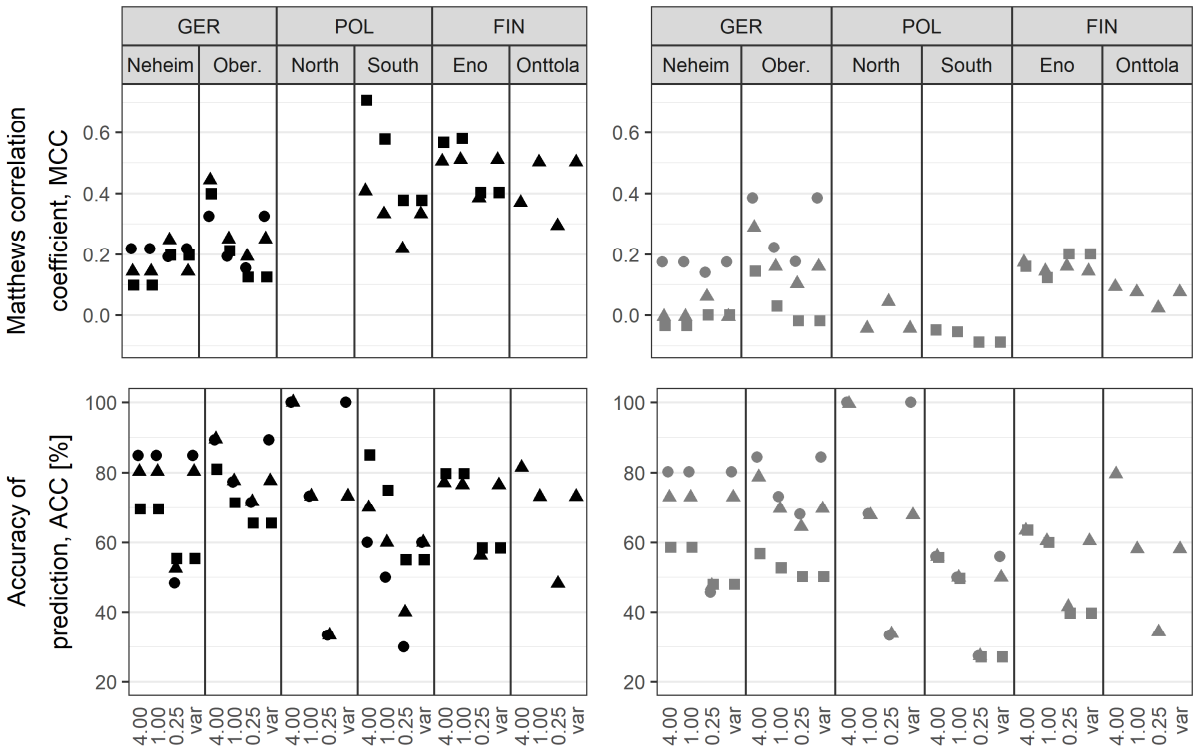

Figure 3-9. Accuracy of prediction, when in-situ measurements were related to scenarios of depth-to-water maps, created with static flow initiation areas (FIA) (x-labels), or when FIA was variable according to current conditions ('var', **Figure 3-4**). Black symbols represent binary values of soil moisture content [%], grey symbols represent binary values of soil strength [MPa] (conditions: *wet* – square, *moist* – triangle, *dry* – point).

Improvement of MCC or ACC due to the condition-specific adjustment of FIA could not be observed (**Figure 3-9**), neither for predictions of SMC (p=0.327, p=1, respectively) nor CI (p=0.603 and p=1, respectively).

3.4. Discussion

The generally close agreement between the occurrence of **wet** soils within areas of a low DTW index (**Figure 3-8**) confirms the main assumption of the concept, stating that water moves gravimetrically, following the flow directions as determined by topographic geometry. The consequent accumulation of water across a landscape leads to areas with a high probability for water saturation. In line with this assumption, peaks of MCC for predictions of **wet** soils were between 0.71 and 0.58, with corresponding ACC between 85% and 75%, respectively (**Figure 3-9**). DTW can be assumed to clearly predict the soil wetness (Ågren et al., 2014). Across the studied countries, ACC averaged at 82% (MCC=0.38) when dummy-transformed SMC values were compared to the binary values of $DTW_{4.00}$. These results are in line with earlier findings: Ågren et al. (2014) revealed an accuracy between 72% and 92% with varying FIA between 0.5 ha and 16 ha. In another Swedish case study, Lidberg et al. (2020) revealed an accuracy of 73%. In agreement, the position of existing wet areas has already been delineated by DTW-maps successfully (Murphy et al., 2011). Remote analysis of Murphy et al. (2007) showed, that discrete wetland areas on Canadian study sites were properly reflected by DTW maps in 51%-67% of cases, improving the knowledge of spatial distributions of such at given forest sites.

However, DTW-related predictions of wet soils are not necessarily successful, as reported in **Chapter 2** where SMC was measured on random positions across two forest sites, but could not be related to DTW

indices significantly. In addition, the same authors (2020) showed that soil strength (CI) did not respond to values of DTW. Also, findings from the Krycklan catchment make a response between CI and DTW look questionable (Ågren et al., 2015).

Site-effects show high influence on the accuracy of DTW-derived predictions of (Mohtashami et al., 2017). Characteristics of soil and bedrock can compromise water accumulation, which is the primary factor simulated by DTW maps. Consequently, the shallow Podzol and Histosol on the Finnish study sites should lead to accurate predictions of **wet** soils since a high share of lateral water movement would occur in the upmost layers there (Bishop et al., 2011). Accordingly, the Finnish data demonstrates relatively successful predictions of binary values of SMC by DTW maps, with ACC between 81% and 71% ($DTW_{1.00}$) and corresponding MCC of 0.23 and 0.35, respectively. With respect to effective water runoff predictions in uppermost soil compartments, the well-drained sandy soils on Polish sites should possess least overlap between **wet** soils and DTW<1 m, as water would drain quickly into deeper horizons there (Singh et al., 2020). However, performance values for the prediction of dummy-transformed SMC were similar as compared to observations made on Finnish data. Although ACC in a comparable range was determined on German sites (47% - 89%, $DTW_{1.00}$), MCC, the more meaningful parameter for predictions (Powers, 2011), was lower there (average: 0.18±0.11, **Figure 3-9**). Deep Cambisols with higher water storage capacity could lead to a less linear flow accumulation of precipitation across the landscape. In addition, lower permeability due to the high clay content on German sites should promote the usage of a small FIA. Nevertheless, our findings did not support this assumption in the conducted field trials. On the Cambisols with high clay-content, the largest FIA surveyed (4.00 ha) showed to lead to highest MCC and ACC, at least at the steep site “Obereimer”. In contrast, at the second German site “Neheim”, a small FIA of 0.25 ha led to best performance during *wet* conditions.

Instead of representing site-conditions, the FIA-derived scenarios of DTW maps were designed to simulate changing overall moisture conditions (White et al., 2012). Yet, we were not able to confirm this idea with the given data. As can be seen in **Figure 3-9**, the season-adjusted DTW did neither improve ACC nor MCC. Most likely, the non-linear behaviour of water runoff, in regard to spatial shifts, hydraulic conductivity with soil depth and water storage (Leach et al., 2017) inhibits the intended season- or condition-adjusted prediction of **wet** soils and low CI through DTW maps. The spatial variability in subsurface permeability and hydrological conditions may work against the seasonal emulation of water runoff and accumulation across sites (Ågren et al., 2015; Leach et al., 2017). The real accumulation of water runoff oscillates in accordance with climate, site characteristics and soil properties, making it hard to find a site- and season specific FIA (White et al., 2012; Ågren et al., 2014; Ågren et al., 2015; Leach et al., 2017; Lidberg et al., 2020).

In addition to the disregard of soil-related hydrological conditions, also crucial factors like root network, available slash, stoniness, stumps and at the end soil strength of areas of interest are not considered in DTW maps but are vital for soil trafficability (Suvinen et al., 2009; Vega-Nieva et al., 2009; Ågren et al., 2014; Ågren et al., 2015). Remote sensing techniques offer a way to estimate information about soil properties (Coleman et al., 1993; Dobos et al., 2001) and moisture (Hu et al., 1997). Additionally, vegetation analysis (Ustin and Gamon, 2010; Fassnacht et al., 2016) can be performed using air- or space-borne approaches. These data might allow for an evidence-based estimation of a more accurate FIA in advance of a DTW-based trafficability assessment and support the prediction of **wet** soils with low strength.

Recent investigations have shown, that machine learning algorithms can successfully be used in the field of digital soil mapping (Baltensweiler et al., 2021) and soil moisture mapping (Ågren et al., 2021). We state, that enhanced computational methods can be deployed for trafficability predictions. An adequate

consideration of site effects (Heung et al., 2016), non-linear hydrological processes (Melander et al., 2020) and weather data (Mattila and Tokola, 2019) could facilitate improved predictive accuracy. Moreover, several variables can be fused with basic DTW predictions by machine learners, including remotely sensed soil moisture conditions (e.g. Reichle et al., 2020a), as conceived in **Chapter 5**.

An appropriate prediction of soil strength and trafficability would enhance sustainable forest management and in turn cost-efficient and environmentally sound harvesting operations (Murphy et al., 2007; Vega-Nieva et al., 2009; White et al., 2012; Mohtashami et al., 2017; Mattila and Tokola, 2019; Picchio et al., 2020; Uusitalo et al., 2020). The DTW concept entails low demands of input data and is numerically robust, allowing for a calculation using DEMs with different resolutions (ideally lower than 5 m). Although rutting per se is possibly not avoidable by the application of DTW maps (Mohtashami et al., 2017; **Chapter 2**), the usage could support harvesting operations through better guidance of machine operators through forest sites, as practical use of DTW-maps has been witnessed, for example in Canada and Sweden. By this, sensitive areas can be effectively avoided or reinforced with brush mats and so can the thereby caused deleterious sediment transport in sensitive areas and perennial streams (White et al., 2012; Ågren et al., 2015; Kuglerová et al., 2017; Lidberg et al., 2020).

3.5. Conclusions

The field trials conducted at various sites across Europe revealed strong temporal variations of SMC, which can be associated with soil strength. During a period of relatively low precipitation, it was possible to correctly predict a high share of wet soils occurring by DTW maps which represented overall dry conditions, especially on sites in Finland and Poland. The prevailingly sandy soil texture at these sites might contribute to a topography-derived and geometric flow accumulation. On the contrary, on German study sites, only 35% of wet soils matched with the predictions made, considering $DTW_{4.00}$ maps (**Figure 3-8**). As compared to predictions of soil moisture, the prediction of soil strength showed to be less accurate. Although overall accuracy reached 76% when binary values of soil strength were compared to $DTW_{4.00}$ maps, 66% of low values occurred on measuring points possessing a $DTW_{4.00}$ index greater than 1 m. We state, that present site effects, such as soil characteristics led to non-linear water accumulation and peculiar spatial variations of soil moisture and strength. The choice of an individual map-scenario enabled accuracy improvements for given sites. Still, the intended representation of moisture conditions by DTW scenarios could not be proven by the data from the conducted time-series. Therefore, no general rules could be formulated in terms of which FIA would result in best site- and condition-specific DTW performance. Current research already addresses this issue and aims in a clear direction – machine learning. Improved supervised learning algorithms may merge spatial with temporal information, cope with non-linear dynamics of a soil state, and support the creation of more accurate trafficability maps in return.

Declaration of Competing Interest

The authors declare no conflict of interest.

Acknowledgements

We acknowledge the valuable suggestions of the three anonymous reviewers, who contributed to the improvement of the paper.

Funding: This work was supported by the Bio Based Industries Joint Undertaking under the European Union's Horizon 2020 research and innovation program, TECH4EFFECT Knowledge and Technologies for Effective Wood Procurement—project, [grant number 720757]; by the cooperation project "BefahrGut" funded by the State of North Rhine-Westphalia, Germany, through its Forest Education

Centre FBZ/State Enterprise Forestry and Timber NRW, Arnsberg/Germany; and by the Eva Mayr-Stihl Stiftung. The APC was funded by the Open Access Publication Funds of the University of Göttingen.

4. Review: Status of trafficability prediction in European forestry

This chapter was accepted for publication in Current Forestry Reports (Springer Journals), on 3rd of December 2021. The original title is: "Trafficability prediction using depth-to-water maps: The status of application in northern and central European forestry". This chapter is currently in print.

Full author list: Stephan Hoffmann[1,2,*], Marian Schönauer[2], Joachim Heppelmann[1], Bruce Talbot[1], Antti Asikainen[3], Emmanuel Cacot[4], Benno Eberhard[5], Hubert Hasenauer[5], Janis Ivanovs[6], Dirk Jaeger[2], Andis Lazdins[6], Sima Mohtashami[7], Tadeusz Moskalik[8], Tomas Nordfjell[9], Krzysztof Stereńczak[10], Jori Uusitalo[11], Morgan Vuillermoz[12], Rasmus Astrup[1]
* Corresponding author

[1] Norwegian Institute of Bioeconomy Research (NIBIO), Ås, Norway

[2] University of Göttingen, Department for Forest Work Science and Engineering, Göttingen, Germany

[3] Natural Resource Institute of Finland (Luke), Helsinki, Finland

[4] Forestry Cooperative UNISYLVA, Limoges, France

[5] University of Natural Resources and Life Sciences (BOKU), Vienna, Austria

[6] Latvian State Forest Research Institute (Silava), Salaspils, Latvia

[7] The forestry research institute of Sweden (Skogforsk), Uppsala, Sweden

[8] Warsaw University of Life Sciences (SGGW), Department of Forest Utilization, Warsaw, Poland

[9] Swedish University of Agricultural Sciences (SLU), Department of Forest Biomaterials and Technology, Umeå, Sweden

[10] Forest Research Institute, Sękocin Stary, Poland

[11] University of Helsinki, Department of Forest Sciences, Helsinki, Finland

[12] Technological Institute (FCBA), Champs-sur-Marne, France

My contributions: Contribution to the development of the review's design and structure; Significant contribution to the literature compilation, review and analysis; Drafting of technical sections of DTW concept; Country reviews Austria and Germany; Significant contribution to the overall writing of the manuscript (contributions stated in accordance with Stephan Hoffmann).

Abstract

Purpose of review: Ground-based logging operations with harvesters and forwarders represent the most applied forestry equipment in Europe but are well-known to potentially cause soil impacts through various forms of soil disturbances, especially on wet soils with low bearing capacity. In times of changing climate, with shorter periods of frozen soils, heavy rain falls events in spring and autumn and frequent needs for salvage logging, forestry stakeholders face increasingly unfavourable conditions to conduct low-impact operations. Thus, more than ever, planning tools such as trafficability maps are required to ensure efficient forest operations at reduced environmental impact. This paper aims to describe the status quo of existence and implementation of such tools applied in forest operations across Europe. In addition, focus is given to the availability and accessibility of data relevant for such predictions. *Recent findings:* A commonly identified method to support the planning and execution of machine-based operations is given by the prediction of areas with low bearing capacity due to wet soil conditions. Both, the topographic wetness index (TWI) and the depth-to-water concept (DTW) are used to identify wet areas and to produce trafficability maps, based on spatial information. *Summary:* The required in-put data is commonly available among governmental institutions, and in some countries already further processed to have topography-derived trafficability maps and respective enabling technologies at hand. Particularly the Nordic countries are ahead within this process and currently pave the way to further transfer static trafficability maps into dynamic ones, including additional site-specific information received from detailed forest inventories. Yet, it is hoped that a broader adoption of these information by forest managers throughout Europe will take place to enhance sustainable forest operations.

Keywords: depth-to-water, remote sensing, digital terrain models, European forestry, precision forestry, trafficability prediction

4.1. Introduction

In central and northern European countries, ground-based harvesting equipment accounts for the vast majority of commercially supplied roundwood. These predominantly cut-to-length operations are usually performed by harvester-forwarder systems unavoidably impacting the soil-ecosystems due to high machine and payload weight transported over sensitive forest grounds (Cambi et al., 2015). Such impacts occur in various forms and include soil deformations such as ruts (Horn et al., 2007; Agherkakli et al., 2010), or soil compaction, which increases bulk density due to a decreasing pore space (Ampoorter et al., 2009; Gerasimov and Katarov, 2010), restricting the permeability of the soil (Labelle and Jaeger, 2011). The occurring degree of damage is a function of the traffic experienced, site conditions such as soil type, climate variables, and machine-operator skills (Cambi et al., 2015; Crawford et al., 2021).

Historically, the primary timber logging season was scheduled for the winter periods when the soils are frozen (Mattila and Tokola, 2019; Uusitalo et al., 2020), making them relatively resilient to impacts due to their increased bearing strength (Šušnjar et al., 2006). Yet, the high ownership costs of modern logging equipment and involving supply chains require these machines to work year-round with the capability to increase their loads for cost reduction in an increasingly complex business environment with global competition (Gabbert et al., 2020). Moreover, time periods of favourable operational conditions, in terms of frozen and thus stable soils, are getting shorter and less frequent (Max-Planck-Institute for Meteorology, 2009; Gerasimov and Katarov, 2010). On the other hand, periods of freeze and thaw cycles with wet or even water saturated soil conditions, are likely to be extended, resulting in vulnerable soils with restricted trafficability (Uusitalo et al., 2015). This leads to a more significant potential for lasting site damages caused by heavy machinery in the form of soil rutting or compaction (Rab, 2004), challenging sustainable forestry in large parts of Europe.

The occurrence of severe soil impacts can be associated with several negative effects, including both economic and ecological aspects. For instance, more machine power is required when machines are driving on soft grounds, resulting in increased fuel consumption, machine wear and technical failures (Ala-Ilomäki et al., 2020; Melander et al., 2020). Moreover, ongoing operations need to be stopped if the occurring rut depth exceeds degrees or extents defined in contracts made between entrepreneurs and forest owners, resulting in high costs due to machine relocations and downtime.

In addition to economic drawbacks, various traffic-induced environmental consequences are of concern. The compaction of soil in a continuous linear pattern, such as a wheel track, restricts the soil's permeability and alters hydrological conditions (Startsev and McNabb, 2009). On steeper slopes, ruts can result in channelling with increasing erosional energy, fortifying the loss of valuable topsoil (Startsev and McNabb, 2000). When exceeding a specific soil bulk density, negative effects on plant available water (Arvidsson et al., 2003) and plant growth (Mariotti et al., 2020; DeArmond et al., 2021) can occur. Moreover, mechanized systems can cause logging wounds on trees, where pathological agents may enter (Sirén et al., 2013). Due to the reduced macropore volume and the altered hydrological conditions, negative effects on various soil faunal groups are reported in the review by Beylich et al. (Beylich et al., 2010), too. In addition, soil disturbance through rutting has also been suspected of mobilizing heavy metals, e.g. Methyl-Mercury, although the direct effect of soil disturbance alone has not been quantified (Ampoorter et al., 2010; Eklöf et al., 2014; Wit et al., 2014).

In consequence, it is critically noted that forestry machines have increased in total weight over the last decades (Nordfjell et al., 2010). However, the pressure exerted by heavy forwarders on the ground did not increase, as a result of likewise increased contact area between machine and soil (Nordfjell et al., 2019). Along with wider and optionally low inflatable tyres (Arvidsson and Keller, 2007), numerous technological solutions aim to mitigate traffic-induced site impact. Hereby, a focus is set on increasing

machine flotation, traction and contact area, as for example through bogie tracks (Labelle and Jaeger, 2019), long-tracked bogie axles (Edlund et al., 2013), triple-bogie axles (Starke et al., 2020), auxiliary axles (Fjeld and Østby-Berntsen, 2020), rubber-tracked bogie axles with support rollers (Engler et al., 2021), large radial tyres with alternative treads (Seixas and McDonald, 1997), the utilization of traction-assist winches (**Chapter 6**), brush mats (Labelle et al., 2015) and innovative steering concepts (Li and Kang, 2020).

However, an efficient utilization of technical soil prevention measures relies upon the information of soil-state in advance of scheduled operations. This enables the selection of adequate equipment and sites to be operated in, actual instructions for machine drivers, as well as a sufficient support during the off-road navigation in forest stands. The potential avoidance of areas and sites possessing a currently high vulnerability to machine impact implies the spatial prediction of risks to severe damages – both, among extensive off-road traffic during clear-cut operations, as common in Nordic countries, but also among single-selection silviculture systems commonly practiced in Central Europe, where machine traffic is often confined to permanent machine operation trails. There, next to the reduction of soil impacts in general, the technical functionality and consequent permanent accessibility into forest stands can be maintained if machine operators know which segments of a machine operating trail to avoid at a given time of operation. Thus, there is an increasing role for planning software solutions expected and demanded in harvesting preparations (Jones and Arp, 2017; Sirén et al., 2019b; Uusitalo et al., 2019).

A number of rut risk prediction tools has been developed in the last decades: A simplified model was suggested by O'Sullivan et al. (O'Sullivan et al., 1999), in which contact areas between soil and tires, soil type, initial bulk density and water content profiles are considered for the selection of an appropriately equipped machine. A similar approach was invented by Canillas and Salokhe (Canillas and Salokhe, 2002), who added external variables like travel speed, axle loads and number of passes to tire and soil variables, to develop a decision support system, providing recommendations for soil management practices on agricultural areas. Still, a regular application of such systems in day-to-day forestry operations is pending. It can be assumed that a reason for a lacking implementation of predictive systems into forest management can be found in the high demand of required input data, or time-intensive efforts for related in-field measurements (**Chapter 2**). Consequently, topical research emphasizes the utilization of openly accessible data, as for example shown by the work of Lidberg et al. (Lidberg et al., 2020), who generated wet area maps based on data from national inventories, fused with topographical information, including the topographic wetness index (TWI) and depth-to-water (DTW) maps. Salmivaara et al. (Salmivaara et al., 2020) developed an integrative tool to predict trafficability, using a spatial hydrological model, inventory data, a wide range of spatial information and data derived from the operating machine.

Such approaches profit vastly from open and cross-border availability of spatial data, as implemented through the European Community INSPIRE Directive (European Commission - Joint Research Centre, 2021b). There, 34 spatial data themes needed for environmental applications, such as elevation, are compiled and organized in a standardized infrastructure for sharing among public organizations, but also providing public access on a European scale, aiming towards an enhanced land-use policy-making across boundaries (European Commission - Joint Research Centre, 2021b).

The increasingly available ALS (Airborne Laser Scanning) derived digital terrain models (DTM) have been verified by the plethora of their various applications, both for practical and scientific purposes. Perhaps one of the most significant applications of ALS derived DTMs in forest operations has been in facilitating the mapping of areas of anticipated high moisture and therewith, potentially high vulnerability to soil damage by vehicle passes. The nowadays wide availability of high resolution DTMs (i.e. 0.5-2 m grid cell size) allows for precise application of spatial parameters useful to determine soil

trafficability sensitivity, such as the TWI developed by Beven and Kirkby (Beven and Kirkby, 1979). This index quantifies the influence of topography on hydrological processes based on slope and upstream contributing area. Researchers have evaluated TWI's successfulness in predicting the ground water table (Seibert et al., 1997), the effect of DTM resolution on its prediction (Sørensen and Seibert, 2007) and how it performs in comparison to a dynamic model (Grabs et al., 2009). There are several possible methods to calculate the contributing area, flow channels and slope out of a DTM for the TWI index, partly with local alterations.

The cartographic DTW concept, developed by Murphy et al. (Murphy et al., 2009; 2011), has proven to be powerful in the prediction of soil state across different landscapes (Vega-Nieva et al., 2009; Murphy et al., 2011). This concept was evaluated to be more independent from the scale of the DTM provided, as compared to other topography-derived algorithms, such as the TWI (Ågren et al., 2014). This allows for reliable results even when the calculations are based on input grid-cells of different resolutions. DTW uses flow lines derived from a DTM to calculate the anticipated vertical distance between any given cell of the DTM to a modelled water layer (Murphy et al., 2011). The resultant metric index can be used to estimate probabilities for a defined area to be water saturated or wet and to delineate perennial and intermittent flow lines (Ågren et al., 2015). Since the susceptibility of soils to deformations is deeply attributed to the soil moisture content (McNabb et al., 2001), maps created using the DTW concept are increasingly used to assess the risk of causing machine-traffic-induced rutting and compaction (Mohtashami et al., 2017; **Chapter 2**). Recent studies reveal a possible fusion of DTW maps with further data sources, including openly accessible spatial information and hydrological modelling, to be used for the prediction of forest soil's trafficability (Lidberg et al., 2020; Salmivaara et al., 2020) and improve the off-road navigation of forest machines (Willén and Hannson; Flisberg et al., 2021).

Once a DTW-map is created, it needs to be adopted by the forest industry and made available to operators to plan and guide their operations. Such a planning approach can be used for instance to identify and avoid potential wet areas, streams which are not visible due to a snow cover, or to optimize the delineation of a machine operating trail across forest stands. An integrated on-board navigation system in harvester and forwarders could then be used to identify and warn operators when approaching sensitive areas within a harvesting unit. Zimbelman and Keefe (Zimbelman and Keefe, 2018) demonstrated the use of geofencing tools to notify workers of high hazard zones in forestry activities. Similar activities could be developed that integrate the mapping of soft soils and actively inform the operator when they approach those areas. However, it would also require additional training to ensure that the operators can quickly implement this information to improve forest management's sustainability.

This paper aims to give an overview and synthesises the readiness-level for the implementation of national terrain simulations, applying the DTW concept. Relevant forestry countries in northern and central Europe have been selected to review the status of available terrain data derived from state-of-the-art airborne laser scanning (ALS) technologies - a fundamental prerequisite to produce DTW-maps. Further, already existing applications of the DTW concept or other means of spatial trafficability prediction to reduce the impact of ground-based logging systems are presented among the selected countries, too. Hence, this paper provides an assessment of the status and the potential integration of such tools to support sustainable forest management by improved operational planning and execution.

4.2. Literature review

Review articles are commonly based on the screening of scientific publications, identified through a search string of selected keywords in combination with Boolean operators applied to a publication data base such as the Web of Science. Although this review approach facilitates a logical identification of publications assigned to a specific topic, it also often leads to hundreds of selections which are not

relevant for the review's objective and need to be manually eliminated through a time-consuming initial examination of at least the title or the abstract.

This review on the DTW concept in the context of trafficability mapping, follows the snowball approach, where the bibliography of a known recent key publication on that topic is used as a starting point to identify further publications. Subsequently, selected publications were reviewed and those' bibliographies used to identify additional publications until no more new references of relevance appeared. This approach was selected since in contrast to a purely keyword focused data base search, the snowball system considers all relevant references, including non-peer reviewed early-stage research, as well as institutional and industry reports. Moreover, the authoring team consists of experts on the topic, being involved in the two multiyear EU projects TECH4EFFECT [grant number 720757] and EFFORTE [grant number 720712], which conducted intensive research in the field of trafficability prediction. Thus, additionally to the relevant state-of-the-art publications, latest findings from ongoing research and technical implementation on national level, could be incorporated into the review process through this rather open approach.

4.3. Conception of the depth-to-water concept

The general premise of the DTW concept is the simulation of water flow and accumulation across the landscape. The concept estimates flow directions between grid-cells and accumulates a hypothetical flow among cells. Thus, each grid cell's accumulated flow value is computed based on the size of the area, converging from the adjacent cells. The accumulated area size is then used to initiate a flowline, depending on a threshold set. This threshold of area size defines the flow initiation area (FIA, m²). For example, if the FIA was set to 2,500 m², an accumulated value of 2,500 m² was sufficient to start a flow line, which continues until leaving the area of interest. If a large FIA is used to initiate a simulated flow line, a low level of soil moisture is represented in return. Contrarily, a small FIA can be used to simulate very wet or sensitive soil conditions, as the network of flowlines expands.

The flowlines created in this way are added as a dichotomous value to the respective DTM. The combination of both flowlines and DTM can be used to compute the vertical difference between each grid cell and the nearest flow line – defining the DTW index. Therefore, a least cost function is applied to estimate the least slope gradients between the grid cells and the flow lines, minimizing equation (9):

$$DTW[\mathrm{m}] = \left[\sum \frac{dz_i}{dx_i}\, a\right] x_c \qquad (9)$$

Where $\frac{dz_i}{dx_i}$ is the slope between a cell i and adjacent cells, a is 1 in case of parallel drainage and $\sqrt{2}$ in case of diagonal drainage, and x_c is the grid cell size [m].

The DTW index can be interpreted as a relative measure of soil drainage condition, which approximates the tendency of a saturated landscape point. Cells with a small DTW value show a trend of surface water or water containing layers in the soil (Murphy et al., 2009). In return, high values of DTW are assumed to indicate dryer soils.

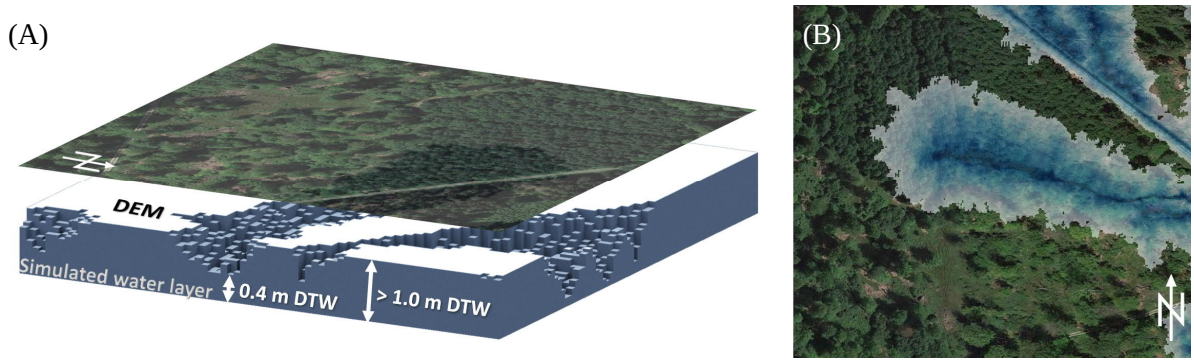

Figure 4-1. The depth-to-water index (DTW) indicates the vertical proximity to the nearest simulated water layer, which is based on flow lines or areas saturated by water. Particularly, this metric index is calculated for each cell of a digital terrain model (DTM). (A) Values less than 1 metre indicate wet areas with high susceptibility for soil deformations, whereas values greater than 1 metre should possess sufficient trafficability for heavy forest machines. (B) Thus, areas with a high risk for soil damage can be shown on maps, as indicated by the blue colouring.

4.4. Country overview and readiness for DTW

Countries are collecting spatial data from regional to national level, characterized by differences in survey technology, processing, and provision to users (**Table 4-1**). In consequence, this determines the DTW-readiness for operational purposes within a specific country. Therefore, a detailed overview of national ALS mapping campaigns and derived DTM accessibility shall be given for selected key forestry countries. Namely, the Nordic countries Finland, and Sweden were selected due to its dominating application of CTL-equipment, as well as a considerable share of sensitive operation sites such as peatlands. Norway, with its more mountainous landscapes completes the boreal forest biome of the Nordic countries. In Central Europe, Germany and France are representing diverse temperate forest regions of major timber producing countries, applying a wide range of silvicultural and operational systems. Austria, following similar forestry approaches, is included to represent the high mountain regions of Central Europe. East-Central Europe is represented by Poland as an important timber producer with vast forest areas shaped by continental climate conditions. Furthermore, Latvia was added to represent the specific Baltic conditions with seasonally waterlogged plains.

Next to the acquisition and provision of terrain data, the current availability or implementation of DTW-maps and non-DTW based trafficability prediction in the selected countries is surveyed within this review. Although forest operation driven soil impacts are occurring in Southern Europe too, this region has been excluded from the review since trafficability limitations related to soil moisture are commonly not of concern in the Mediterranean region.

Table 4-1. Overview of the availability and quality of digital terrain models in selected European countries.

Country	Grid cell size	Data acquisition	Year of national campaign	ALS resolution	Source	Costs
Austria	10 m	national ALS campaign	2013	4 pts/m²	www.data.gv.at	Open access
	1 m (0.5 m)	state-individual ALS campaigns	varying between states			
Finland	2 m	national ALS campaign	accomplished 2020	0.5 to 1 pts/m²	www.paituli.csc.fi	Open access
France	national ALS campaign under planning					
	25, 75 and 250 m	various sources according to regional acquisition approaches		not applicable		Open access down to 75 m, 25 m with costs
Germany	200 m	various sources according to regional acquisition approaches	update based on regional data provision	diverse	www.bkg.bund.de & www.geoportal.de	Open access
	5 m					Individualized licensing scheme
	1 m		varying between states			
Latvia	20 m	national ALS campaign	2013-2019	4 pts/m²	www.lgia.gov.lv	Open access
Norway	10 m (national level, locally higher)	national ALS campaign & regional orthophotos	updating campaign 2016-2022	min. 2 pts/m² (locally higher)	www.hoydedata.no	Open access
Poland	0.5 m (1 m)	national ALS campaign	since 2011-2014	4, 6 and 12 pts/m²	www.gugik.gov.pl	Open access
Sweden	2 m	national ALS campaign	2009-2016 (new campaign since 2018)	0.5-1 pts/m²	www.lantmateriet.se & www.geodata.se	Yearly subscription fee for research, education and non-commercial operation
	50 m	various sources according to regional acquisition approaches		not applicable		Open access

Finland: state of operational moisture driven trafficability modelling

Forest owners in Finland can estimate forest soil trafficability with two alternative methods; with the DTW maps or with the static trafficability maps developed by Arbonaut Oy.

The DTW maps are based on 2 m DTMs practically available for the whole country. Various stream networks are calculated by using 0.5 ha, 1 ha, 4 ha, and 10 ha threshold on the flow accumulation raster. The DTW is finally calculated based on these stream networks and slope with cost accumulation. The calculation has been executed per watershed. The calculation has been carried out by Luke and the maps are available in the national spatial data download service (www.paituli.csc.fi).

The static trafficability map presents the classification of forests in 6 different trafficability classes. The map product, developed by Arbonaut Oy, combines classic topographic DTW information to tree volume and soil type (peatland or mineral soil). The trafficability classes are based on seasonal changes

in bearing capacity of forest floor in Finland. The map provides information about the season when harvesting operations may take place with standard logging machinery (i.e. a harvester and a forwarder) without causing substantial damages on forest soil. The mapping unit is a pixel of 16 m size compatible with the forest resource information provided by the Finnish Forest Centre. Each pixel is classified in one of the following classes: 1. Operations possible in all seasons 2. Operations possible in summer, mineral soils 3. Operations possible in summer during dry season, mineral soils 4. Operations possible in summer, peatlands 5. Operations possible in summer during dry season, peatlands 6. Operations possible only during frost or thick layer of snow

The trafficability maps are available for the whole country. The data is distributed as open access data by The Finnish Forest Centre. The data can be accessed via a map application and a web map service WMS. Also, the raster maps can be downloaded from The Finnish Forest Centre's www-site (https://aineistot.metsaan.fi/avoinmetsatieto/Korjuukelpoisuus) as Tiff-files. In addition, forest owners can access the data in www.metsaan.fi service portal. Metsaan.fi is a service for forest owner to easily access the information of their own forest and to use digital forest services. The trafficability maps are today widely used in Finnish forestry by forest operation managers and forest machine operators.

Sweden: state of operational moisture driven trafficability modelling

The Swedish Mapping, Cadastral, and Land Registration Authority, Lantmäteriet, scanned the entire country with high-resolution ALS technology between 2009 and completed in 2016 to provide detailed terrain model required for climate change adaptation programs and other environmental programs. The scanning was performed from airplanes at an altitude of 1,700-2,300 and up to 3,500 m in the mountains), on areas of 25 × 50 km, and collect data in the form of point clouds. The point intensity in scanning varies between 0.5- 1 per m². It has an average error of 25 cm planar direction in the reference system SWEREF 99 TM and 5 cm in elevation in the reference system RH 2000. Using Triangular Irregular Network (TIN) interpolation, the point data is transformed to a 2-m elevation grid with a precision that is better than 10 cm in height and 30 cm in planar (Lantmäteriet, 2020). The dataset is available for a subscription fee but may be free for research and education pending an application. Elevation data, grid 50, is another terrain model available at the Swedish Mapping, Cadastral and Land Registration Authority. This model is built based on either the 1) national terrain model or 2) the elevation data bank (from 1980s) and are used in more general applications, e.g. height contours generations and correction of satellite images.

A new nationwide LiDAR campaign has just started in spring 2018, mainly to update the forest estimations, e.g. tree volume, height, average diameter, and biomass. The product will be prepared for areas of 2.5 × 2.5 km (Lantmäteriet, 2020).

Depth to Water (DTW) maps were prepared by the Swedish forest agency over the whole country since 2014 and were freely available through their online map services. The maps had been used by majority of forestry companies since about five years and contributed to improved planning of different forest operations.

A new version of soil moisture maps has been developed at the Swedish University of Agricultural Sciences (SLU) and is available at online map services of the Swedish forestry agency since beginning of 2021. Using Artificial Intelligence (AI) information from various (24) data layers, e.g. soil type, topography and climate, which are combined to estimate a moisture index representing a yearly average of soil moisture in raster layers of 2 × 2 m resolution (Lidberg et al., 2020).

Norway: state of operational moisture driven trafficability modelling

The Norwegian Mapping Authority (Kartverket), in conjunction with partner organizations, collects, systemises, processes, manages and disseminates national geographical information. In 2016, a national

program was started to generate a new detailed terrain model based on ALS, for areas with vegetation/forest cover, and image matching for mountain areas with little to no vegetation. The new terrain model is scheduled to be completed for the whole country (325,000 km²) by 2022. Private vendors were awarded project wise to conduct the scanning campaigns with a coverage of at least 2 pts/m², delivering classified point clouds to the Norwegian Mapping Authority. Classes vary between ALS-projects, but always include the class "ground points". In addition to the contracted deliveries, existing regional ALS data of higher quality, but also photogrammetric image matching for high mountain plateaus, is used by the Norwegian Mapping Authority to generate the latest national DTM. The density of the point cloud behind the updated national DTM can therefor regionally differ but is constantly updated if higher quality data is available. The latest data sets can be visualized with a variety of web map services at the portal "hoydedata.no". Both, the ALS point cloud data and a 1-meter resolution DTM can freely be downloaded. A second acquisition of a national ALS data set at a later point in time is not planned so far. The digital elevation data will be updated using photogrammetry based on aerial images that are acquired in regular intervals (5-10 years) (Kartverket, 2021).

Based on the DTM availability, two DTW-maps (Markfuktighetskart) presenting the soil moisture in a grid either as classes or in centimetre towards the soil surface and are openly available on national level (www.kilden.nibio.no). The DTW-maps are to varying degree used by foresters in the planning of forest operations in Norway. Further developments of the DTW-maps will include a dynamic approach for trafficability mapping that combines weather data and DTW maps to predict trafficability.

France: state of operational moisture driven trafficability modelling

At the end of 2020, plans for the initiation of the first national French ALS campaign, conducted by the National Institute of Geographic and Forest Information (IGN = public administrative establishment placed under the joint authority of the Ministries in charge of ecology and forestry) were announced. Although no starting date finalized so far, it is supposed to be implemented with countrywide coverage over a period of five years. Yet, sub-regions are identified as priorities for EU CAP monitoring purpose and are expected to be accomplished by 2023. The scanning campaign is envisaged to be conducted with a coverage of 10 pts/m², and the data will be used to produce DTMs and DSMs, after completion openly available through the national geo-portal (https://www.geoportail.gouv.fr/). Additionally, an initiative from the Ministry of Agriculture intends to update the spatial data on three-year intervals through 25 cm IR photography. But currently, the BD Alti, based on various regional data acquisition techniques is the only nationwide available DTM, with highest resolution of 25 m grids, only.

For forest soil trafficability assessment, a model developed for agriculture (SoilFlex; developed by Keller et al. (Keller et al., 2007)) was also tested on two French forest sites. The purpose of the model was to predict compaction risks and rutting from a set of accessible parameters to practitioners for either agriculture or forestry. Results were, for the most part, successful. The exception occurred for the inclusion of the surface organic layer. This organic layer includes a high organic carbon and moisture and a smaller deformation than predicted by the model (Goutal et al., 2013). During the last decade, experimental plots were instrumented and monitored to document hydric transfer phenomena and forest soil reaction after compaction. Such fundamental research has been limited to few plots established on state-owned forest (two sites in Lorraine region) or via the network F-ORE-T with two sites partially focused on and instrumented for these topics. Monitoring of experimental sites for the long-term productivity shows that after two of the routing cycles of a forwarder and the sensitive forest soils are quickly degraded, their restoration takes longer than seven years (Goutal-Pousse et al.). Moreover, active restoration following soil compaction is difficult.

Germany: state of operational moisture driven trafficability modelling

Owing to the federal organization in Germany, generation and provision of geo-data is administered at different regional scales. The 16 individually organized state surveying offices of Germany are responsible for their respective data acquisition, including ALS campaigns to create terrain models. Although the resultant DTMs possess a high variability in terms of technology used and updating, they are available in all states with a grid cell size of 1 m, since the completion of the state Saxony in 2020 (Arbeitsgemeinschaft der Vermessungsverwaltungen der Länder der Bundesrepublik Deutschland, 2021). Access and retail fees depend on individual policies, ranging from open data DTMs, as provided via a web coverage service for the area of North Rhine-Westphalia (Bezirksregierung Köln, 2020) to commercial products as available for the area of Lower Saxony (Landesamt für Geoinformationen und Landesvermessung Niedersachsen, 2020).

The Federal Agency for Cartography and Geodesy, BKG (Bundesamt für Kartographie and Geodäsie), in fulfilment of the Federal Geo-data Reference Act (BGeoRG), maintains geodetic reference systems and collects and provides data for utilization by other national authorities and to fulfil its international obligations (Bundesamt für Kartographie und Geodäsie, 2017). The BKG delineates and updates country wide DTMs as soon as new data is submitted by one of the 16 state surveying offices. The state-wide DTMs are merged to country wide DTMs with a grid cell size ranging from 5 m to 1,000 m. A country-wide DTM with a grid cell size of 200 m is openly accessible as part of the INSPIRE program (European Commission - Joint Research Centre, 2021b), same applies to the digital CORINE landcover map “LCL5”, providing land-use classification at 5 ha resolution. DTMs with a higher resolution, covering the whole area of Germany, are retailed as commercial products by the BKG. Among these, the “DGM5” (5 m grid cell size) has the highest resolution, with prices dependent on area size and type of utilization.

Despite of the availability of DTMs, trafficability of forest management units in Germany is currently rather statically, and non DTW-based evaluated, besides at a current regional research activity in North Rhine-Westphalia **Appendix III**. Terrain accessibility maps for 4 case study areas.. Site information and terrain slope classifications, in combination with the local forest manager’s experience on trafficability are a common way to select appropriate machine systems and schedule the most suited time of the forest operation. However, soil mapping has been conducted intensively in Germany, and digital soil maps are available, although highly varying between states. Based on such soil maps, regional solutions were developed to support the common practice for mechanized forest operations. For instance, the state forest enterprise of Lower Saxony introduced trafficability risk maps, consisting of four risk levels (Niedersächsische Landesforsten, 2017) and made available for forestry stakeholders through an internal online GIS (Geographic Information System). Another approach was developed to evaluate operational systems according to technical limitations by the site classification, and in addition to observed stand development phases and weather conditions during the scheduled harvesting period (Kuratorium für Waldarbeit und Forsttechnik e.V.). Going a step further, the State Office for Environment, Agriculture, and Geology in the state of Saxony (LFULG) already provides a digital map showing soil’s sensitivity to compaction at a scale of 1:50,000 (Feldwisch and Friedrich, 2016). It is based on the governmental digital soil map “digBK50”, interfaced with monthly climatic water balance values recorded from 1993 onwards, and allows to consider soil compaction sensitivity according to various soil features during the seasons for large area planning, such as agricultural or construction operations. Although this is one of the first attempts of a soil moisture driven trafficability modelling, the scale is too large to suit individual forestry operations.

Austria: state of operational moisture driven trafficability modelling
Based on the INSPIRE programme of the European Parliament (European Commission - Joint Research Centre, 2021b), and legally ratified through (BMDW, 2010), a DTM with a grid cell size of 10 m is openly accessible for the whole area of Austria. This DTM has been retrieved from the first cycle of scan flights by ALS, in 2013. Due to the country's federalism, the geospatial data are managed individually by the nine states. A second and third cycle was performed by each state independently. The data density for the first cycle, in general, was 4 pts/m², while the intended value for ongoing measurements was 8-16 pts/m².

Austria has an open geodata portal, operated by the governmental provider (Cooperation OGD Österreich, 2021). The availability of geospatial data varies between the states: For instance, in Upper Austria, all the data are made freely available by the state office and contain DTMs with a grid cell size of 0.5 m or 1 m for each municipality. A guidance for merging and processing the XYZ-tiles, using open tools, is provided too (Land Oberösterreich, 2021). In line with this data organization, several Austrian states openly provide DTMs with a grid cell size of 1 m. However, for the area of Burgenland, Tyrol, or Lower Austria, freely accessible DTMs show a lower grid cell size (5 m, or 10 m). For the area of Vorarlberg, contour lines are available only, either as a shapefile or rasterized.

Although the DTMs available for a large area of Austria are sufficient and the country declared a mandatory conservation of soils (Alpine convention, 1995, 1998), an implementation of machine-induced impacts through trafficability predictions is pending so far. Still, soil mappings and additional geospatial data for various topics such as forest, natural hazards, nature conservation, flood, and aerial images are offered partially.

Poland: state of operational moisture driven trafficability modelling
In Poland, the data covering now whole country and first large acquisition is from one ALS campaign completed between 2011-2014. It was completed to fulfil obligations imposed on EU countries by the Directive 2007/60/EC of the European Parliament and the Council on the Assessment and Management of Flood Risks (23 October 2007). To assess flood risk, the Polish Government decided to start the project entitled "IT System for the Country's Protection Against Extraordinary Threats" (in Polish: ISOK – "Informatyczny System Osłony Kraju przed nadzwyczajnymi zagrożeniami"). Under this project, 92% of the total area was covered with ALS data, and based on DTM generated from ALS data, the flood risk assessment was determined. Before this period, there were obtained ALS data just from single projects and covered relatively small areas. The area scanned under the ISOK project was 288,806 km², from which 267,403 km² was completed with density of 4 pts/m², 8,148 km² with 6 pts/m² - priority areas, and 13,769 km² with 12 pts/m² - cities (Wężyk, 2015). The derived DTMs are available with a grid cell size of 0.5 and 1 m. After 2014, new campaigns of ALS data acquisition were carried out and now almost whole Poland is covered at least with one ALS data set.

The authority which hosts the National data is the Department of Photogrammetry at the Geodesic and Cartographic Documentation Centre in Warsaw. All data are freely available for any purpose. But currently the data has not been used to implement a DTW or other spatial approach to predict forest trafficability. However, on a pilot site, DTW-maps have recently been applied for trafficability prediction on research level (**Appendix III**).

Latvia: state of operational moisture driven trafficability modelling
In Latvia, 50.1% of the territory is covered by forests; agricultural land is covering 22.8%, grasslands 15.9%, wetlands 6.2% and settlements 4.8% (Krumsteds et al., 2019). One-time coverage of ALS data is provided for the whole territory of the country and data collection has been organized by the Latvian Geospatial Information Agency (LGIA) by hiring foreign companies. ALS surveys were performed in

the period from 2013-2019. The Leica ALS70, Riegl LMS-Q680i and Riegl LMS-Q780i scanners were used for scanning. ALS scanning was performed on both the leaf-on and leaf-off periods. The total point density is at least 4 points per square meter, while the density of ground points is at least 1.5 points per square meter. The ALS point cloud is automatically classified by ground points, as well as low, medium, and high vegetation classes, but infrastructure and other objects are manually classified. The data is freely available on the LGIA website, as well as a generated DTM of 20 m resolution. Negotiations are underway for a second ALS campaign.

At the beginning of 2021, ALS data in Latvia were used to generate DTW maps nationwide in 5 m horizontal resolution and individual map sheets can be downloaded from the LSFRI Silava website (http://www.silava.lv/produkti/Kartografiskie-materiali.aspx). In parallel, work is underway to develop a wet area map for the entire country according to the methodology described by Ivanovs and Lupikis (Ivanovs and Lupikis, 2018). Wet area mapping uses various indices obtained by processing DTM, such as depression maps, normalized elevation index, slope, TWI, DTW and other indices. These maps are planned to be popularized in forestry industry seminars and put into practice in forest management planning.

4.5. Discussion

This review indicated that there is a potential to mitigate impacts from ground-based harvesting by improved planning aided by DTW-derived predictions of sensitive soil conditions. The review of the country-wise status of trafficability predictions illustrated that basic requirements for applications in forestry industry are expanding throughout northern and central Europe with the increasing availability of highly accurate ALS-derived DTMs (**Figure 4-2**A). However, it is merely in the Nordic countries that national DTW-maps are publicly available with close to national coverage (**Figure 4-2**B).

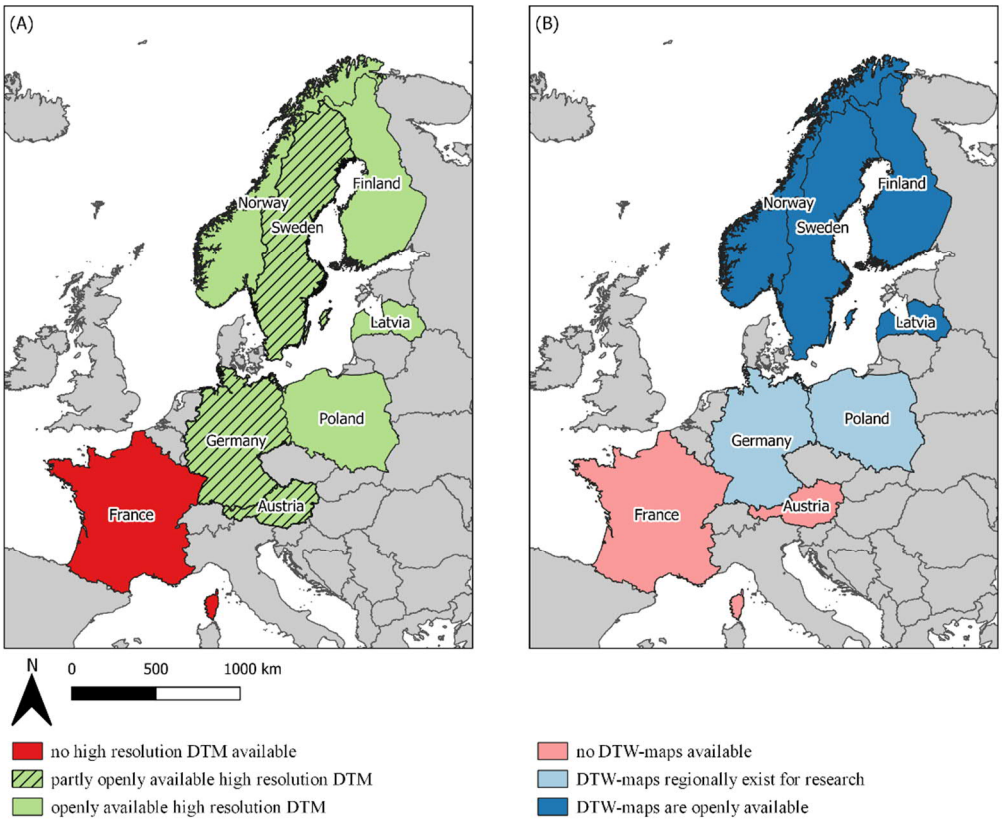

Figure 4-2. Availability and accessibility of (A) high resolution digital terrain models (DTM) and (B) depth-to-water (DTW) maps among the European countries included in the review about current state of trafficability prediction.

Since most European countries have initiated national ALS flight campaigns, country- or state-wide DTMs are available, enabling the creation of DTW maps for practical and scientific purposes. The creation of country wide DTW-maps has already been facilitated by specific public or private institutions in the Nordic countries such as Sweden, Norway, Finland, and Latvia. In order to actually enable the widespread use of high-resolution DTW-maps in forest operations, the maps will very likely have to be produced by a central organization as it seems unrealistic that small and medium sized individual organizations are able to execute the acquisition of openly available data or the commercial purchase of DTMs from governmental providers. The availability of DTMs ranges between openly accessible DTMs with a grid cell size of 0.5 m to complex hybrid business models requiring the purchase of DTMs with such a high spatial resolution. For instance, in the case of large areas of Austria and Germany, a fee is required for high resolution DTMs. There, only DTMs with a grid cell size of 5 m, 10 m or 200 m, respectively, are made openly accessible according to the INSPIRE programme (European Commission - Joint Research Centre, 2021b). Although the application of the DTW concept is generally robust to DTMs of different size (Ågren et al., 2014), but should not exceed 5-10 m resolutions, and ideally be even less than 5 m (**Chapter 3**). Thus, DTW modelling is technically also possible on DTMs with a low resolution of e.g., 200 m, but the resulting DTW map would not be practical for operational implementation to determine machine trafficability on a logging site (Ågren et al., 2014).

Generally, it can be stated that the availability and accessibility of high resolution DTMs is not a major limitation for the creation of DTW-maps anymore. All surveyed countries already provide DTMs with a sufficient resolution, or as in the case of France, are on the way to facilitate national ALS campaigns.

The more fundamental bottleneck might be the actual calculation of the DTW concept for the application of such maps as tools to increase soil conservation. Currently, DTW maps in most countries are produced by researchers and individual authorities (Ågren et al., 2014) for an intended user, who covers the costs, or possesses specific project funds. For a wide-spread practical application, supporting day-to-day forest operations, the maps should be generated on behalf of forestry stakeholders by dedicated experts, since entrepreneurs might not have the capability to create DTW maps. Although not solely DTW-based, the currently available static trafficability maps in Finland, are a good example how information about trafficability can be made openly accessible and support sustainable forest operations at small-scale (Kankare et al., 2019). Another big asset of the Finish maps is also the classification according to seasonal recommendations for the execution of operations (Kankare et al., 2019). Such a feature current DTW maps are generally lacking, since they just define an area as “wet” or “dry” (Lidberg et al., 2020), although attempts to further classifications into various wetness categories are in progress (Ågren et al., 2021). Therefore, it would be a worthwhile endeavour to governmentally provide comprehensive trafficability maps, covering European forests. In addition, the open accessibility to DTMs with a sufficient resolution as well as to remaining geospatial data would support and promote both practical applications and purposes, as confirmed by Melander et al. (2020).

Regardless of the origin of DTW-maps, an enhanced soil conservation through cartographic material requires a user specific interface. Modern forest machines are capable to read and display geospatial grids, such as DTW maps. Apart from that, the “TECH4EFFECT Mapping App” (Schönauer, 2019) is a good example following the open geo-spatial information philosophy, by providing such an interface through a no-cost Android OS mobile application. The app is conceived primarily as a visualisation tool for machine operators to be able to adopt their path of travel in accordance with the geo-referenced location and displayed DTW maps. Additionally, such apps usually allow for incorporating further spatial information about additional “no-go areas”, such as protected areas, with the option to prompt the user with a signal when approaching these.

Displaying DTW-maps by machine's on-board computers, integrated into mobile GIS applications, can provide the operator with site-specific information to choose the extraction route that combines consideration for both benefits for soil conservation and operational efficiency. The latest GNSS (Global Navigation Satellite System) receivers are standard features on state-of-the-art logging equipment, setting the basis for such an approach. Yet, precise machine positioning, as through RTK (real-time kinematic) support (Noordermeer et al., 2021), and in-field access to DTW-maps, which could be provided as web-map-service, require mobile networks with high data transmission standards, also in remote forest areas (Müller et al., 2019). But in many European regions the mobile network infrastructure does not meet these requirements yet (GSM Association, 2021). It is therefore the responsibility of the relevant government agencies of the individual countries to build-up the demanded standards. Until then, standalone applications, functioning in off-line modes, will be the focus of intermediate solutions (Müller et al., 2019).

Besides technical and administrative challenges, a full-range implementation of DTW-based trafficability maps would require a dynamic approach, accounting for seasonal variation of soil moisture (**Chapter 3**, Leach et al., 2017; Heiskanen et al., 2020). Research activities currently address this issue, for example by sequential combination of DTW-maps and additional, freely accessible weather data. This led to a recently conducted dynamic approach, integrating information about topography, soil and vegetation (Launiainen et al., 2019), used for trafficability prediction on pilot sites in Finland, creating suitable outputs with a grid cell size of 16 m (Salmivaara et al., 2020). Including real-time weather forecasts in the trafficability models would further enhance prediction quality at a dynamic level (**Chapter 3**, Leach et al., 2017; Heiskanen et al., 2020).

Further to dynamic information about moisture driven trafficability, operational information is required to optimize quasi-instantaneous planning, the actual most efficient routing of forestry equipment to ensure productive operations with minimal impact. The “BestWay” decision support system (Flisberg et al., 2021), shows on a case-study level in Sweden, how DTW-maps, in combination with further detailed information on operational site features, can be used for optimized routing. Detailed information on forest volume, its density and concentration, position of landings, areas for natural conservation, as well as known unavoidable crossings in the terrain, are used in complementing the DTW-maps. By this, the least cost extraction route with lowest expectable soil damage can be identified. Despite its promising results, evaluated under scientific settings, the “BestWay” system is too complex and processing capacity demanding for practical applications (Lidberg et al., 2020). However, principles of the “BestWay” decision system have been adapted to develop the more basic, but operational commercial planning tool “Timbertrail”, which is well acknowledged by first user experiences (Creative Optimization AB, 2021). This pinpoints on the relevance to further implement additional spatial and site-specific information to reach sufficient trafficability prediction systems.

Site-specific information, such as information derived from forest inventories or soil mapping, are commonly gathered by national institutions, but not always openly accessible for every forestry stakeholder. National forest inventories were initiated in Europe already a century ago, providing detailed information on the forest condition and other related parameters for decision support, collected through sample plots, but also remote sensing approaches, continuously improving on the fine resolution of this data (Breidenbach et al., 2021). In addition, soil mapping on national level has a long tradition in Europe too, and initiatives are in place to merge national attempts to a digital and thematic soil map database – yet this is a long-term process, and the resulting spatial information will only be available at a coarse resolution (Kristensen et al., 2019). The accessibility to various geospatial data gathered by national authorities and consequently the ability to integrate such data in topical trafficability predictions should be improved by open access data bases.

Current research demonstrated already, how openly available geospatial and temporal data can be used to improve predictions of soil moisture and trafficability. Recent findings of Schönauer et al. (**Chapter 5**) showed a method how information of different origins and spatial resolutions was fused, in order to achieve a spatiotemporal prediction of soil moisture on different forest sites in Europe. Moreover, spatial predictive systems can be merged with operation-specific information, captured in real-time through forestry machine-based sensors itself (Lidberg et al., 2020; Melander et al., 2020; Salmivaara et al., 2020). Fully mechanized harvesting operations are eminently suitable for such an approach, since the forwarder extraction is invariably consecutive to the harvester traffic, allowing forwarder routing to be adapted based on the previously captured data. The international forest machine standard StanForD, compiles operational data for various components of forest machines and can be used to determine the felled and loaded timber on each machine; thus, the pile volumes can be constantly updated as well as the gross weight of the vehicle. In addition, the CAN-bus (Controller Area Network) system captures data from the engine and drive train, which are valuable for trafficability purposes, too. As soon as telecommunication infrastructure will allow for improvements of accurate RTK supported positional data from the GNSS, wheel slip can potentially be computed (Suvinen and Saarilahti, 2006), based on machine internal CAN-bus recordings (Ala-Ilomäki et al., 2020). The CAN-bus data therefore can contribute to computationally producing a mobility map for optimal routing of the forwarder, as rut formation after a harvester pass has been a good predictor of the rut formation in forwarding, both on mineral and on peatland soils (Sirén et al., 2019b; Sirén et al., 2019a). In addition, forest machine-mounted LiDAR (Light Detecting and Ranging) proved to be able to measure rut development during forwarder operations and can be used as another potential component to be integrated in an active routing system of a forwarder (Salmivaara et al., 2018; Melander et al., 2020).

With GIS expertise nowadays in place in forestry institutional and corporate settings, and the DTW concept available through open access data repositories (**Appendix IV**), the corresponding maps can be easily created for regional applications, as long as access to a sufficient DTM is granted. Thus, the required economic resources, can be considered as moderate in comparison to the benefits of improved operational planning and increased efficiency during timber harvesting. Moreover, since static DTW-maps once created can easily be used on mobile devices or standard forest machine map interfaces, no further running costs can be expected. Although further improvements towards a dynamic approach with further input requirements could demand services and system infrastructure which add to costs of using such systems but should also be weight against the multiple environmental benefits associated to higher consideration of soil conservation. Further, it is also worth mentioning that DTW-maps can support multiple other application areas in forestry. DTW-maps were reported as being promising tools in enhancing water protection through a better spatial knowledge of perennial and intermittent streams, an important asset for the implementation of riparian buffer zones as best management practice among sustainable forest operations (Picchio et al., 2021). Even in winter months, when the surface was covered by snow, and streams were invisible such maps helped to avoid machine passes in these sensitive areas (Kuglerová et al., 2014; Ågren et al., 2015). Further, Bartels et al. (2018) used DTW-maps to relate bryophyte assemblages to wet forest areas, indicating the potential use of the concept to select between harvest areas and sites relevant for biodiversity conservation within a landscape management approach. In addition, DTW-maps were recently used to monitor site indices. A variation in productivity was adequately portrayed in a survey by Bjelanovic et al. (2018), who reported a potential application to model forest growth and yield. Finally, a combination of DTW-maps with data of annual precipitation was used to delineate drought-prone areas during periods of low moisture conditions (Kuglerová et al., 2014; Ågren et al., 2015).

4.6. Conclusions

DTW-maps are eligible to support forest management towards a mitigation of traffic-induced soil impacts, by identifying sensitive areas that should be avoided during mechanized operations. It is therefore supportive during the planning phase, but also during the execution of operations. The creation of practicable DTW maps relies on the availability of high resolution DTMs. Most of the European countries have programs to capture ALS data and produce high resolution DTMs with increasing data quality or are on the way to do so. However, the DTMs and other spatial information is not always openly available, or just in lower resolutions. In order to generate and apply DTW-based trafficability maps to aim for sustainable forest operations on a wider range, the already proceeding European open access policy for spatial data should be further intensified and be more consolidated across the continent. This should not only cover spatial terrain data, but also forest inventory, soil mapping, climatic conditions and other relevant information currently envisaged to further improve upon the potential of dynamic trafficability mapping and post-harvest impact monitoring. Furthermore, additional work is needed to integrate this information through consistent applications and interfaces to enable a full usage of such systems by forest planners and machine operators. Despite all that, DTW maps already found their way into forest operations and first attempts to make them dynamic are in place. The Nordic countries, in particular Sweden adopt a forerunner position, but the other reviewed countries initiate similar approaches, and it can be expected that in foreseeable time dynamic trafficability maps will become a standard tool to support sustainable forest operation practices.

Funding: This research was funded by the Bio Based Industries Joint Undertaking under the European Union's Horizon 2020 research and innovation program, TECH4EFFECT Knowledge and Technologies for Effective Wood Procurement - project, [grant number 720757], and EFFORTE Efficient forestry by precision planning and management for sustainable environment and cost-competitive bio-based

industry – project, [grant number 720712]. The contributions from the University of Göttingen were further financially supported by the Eva Mayr-Stihl Stiftung.

Declaration of Competing Interest: The authors declare no conflict of interest.

5. Spatio-temporal prediction of soil moisture

This chapter has been submitted to the International Journal of Applied Earth Observation and Geoinformation. The original title of the preprint is “Spatio-temporal prediction of soil moisture using soil maps, topographic indices and NASA Earthdata” (2021b). It is available at: https://doi.org/10.5281/zenodo.5691526

Full author list: Marian Schönauer [1,*], Robert Prinz [2], Kari Väätäinen [2], Rasmus Astrup [3], Dariusz Pszenny [4], Harri Lindeman [2], Dirk Jaeger [1]

* Corresponding author

[1] Department of Forest Work Science and Engineering, University of Göttingen, Göttingen, Germany

[2] Natural Resources Institute Finland (Luke), Helsinki, Finland

[3] Norwegian Institute of Bioeconomy Research (NIBIO), Ås, Norway

[4] Warsaw University of Life Sciences – SGGW, Warsaw, Poland

Author's contributions: Marian Schönauer: Conceptualization, Methodology, Formal analysis and Visualization, Investigation and Resources, Writing – Original Draft, Writing – Review and Editing. **Robert Prinz:** Investigation and Resources, Writing – Review and Editing. **Kari Väätäinen:** Investigation and Resources, Writing – Review and Editing. **Rasmus Astrup:** Writing – Review and Editing, Project administration, Funding acquisition. **Dariusz Pszenny:** Investigation and Resources. **Harri Lindeman:** Investigation and Resources. **Dirk Jaeger:** Writing – Review and Editing, Supervision, Project administration, Funding acquisition.

Abstract

Introduction. Milder winters and extended wetter periods in spring and autumn limit the amount of time available for carrying out ground-based forest operations on soils with satisfactory bearing capacity. Thus, damage to soil in form of compaction and displacement is reported to be becoming more widespread. The prediction of trafficability has become one of the most central issues in planning of mechanized harvesting operations. *Material and methods*. The work presented looks at methods to model field measured spatio-temporal variations of soil moisture content (SMC, [%vol]) – a crucial factor for soil strength and thus trafficability. We incorporated large-scaled maps of soil characteristics, high-resolution topographic information - depth-to-water (DTW) and topographic wetness index - and openly available temporal soil moisture retrievals provided by the NASA Soil Moisture Active Passive mission. Time-series measurements of SMC were captured at six study sites across Europe. This data was then used to develop linear models, a generalized additive model, and the machine learning algorithms Random Forest (RF) and eXtreme Gradient Boosting (XGB). The models were trained on a randomly selected 10% subset of the dataset. *Results*. Predictions of SMC made with RF and XGB attained the highest R^2 values of 0.49 and 0.51, respectively, calculated on the remaining 90% test set. This corresponds to a major increase in predictive performance, compared to basic DTW maps (R^2=0.02). Accordingly, the quality for predicting wet soils was increased by 49% when XGB was applied (Matthews correlation coefficient=0.45). *Conclusions*. We demonstrated how open access data can be used to clearly improve the prediction of SMC and enable adequate trafficability mappings. Spatio-temporal modelling could contribute to sustainable forest management.

Key words: trafficability prediction, forest operations, machine learning, precision forestry, eXtreme Gradient Boosting, Soil Moisture Active Passive

5.1. Introduction

Topography-derived modelling, based on digital elevation models presents a plethora of potential applications to the forestry industry. For example, Echiverri and Ellen Macdonald (2020) detected forest specific responses between species richness and a cartographic wetness index, Oltean et al. (2016a) delineated drought-prone areas through moisture modelling, while Jones and Arp (2019) demonstrated the relationship between predicted soil moisture and soil strength. Specifically, accurate information of soil strength is one of the most significant parameters in ground-based forest operations. Predictions of soil strength are subsequently sought by forest managers, motivated by practical needs to enable efficient and environmentally sound forest operations (Akumu et al., 2019).

The use of modern forest machines has facilitated major improvements in work safety and efficiency. To improve production efficiency, the weight of forest machines has steadily increased over the last decades (Nordfjell et al., 2019). To counter the increased weight, machine manufactures have improved machine designs with features such as additional axles, with improved tires and tracks that all reduce ground pressure (e.g. Bygdén et al., 2003; Ala-Ilomäki et al., 2021). Yet, forest operations are still frequently associated with severe soil impacts, particularly on sites with high soil moisture content. Since the bearing capacity of wet soils is often too low to withstand the forces exerted by forest machines, traffic can result in soil disturbance, such as displacement and compaction and the creation of deep ruts (Ampoorter et al., 2012; Poltorak et al., 2018). These physical impacts can initiate negative consequences for water and gas permeability, soil fauna and biota, tree regeneration and plant growth in general (Crawford et al., 2021).

Knowledge of time periods with best trafficability characteristics for a specific location is an important information criterion for efficient operational planning (Vega-Nieva et al., 2009; Mattila and Tokola, 2019; Picchio et al., 2020). Using detailed spatio-temporal information about soil moisture and soil trafficability allows for better planning of machine and work resources, to enable environmentally sound forest operations with less impact on the site. In return, this would improve machine productivity with less delays and well-informed production estimates along the supply chain for improved scheduling of subsequent logistical processes.

Topographic modelling of wet areas has been suggested as a potential solution to predict trafficability on forest sites (e.g. **Appendix III**). The depth-to-water (DTW) concept (Murphy et al., 2009) and the topographic wetness index (TWI, Sørensen et al., 2006) consider upstream contributing areas in order to calculate indices which allow for soil moisture estimates. Both indices were associated with soil moisture (Ågren et al., 2014; Lidberg et al., 2020). Whereas TWI reveals a unique map for all conditions, DTW can be used to create different map-scenarios, aiming towards a representation of overall moisture conditions on sites. However, the ability of DTW map-scenarios to represent moisture conditions was not confirmed in **Chapter 3**.

The literature highlights that temporal variations of soil moisture can be derived from a wide variety of approaches and data sources (Li et al., 2021). Launiainen et al. (2019) described a method, where the influence of topography, soil, and vegetation was considered to model water discharge of forest stands. Daily grids of soil moisture are provided for all of Germany (Samaniego et al., 2010), mainly with the focus of drought monitoring for agricultural purposes. The Soil Moisture Active Passive mission (SMAP, Reichle et al., 2020a), run by NASA-USDA, uses radar and radiometers to globally measure soil moisture, and makes the resultant three-hourly retrievals, with a spatial resolution of 9 by 9 km, openly accessible. Yet, neither remotely-sensed nor hydrologically modelled information of soil moisture has been merged with high-resolution topographic indices for predicting soil moisture on forest sites.

Machine learning (ML) algorithms have been repeatedly used for mapping soil properties such as soil carbon content (e.g. Keskin et al., 2019), digital soil mappings (Baltensweiler et al., 2021), or to create soil moisture maps (Ågren et al., 2021). Yet, ML approaches were commonly trained on a relatively large portion of data, and validated on a relatively small testing set. Challenges related to the successful implementation of ML for enhanced forest management lie in the limited data availability. Extensive efforts are needed for in-field measurements, which in-turn do not allow for predictive systems with high input data demands.

In this work we investigated the possibility of creating a model which incorporates high-resolution topographic indices, openly available soil parameters, and remotely sensed soil moisture retrievals in order to predict spatio-temporal variability of in-field measured soil moisture. In particular, we wanted to assess

- the possibility to achieve spatio-temporal modelling of soil moisture by merging spatial information with daily updated remote sensing products,
- the performance of selected ML algorithms, and
- the performance and adaptability (generalizability) of models, which were trained on only a few in-field measured observations, but were used to predict temporally varying soil moisture over large areas.

5.2. Material and methods

Soil moisture was measured in a time-series fashion on six different forest sites, merged with other data sources, and modelled using four statistical methods. The models were tuned by a cross-validation on an 80% partition of the data. Then, generalizability of the models was assessed by restricting the training to a 10% set, and validating the models on the remaining 90% test set.

5.2.1. *In-field measured soil moisture content (SMC)*

The response variable to be modelled, **SMC** [%vol], was measured with a capacitive soil moisture meter (HH-2 moisture meter, Delta-T Devices Ltd, England), on forest sites in Finland, Germany and Poland, along 23 measuring transects, with 21 measuring points per transect (see **Chapter 3** for site characteristics and the common measurement protocol). It was observed that the moisture measurements tended to overestimate **SMC** of relatively wet soils. Therefore, values above water saturation were cut off, and the texture-specific water saturation was assigned (see **Chapter 3** for details about soil sampling and definition of saturation). Measurements were repeated monthly, executing 6 field campaigns in Finland, 11 in Germany and 10 in Poland, between September 2019 and November 2020, resulting in 2,954 observations measured on 483 positions.

Since the susceptibility towards soil displacement increases considerably above a certain threshold of moisture (McNabb et al., 2001; Poltorak et al., 2018), values of **SMC** were also transformed into a binary variable, where texture-specific field capacity was considered to classify **wet** and **non-wet** values (see **Chapter 3** for details). The field capacity was defined at 1.9 pF matrix potential, resulting in **SMC**-thresholds of 35 %vol for data measured on Finnish study sites, 42 %vol on German sites and 19 %vol on Polish sites.

5.2.2. *Spatial and temporal predictor variables*

European Soil Database

The European Commission - Joint Research Centre (2004) provides a harmonized soil database for Europe (ESDB) at a scale of 1:1,000,000. Herein, maps of the main soil classification, following the World Reference Base (IUSS Working Group WRB, 2015), and several additional variables (see European Commission and the European Soil Bureau Network, 2004) were extracted at each measuring point and added as attributes (see **Appendix VII**).

Topographic indices

Two topographic indices were calculated for the study sites in each participating country, based on digital elevation models with high spatial resolution, as available from the National Land Survey of Finland (2 by 2 m), Bezirksregierung Köln (2020, Germany, 1 by 1 m) and the Head Office of Geodesy and Cartography (Poland, 1 by 1 m).

A DTW map was calculated, following the procedure described by in **Appendix IV**. A flow initiation area of 4.00 ha was used. Values of this map were extracted at the measuring positions and saved as new variable $\mathbf{DTW_4}$ [m].

We calculated a topographic wetness index as defined by Sørensen et al. (2006), and extracted values to each measuring position (**TWI**, dimensionless). The digital elevation models were resampled to obtain a lower spatial resolution of 5 by 5 m to achieve robust values (Southee et al., 2012). Afterwards, the function 'r.watershed' of the free toolbox GRASS GIS (Awaida and Westervelt, 2020) was run, creating the TWI map as an output.

Soil Moisture Active Passive Mission (SMAP)

SMAP (Reichle et al., 2020a), provides soil moisture data across the globe. SMAP was launched in January 2015. Ever since, it has generated global information about surface and subsurface soil moisture, using radiometers and radar sensors. The captured brightness, and backscatter cross-section of the earths' surface is used to determine soil moisture, including corrections for vegetation and surface roughness (Entekhabi et al., 2014).

Global grids of surface soil moisture (format: HDF5) were downloaded for each measuring day in the study period. The grids were transformed into a raster stack (see **Appendix V**), containing one layer for each measuring day. Retrievals of surface soil moisture for each measuring day were extracted at the locations of the study sites (**Chapter 3**, **Figure 3-1**, **Table 3-1**), assigned to the corresponding measuring campaigns and saved as a new variable $\mathbf{SSM_{SMAP}}$ [%vol]. By this we incorporated a temporal component, which allowed for the spatio-temporal modelling.

Soil constants provided by the SMAP mission allow for a further interpretation of geophysical fields. Several numerical and categorical parameters, as available from SMAP "Land Model Constants" were included (see the user guide of Reichle et al. (2020b)) as predictor variables for the proposed modelling approach (**Appendix VI**).

5.2.3. *Data analyses*

Data was merged and analysed using the free software language R (R Core Team, 2020), interfaced with Rstudio (version 1.4.1103, RStudio, PBC, Boston, MA). Pre-processing of the predictor variables was performed: the strongly skewed predictor $\mathbf{DTW_4}$ was transformed by natural logarithm, after adding a value of 0.01, since zero-values were present. Subsequently, a linear min-max-normalization (between

0 and 1) of all numerical predictors was performed (R library: "caret", Kuhn, 2020). The high amount of >100 predictor variables was checked for identifying characteristics (e.g. sample numbers in ESDB), co-variation, redundancy, and the number of factor levels being greater than one. The data used for modelling was thereby reduced to 54 predictor variables, which consisted of **SSM_{SMAP}, DTW_4, TWI**, several land model constants (SMAP), and soil properties (ESDB), see *-marked values in **Appendix VI** and **Appendix VII**).

Data partitioning

For modelling, the full dataset was portioned into training and validation data in two different ways (**Table 5-1**): (1) **Part80-20**: 80% of the measuring positions were selected to define the training set, using the factor 'study site' as an attempt to balance the class distributions within the splits. The remaining 20% were kept aside as a test set. (2) **Part10-90**: To assess generalizability of models, a second and individual partition was created, consisting of observations measured on 49 out of 483 measuring positions in the training set, and the data measured on the remaining 434 position kept aside as a testing set.

Table 5-1. Data was split into two partitions: **Part80-20**, containing randomly selected training data (80% of measuring positions) and a 20% test set, and **Part10-90**, where data originating from 10% of measuring positions was used for training, whereas the remaining 90% were used for model validation.

Site	**Part80-20**		**Part10-90**	
	training	testing	training	testing
FIN_E	396	108	36	468
FIN_O	414	90	66	438
GER_N	748	176	99	825
GER_O	536	135	64	608
POL_N	130	20	10	140
POL_S	140	60	20	180

Basic predictions by the topographic indices

Simple linear models were fitted to carry out regressions between **SMC** ~ **DTW_4** or **TWI**. This was done to calculate the coefficient of determination (R^2, equation (1)), with the inclusion of model intercepts. For predictions derived from **DTW_4**, Matthews (1975) correlation coefficient (MCC, equation (2)) and accuracy of predictions (ACC, equation (3)) were calculated based on the created confusion matrix (**Table 5-2**).

Model building and tuning

Based on existing studies that modelled spatial aspects of soil properties (Hengl et al., 2018; Ågren et al., 2021; Baltensweiler et al., 2021), four statistical modelling approaches to test in this study were identified: a generalized linear model, an additive model, and two ML algorithms.

As a first step, 'full' models, consisting of 54 predictor variables of the 80% training dataset, were reduced, until a decrease of goodness-of-fit (>1%) occurred. Then, the tuning of the reduced models was performed through a 10-fold cross-validation (R library: "caret", Kuhn, 2020), aimed at attaining the highest possible of R^2 (equation (1)), calculated on the 10th chunks of the cross-validation.

Afterwards, the hyperparameters determined through the cross-validation (on the 80% training dataset) were used to build new models based on the 10% training set. Validation of the reduced and tuned

models was performed on the unseen testing datasets, either comprising of 20% or 90% of the entire dataset, respectively.

Generalized Linear Model with Stepwise Feature Selection (GLM)
The goal of the GLM was to select predictors that fitted the response variable well (library: "MASS", Venables and Ripley, 2002). To reduce the full model to important predictors only, Akaike's information criterion was assessed step-wise throughout the iterative variable selection procedure. The reduced model of the GLM included **SSM_{SMAP}**, **DTW_4**, **TWI**, **clsm_poros**, **clsm_veghght**, **clsm_cdcr2** and **clsm_dzpr** (Reichle et al., 2020b) as predictor variables. These variables were used to fit models to both training datasets, and make predictions on the corresponding testing datasets.

Generalized Additive Model with Loess function (GAM)
The GAM is a generalized linear model in which the response was fitted to predictions made with a Loess smooth function (R library: "gam", Hastie, 2020). Thereby, GAM can cope with non-linear responses. For model tuning, a *span* between 5 and 50 was considered.

Random Forest (RF)
The RF model is a tree-based learner, which randomly partitions the data into nodes, aiming to maximize the within-node homogeneity and the between-node heterogeneity (Breiman, 2001). The feature reduction was run with default settings (R library: "ranger", Wright and Ziegler, 2017, $min_{nodesize}$=5, $m_{try}=\lfloor\sqrt{p}\rfloor$, where p is the number of predictor variables), executing a stepwise recursive elimination of the least important predictors, where five predictors were removed at once. The reduced model included **SSM_{SMAP}, DTW_4, TWI,** and **PARMADO,** and possessed the highest out-of-bag variation explained by predictions. Using these predictor variables, values of m_{try} between 1 and p, and $min_{nodesize}$ from 1 to 10 were considered for the tuning.

eXtreme Gradient Boosting (XGB)
The XGB mostly combines a number of regression trees and uses optimized distributed gradient boosting – an iterative way of putting more weight on large pseudo-residuals (R library: "xgboost", Chen et al., 2021). The full XGB model was built using a random setting of hyperparameters. Thereafter, the four most important predictors, **SSM_{SMAP}, DTW_4, TWI,** and **clsm_dzpr** were used for further tunings, following the procedure described by Ågren et al. (2021). Yet, hyperparameters were confined to conservative ranges: max_{depth}=2, 3 and 4, *eta*=0.05, 0.10 and 0.15, $rate_{drop}$ and $skip_{drop}$=0.25, 0.50 and 0.75, $min_{childweight}$=10, 20 and 30, *gamma*=0.8, 0.9 and 1.

Evaluating predictive performance

For reducing the full models to reduced/final models, and for the comparison of such to each other, goodness-of-fit was assessed. Therefore, differences between observed and predicted values, were considered to calculate R^2 (equation (1)). With observed values y_i, predicted values $\hat{y}_i$, mean values of observed values $\bar{y}$, for i observations:

$$R^2 = 1 - \frac{\sum_i (y_i - \hat{y}_i)^2}{\sum_i (y_i - \bar{y})^2} \quad (1)$$

Matthews correlation coefficient (MCC, equation (2)), and accuracy of predictions (ACC, equation (3)) were calculated on a confusion matrix between predicted and measured values (**Table 5-2**). Therefore, binaries of measured and predicted **SMC** were compared, after adding a constant of 5 %vol to model-derived predictions and applying the same texture specific thresholds.

Table 5-2. Two confusion matrices were created, by comparing the occurrence of binary values of in-field measured soil moisture content **SMC** to depth-to-water values (**DTW$_4$**) or predicted values of **SMC** (after adding a constant of 5 %vol). The thresholds for the two levels of **SMC** were 35 %vol (Finland), 42 %vol (Germany) and 19 %vol (Poland).

classification	abbr.	measured **SMC**	predicted (**SMC** + 5)	**DTW$_4$** [m]
true positive	TP	**wet**	**wet**	<1
true negative	TN	**non-wet**	**non-wet**	≥1
false positive	FP	**non-wet**	**wet**	<1
false negative	FN	**wet**	**non-wet**	≥1

$$\mathrm{MCC} = \frac{\mathrm{TP} * \mathrm{TN} - \mathrm{FP} * \mathrm{FN}}{\sqrt{(TP + FP)(TP + FN)(TN + FP)(TN + FN)}} \tag{2}$$

$$\mathrm{ACC} = \frac{\mathrm{TP} + \mathrm{TN}}{\mathrm{TP} + \mathrm{TN} + \mathrm{FP} + \mathrm{FN}} \tag{3}$$

5.3. Results

Overall moisture conditions clearly differed between the three countries with mean values of 14.0 %vol measured in Poland, 29.3 %vol measured in Finland, and 30.3 %vol measured on German study sites. Eleven consecutive measuring campaigns were conducted in Germany, resulting in mean values per measuring day and site ranging from 13.6 %vol to 44.1 %vol (**Figure 5-1**). Lower extents of campaign-to-campaign variation could be observed on Finnish and Polish study sites, where means ranged between 21.9 %vol and 38.4 %vol, and5.3 %vol and 21.1 %vol, respectively. Overall, **SSM$_{SMAP}$** was in relatively close alignment with mean values of **SMC** in most of the study sites, except in 'POL_S' (**Figure 5-1**).

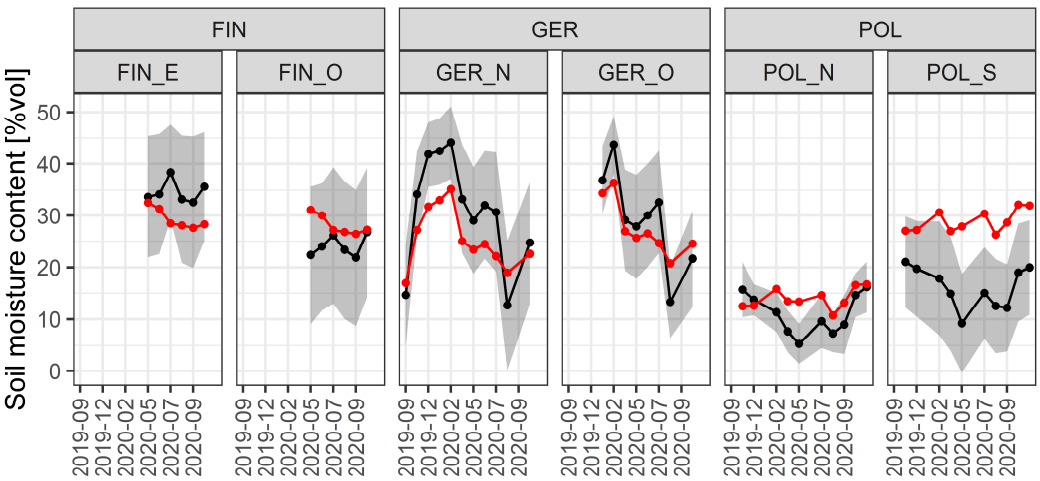

Figure 5-1. Soil moisture content (**SMC**) was measured on six sites in three countries (FINland, GERmany, POLand), in a time series fashion (year-month). Black dots show mean values of **SMC** for each site and day of measurement; the shading indicates the corresponding standard deviation. Red dots indicate remotely-sensed surface soil moisture (**SSM$_{SMAP}$**), as available from the Soil Moisture Active Passive mission.

5.3.1. *Prediction of SMC*

Simple linear models were used to compare **SMC** and **TWI** of the 80% training dataset, indicating a significant correlation ($p<0.001$), but a high proportion of variation was unexplained ($R^2=0.049$). Another linear model was fitted to **SMC** and **DTW_4** of the 80% training dataset, revealing a significant correlation between the two variables ($p<0.001$). The goodness-of-fit of **DTW_4** derived predictions of **SMC** was different between the measuring sites, with $R^2=0.16$ when only the Finnish data was considered, and $R^2=0.42$ for Polish data. Yet, the over-representation of German data (**Table 5-1**), where R^2 was 0.019, as well as site-specific intercepts resulted in an overall $R^2=0.022$ for the 80% training dataset (**Figure 5-2**A).

Ideally, all **wet** values would coincide with **DTW_4**<1 m (**Table 5-2**). The actual occurrence of **wet** values was correctly predicted by **DTW_4** for 38% of observations (=TP/(TP+FN), **Table 5-3**), participating to a total MCC=0.31 (**Figure 5-3**A).

Table 5-3. Soil moisture content was predicted by depth-to-water (DTW, simple linear model), and spatio-temporal models based on several predictors: A generalized linear model (GLM), generalized additive model (GAM), random forest model (RF) and extreme gradient boosting (XGB) were tested.

	Classes of confusion matrix (**Table 5-2**)			
Prediction	TN	FP	FN	TP
DTW	1713	2230	442	274
GLM	1522	421	257	459
GAM	1521	422	254	462
RF	1488	455	222	494
XGB	1446	497	186	530

The ability to explain the goodness-of-fit was clearly improved when applying more predictor variables to the XGB and RF modelling approaches, compared to basic **DTW_4** predictions. R^2 calculated by the cross-validation ranged between 0.43 (GLM) and 0.80 (XGB, RF) (**Figure 5-2**A). When trained on the 80% dataset, the two ML algorithms RF and XGB revealed similar predictions of **SMC**, with a tendency towards higher R^2 for the training dataset, compared to the test dataset. When the model training was performed on the 10% set, minor differences occurred between the RF and XGB (**Figure 5-2**B). When applied to the 90% test dataset of German sites, robust predictions were derived from the GLM (**Figure 5-3**B) and GAM, with R^2 equal 0.44 and 0.45, respectively. However, significantly lower R^2-values were observed for the remaining observations made in Finland and Poland (**Figure 5-2**).

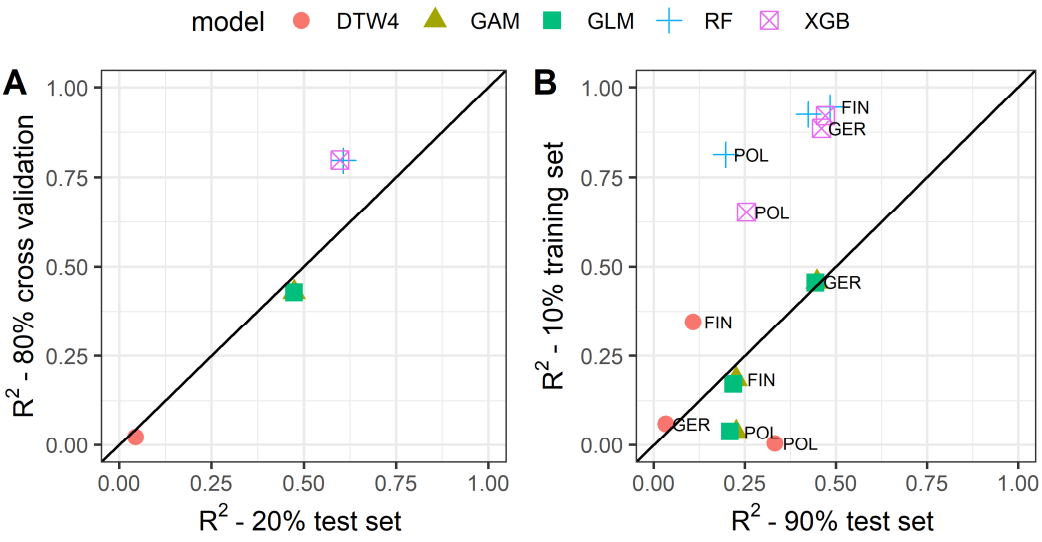

Figure 5-2. R^2 (equation (1)) was calculated by a 10-fold cross-validation of the 80% training set (A), and by a 10% training dataset (B), and the remaining test sets of 20% and 90%, respectively. Depth-to-water maps (DTW), a general additive model (GAM), a generalized linear model (GLM), random forest (RF) and extreme gradient boosting (XGB) were used to predict soil moisture content for sites in FINland, GERmany and POLand.

The methods RF (n_{trees}=500, m_{try}=2, $min_{nodesize}$=2) and XGB (n_{rounds}=500, *eta*=0.10, max_{depth}=4, *gamma*=1, $colsample_{bytree}$=0.50, $min_{childweight}$=5, $rate_{drop}$=0.25, $skip_{drop}$=0.75, *subsample*=0.5) were applied to the predictor variables $\mathbf{SSM_{SMAP}}$, **TWI**, $\mathbf{DTW_4}$ and either **PARMADO** or **clsm_dzpr**, respectively. For both models, $\mathbf{SSM_{SMAP}}$ was the most important predictor, followed by the two topographic indices and one soil parameter. In effect, the soil parameter acted as a grouping variable, since unique values were present for each participating country (**PARMADO**, i.e. dominant parent material, derived from ESDB), or site (**clsm_dzpr**, i.e. thickness of profile soil moisture layer, derived from SMAP). Based on these predictors, RF and XGB models were trained on the 10% dataset and validated on the 90% test dataset (Figure 5-3C), resulting in **SMC** predictions with an overall R^2=0.49 for both models – a significant increase compared to the simple linear model with $\mathbf{DTW_4}$ as independent variable (R^2=0.022). Accordingly, MCC was increased by approximately 48%, from 0.30 ($\mathbf{DTW_4}$), to 0.40 (GLM) and 0.44 (XGB), calculated on the 90% test dataset.

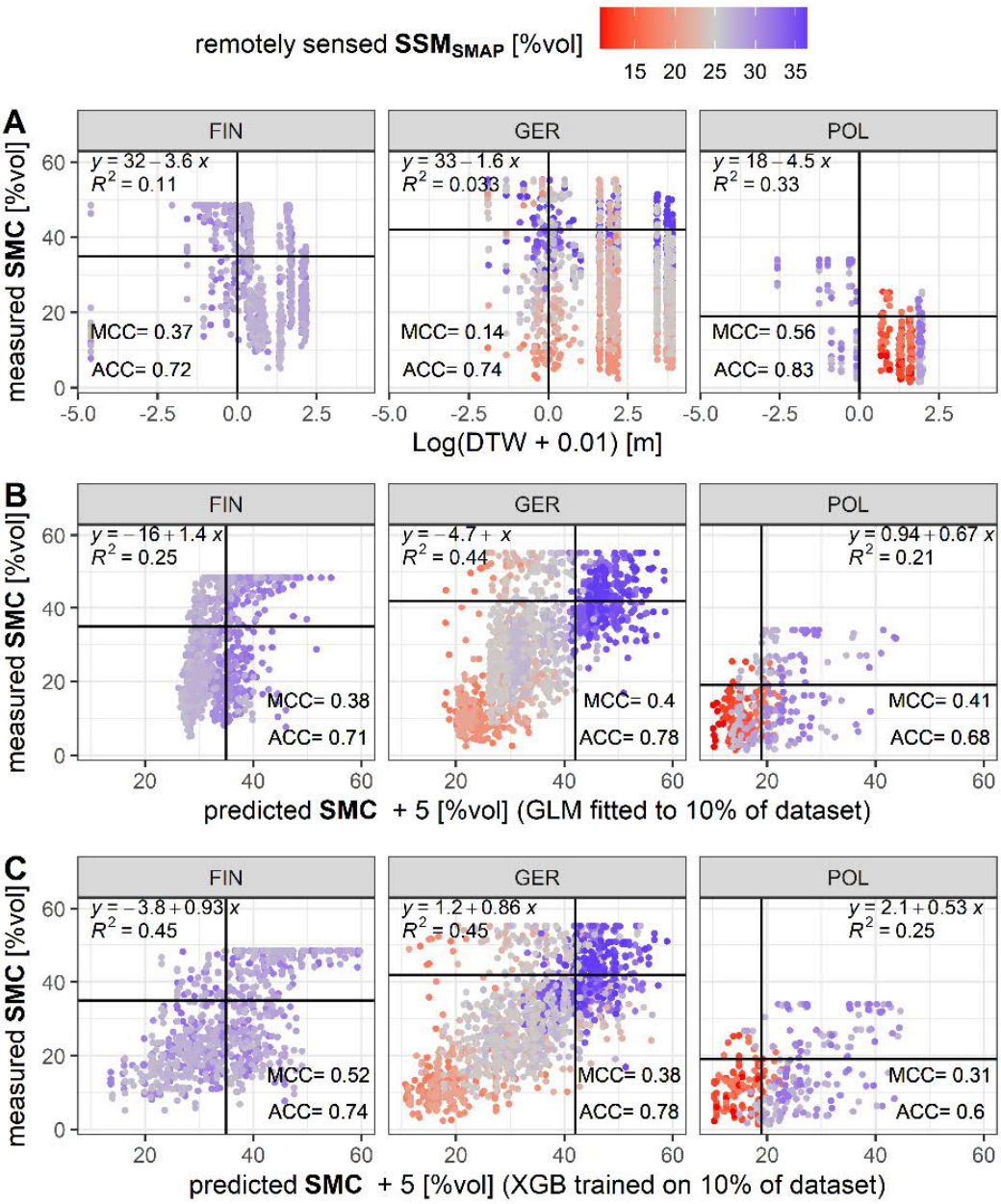

Figure 5-3. Soil moisture content (SMC) was measured on forest sites in FINland, GERmany and POLand. The values were compared to depth-to-water (DTW) values (**A**). A generalized linear model (GLM, **B**) was fit, and the machine learning algorithm eXtreme Gradient Boosting (XGB, **C**)) was trained on a 10% subset of data, and used to predict SMC of the remaining 90%. Colouring indicates remotely sensed surface soil moisture (**SSM_{SMAP}**). With regression equations, R^2, MCC and ACC, according to equations (1), (2) and (3).

5.4. Discussion

In the present study, we illustrate how spatio-temporal variation in soil moisture can be predicted and hence serve as an important tool for reduced soil impacts in forest operations. For several decades, topography derived indices have been developed, aimed at supporting low-impact forest operations through predictions of soil moisture across large landscapes, with low demands of input data. An example of such an index is DTW, introduced by Murphy et al. (2009), who intended to simulate overall moisture conditions by different map-scenarios. This concept was motivated by the urgent need of forest

managers for dynamic predictions (Akumu et al., 2019), yet the ability of representing seasonal moisture conditions by DTW map-scenarios was not confirmed in a recent study **Chapter 3**. The latter showed, that one map-scenario resulted in the highest predictive performance on a given site, across several seasonal conditions. In agreement, Ågren et al. (2014) and Mohtashami et al. (2017) showed, how differently calculated map-scenarios led to enhanced predictive performances on different sites. These predictions were driven by diverse soil-related, geomorphological and climatic influences on water accumulation on sites.

The complexity of temporal variations of moisture and spatial variations of soil characteristics, can be captured by ML approaches, which are designed to make predictions for complex phenomena with many interactions (Heung et al., 2016). Current research demonstrated and corroborated the potential of such methods for mappings of soils' carbon content (e.g. Keskin et al., 2019), soil characteristics (e.g. Baltensweiler et al., 2021), and for creating static moisture maps in Sweden (Lidberg et al., 2020; Ågren et al., 2021). Although temporary, dynamic maps of soil moisture have been made available by different sources (Li et al., 2021), but the low spatial resolution (e.g. 9 by 9 km, SMAP) of such would not allow for direct utilization for forest operations (Zeng et al., 2019). In this work, we demonstrated how low-resolution SMAP grids were merged with high-resolution DTW and TWI maps, resulting in the spatio-temporal prediction of **SMC** on different sites in Europe – a system which could gain value for sustainable forest management, currently challenged by increases in climatic variability and less favourable operational conditions (Pfeifer et al., 2021). Among the investigated modelling approaches, best predictive performance was attained by two investigated machine learning algorithms. Both models can be used to create maps of **SMC** on a daily basis (**Figure 5-4**).

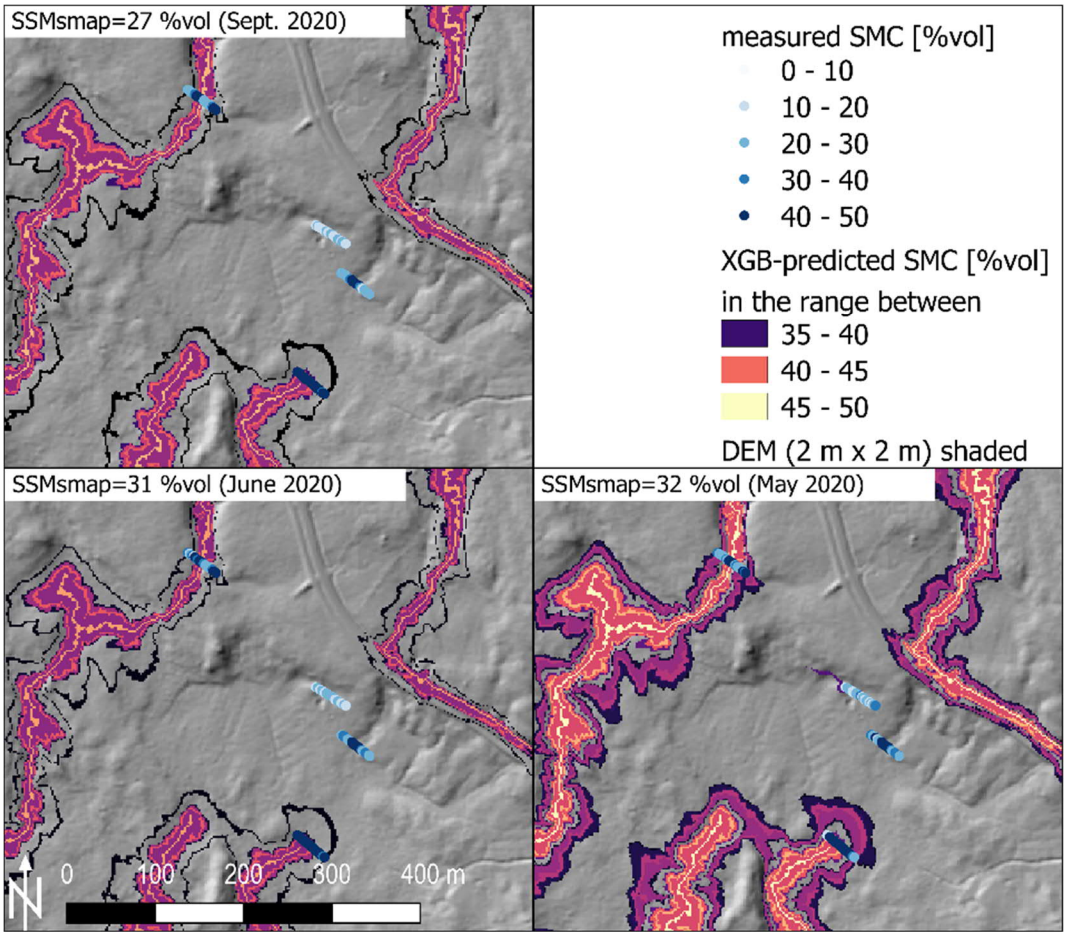

Figure 5-4. A spatio-temporal modelling of soil moisture content (SMC) was achieved by merging spatial and temporal information, and the application of the machine learning algorithm eXtreme Gradient Boosting (XGB). Remotely sensed soil moisture (**SSM_{SMAP}**), two topographic indices, based on digital elevation models (DEM) and large-scaled soil properties were used. The maps show a shaded DEM and the coloured predictions highlight the extent of wet soils (SMC≥35 %vol).

Although the performance of ML models deeply relies upon the quality and quantity of input data used for training (Heung et al., 2016), a system for trafficability prediction should work on low quantities of input data – an inevitable prerequisite for achieving a practical application to enable day-to-day support for forest management over large areas. Therefore, we assessed the predictive ability of the models, when only limited input data was selected for model training. In a separate mode of modelling, the training set was confined to data captured on only 10% of the measuring points to avoid auto-correlation between repeated measurements made on identical measuring positions. The validation of the trained models on the remaining 90% test dataset revealed a reduction in predictive performance compared to the 20% test dataset. When XGB was applied, R^2-values of 0.25 and 0.45, were reached on sites in Poland, and Finland and Germany, respectively (**Figure 5-3**). This corresponds to a more than 3-fold increases in R^2 for Finnish data, a 39%-decrease for the data measured in Poland, and an almost 14-fold increase for the data measured on German sites, compared to basic DTW predictions. The improvements of predictive performance within the data from Germany can be partly explained by the clear influence of **SSM_{SMAP}** within the ML models (**Figure 5-3**). On German sites, the highest variations of **SMC** between the measuring days occurred – a vector that was adequately reflected by **SSM_{SMAP}** (**Figure 5-1**).

Accordingly, MCC, an informative and truthful indicator for the assessment of classifications (Powers, 2011) was increased from 0.30 (binary values of **DTW_4**) to 0.44 (XGB). It has to be noted though, that a constant of 5 %vol was added to the model-derived predictions before classifying the predicted values of SMC into **wet** and **non-wet**. We assumed, that the underrepresentation of **wet** values, which accounted for 36% of the entire dataset, led to an underestimation of such. Yet, after adjusting the predictions, 74% of **wet** values were predicted correctly (**Table 5-3**) – a considerable improvement compared to basic DTW predictions.

Only a few predictor variables were sufficient to explain a large share of the variation of **SMC**. The initially large number of predictors was reduced to four predictors, consisting of **SSM_{SMAP}**, **DTW_4**, **TWI** and one soil parameter, either derived from the land model constants from SMAP (**clsm_dzpr**), or the ESDB (**PARMADO**). It was decided to include DTW maps calculated with a flow initiation area of 4.00 ha (Jones and Arp, 2019), based on three arguments: (I) DTW values from different map-scenarios were partially autocorrelated, (II) since the measuring transects were specifically located on DTW gradients (see **Chapter 3** for details), only **DTW_4** comprised of topographic gradients between the transects. When a DTW map-scenario for moister conditions was chosen, all transects would show zero-values in the centre with similar increases of DTW at the outer parts of each transect. (III) Although high explanatory power was reached when including different DTW map-scenarios, raster predictions made with such models led to unreasonable maps – an aspect which has to be accounted for when modifying the predictors (Meyer et al., 2019). When two DTW maps were included, chequered patterns were observed in the grid predictions made, an indicator for overfitting caused by repeated use of similar predictors and spatial autocorrelation (Nussbaum et al., 2018).

Data used for the developed modelling was openly accessible, allowing for a spatio-temporal prediction of **SMC** in all regions where high-resolution DEMs are available. The validation performed here was limited to six selected sites. However, on each site only a few repeated measurements (in this case, 10 to 99) were required to predict a total of 2,660 values of **SMC**, covering a time span of more than a year. It would be possible to consolidate moisture data of different origins, more accurate soil mappings and weather data to extend **SMC** predictions to a wide range of landscapes and seasons. Applications of created prediction maps could be manifold, including a potential utilization for agricultural purposes, drought monitoring and irrigation scheduling (Li et al., 2021). In the field of forest operations, accurate spatio-temporal predictions can support mitigating measures, and thereby enhance environmentally sound and economically efficient forestry practices as a whole.

5.5. Conclusion

This study showed a successful prediction of **SMC** values at six study sites in Europe. Through the utilization of machine learning, site-specific and non-linear effects on **SMC** could be captured, setting a direction for further solutions towards a large-scaled, temporal and precise support for harvesting operations. The freely available data, provided by the SMAP mission, showed to be an adequate proxy to be used for predictions of **SMC**. The variable **SSM_{SMAP}** strongly contributed to model **SMC** with the XGB and RF algorithms, along with the topography-based **DTW_4** and **TWI** and the one remotely sensed soil parameter. Applying the XGB resulted in MCC of 0.45, with 74% of **wet** values predicted correctly, and R^2 of 0.51 – a significant improvement compared to basic **DTW_4** derived predictions, where MCC was 0.30 (38% of **wet** values predicted correctly), and R^2 was 0.02. A 10% subset of the entire data was sufficient to predict the remaining 90%, corresponding to 10 to 99 in-field measurements necessary per site. A low demand of input data might be a crucial prerequisite to achieve a modelling approach which can be applied for day-to-day forest management. We are confident though, that increasing possibilities in modelling spatio-temporal dynamics of soil moisture, innovative and interactive sensor networks and

more than anything, increasing amounts of field data, will enable further developments towards accurate predictive systems which support year-round timber mobilization with lower environmental impacts.

Declaration of Competing Interest: The authors declare no conflict of interest. **Funding:** This work was supported by the Bio Based Industries Joint Undertaking under the European Union's Horizon 2020 research and innovation program, TECH4EFFECT Knowledge and Technologies for Effective Wood Procurement—project, [grant number 720757]; by the cooperation project "BefahrGut" funded by the State of North Rhine-Westphalia, Germany, through its Forest Education Centre FBZ/State Enterprise Forestry and Timber NRW, Arnsberg/Germany; and by the Eva Mayr-Stihl Stiftung.

Data statement: Data will be made available at doi: 10.5281/zenodo.5659098

6. Field trial of a logging operation on relatively dry ground

This chapter was published under the title “Effect of a traction-assist winch on wheel slippage and machine induced soil disturbance in flat terrain” in the International Journal of Forest Engineering, November 2020 and is available at: https://doi.org/10.1080/14942119.2021.1832816

Full author list: Marian Schönauer [1,*], Thomas Holzfeind [2],
Stephan Hoffmann [1,3], Franz Holzleitner [2], Bastian Hinte [1], Dirk Jaeger [1]
* Corresponding author

[1] Department of Forest Work Science and Engineering, Georg-August-Universität Göttingen, 37077 Goettingen, Germany

[2] Institute of Forest Engineering, Department of Forest and Soil Sciences, University of Natural Resources and Life Sciences Vienna, 1190 Vienna, Austria

[3] Chair of Forest Operations, Albert-Ludwigs University Freiburg, 79085 Freiburg, Germany

Author's contributions: S.H. and M.S. conceived and designed the experiments; M.S., S.H., B.H., T.H. and F.H., performed the experiments; data preparation, M.S. and T.H.; data analysis and interpretation, M.S., T.H., S.H., B.H. and F.H.; writing – original draft preparation, M.S., S.H., T.H., F.H. and B. H.; writing – review and editing, M.S., S.H., T.H., F.H., B. H. and D.J. ; supervision, D.J.; project administration, D.J.

Abstract

Introduction: Recently, forest operations are facing unfavourable climatic conditions more frequently. In Central Europe, machine trafficability and induced soil disturbances, are negatively affected by periods of high precipitation and less intensive frost during ground-based harvesting operations. Winch-assist technology is assumed to reduce soil disturbance by forest machines in steep terrain. Still, the potential positive effects of winches to assist traction of forest machines in flat terrain have rarely been surveyed. In this study, a field trial has been conducted in flat terrain (slope < 5%). *Material and methods:* There, a forwarder with an integrated traction-assist has been monitored during six consecutive machine passes on a permanent machine operating trail. The first section of the machine operating trail was passed without traction-assist, the remaining section with traction-assist, resulting in two treatment groups. To assess soil impacts, three test plots were positioned per treatment group. Within these plots, pre- and post-operational soil bulk density, soil displacement and rutting were determined. Additionally, wheel slippage and cable tensile force were examined, using incremental rotary encoders and a flexible tensile force measurement kit, respectively. *Results and conclusions:* It was observed, that wheel slippage responded inversely with tensile force. Traction-assist technology reduced wheel slippage from 5.3±11.9% to 0.37±10.19% along the section of the machine operating trail, as compared to results from the unassisted section. Although wheel slippage was significantly reduced, no mitigating effect by the usage of traction-assist technology on soil disturbance could be observed, probably due to the low volumetric water content of 27%.

Keywords: forwarder; trafficability; winch-assist; soil impact; rutting; forest operation.

6.1. Introduction

In the context of climate change, forest management is facing numerous challenges, such as drawbacks of established silvicultural systems and the frequency and intensity of disturbances (Kirilenko and Sedjo, 2007; Reyer et al., 2017). In addition, the changing precipitation regime with periods of highly intensive rainfall, but also the shorter and less intensive frost periods during the winter, have negative consequences for forest operations with respect to machine trafficability (Maracchi et al., 2005; Ringdahl et al., 2012). For example, Berendt et al. (2017) estimate that the area suitable for conventional forwarder extraction in the state of Baden-Wuerttemberg/Germany will decrease from 40% to 19% due to climate change induced forest structure change and unfavourable conditions, especially on sensitive soils with limited bearing capacity. Such limitations impede the implementation of sustainable forest operations (Marchi et al., 2018), and thus threaten efficient resource supply chains for the establishment of a forest-based bio-economy within the fulfilment of the United Nations 'Sustainable Development Goals' (Alberdi et al., 2020).

Fully mechanized harvesting operations on sensitive sites can be enabled by advanced equipment, like adapted tires, tracks or a tire inflation management (Cambi et al., 2015; Abbas et al., 2017). This improved and innovative technology decreases wheel rutting and soil displacement during harvesting on such sites. However, it also causes logistic and operational challenges during in-stand relocation activities due to changing machine dimensions, weight and driving properties on forest roads (Labelle and Jaeger, 2019).

In addition, traction-assist technology can also contribute to improve traction during driving, keeps wheel slippage low, and reduces unnecessary soil disturbance (Haas et al., 2018; Cavalli and Amishev, 2019). The initial idea behind the development of this technology was to use it with wheel-based machinery on flat terrain to assist the machines during driving activities on soils with low bearing capacity. At the same time, entrepreneurs have seen the advantage to push ground-based harvesting systems through winch-assist technology into steep terrain to replace cost intensive cable yarding operations and substitute motor-manual work (Visser and Stampfer, 2015). The terms "winch-assist" and "traction-assist" has been used interchangeably with others, e.g. "tethered" or "cable-assist". However, "winch-assist" refers to operations in steep terrain, whereas "traction-assist" addresses purely the traction support in flat terrain operations (Holzfeind et al., 2020).

Wheel slippage, caused by traction loss, substantially increases machine induced soil impacts in form of horizontal and vertical soil displacement (Horn et al., 2007; Ringdahl et al., 2012). In addition, intensive forest machine traffic can negatively affect physical, microbial and functional characteristics of soils, and thus reduces forest productivity (Ampoorter et al., 2009; Cambi et al., 2015).

The implementation of assisting winches to improve traction, can contribute to soil protection efforts in steep as well as in flat terrain (Haas et al., 2018; Cavalli and Amishev, 2019; Garren et al., 2019). Especially in flat terrain, with a focus on sensitive sites, where trafficability is restricted due to varying soil physical properties and high wetness, traction-assist ground-based equipment offers high potential to reduce soil damages caused by timber harvesting operations (Ampoorter et al., 2009; Cambi et al., 2015). However, empirical studies quantifying the effect of traction-assist equipment in flat terrain are lacking, leaving a knowledge gap for operational planning.

Therefore, it is of general interest to determine potential advantages of traction-assist technology compared to conventional operational set-ups. Thus, the objective of this experiment was to generate first field experiences, comparing a forwarder with and without traction-assist, on a sensitive site in flat terrain, and to quantify differences in wheel slippage, rutting and soil displacement.

6.2. Material and methods

6.2.1. *Study site and machine*

The study was carried out in the state of Rhineland-Palatinate, Western Germany, close to the town of Hermeskeil (49°41'27"N; 7°00'42"E). An experimental site was selected in a 75-year-old stand dominated by Norway spruce (*Picea abies* [L.] Karst.), located in the forestry district Thiergarten (forestry office Hochwald), 620 m above sea level. The prevailing soil types are acidic brown soils (contents of sand: 36±3%, silt: 36±7% and clay: 28±8%, based on an analysis as described below) with duff humus forms. Despite its location in a mountainous region, the site is characterized by a wide-ranging plateau (<5% slope) which is strongly influenced by the local water regime. This causes wet and generally sensitive soil conditions, restricting the permanent access to the site with ground-based harvesting machinery. Yet, during data collection in November 2018, unexpected favourable conditions prevailed due to a period of unusually low precipitation before the study was conducted. The volumetric water content was low with an average value of 27% across the machine operating trail, ranging from 25% to 28%. The night before the experiment was carried out, a thin coating of snow covered the whole region, but humus and mineral soil were not frozen.

The experiment was conducted with a standard forwarder Rottne F10^{b} (Rottne Industri AB, Sweden), equipped with an integrated assisting winch system Herzog Synchronwinde HSW 9 (Herzog Forsttechnik AG, Switzerland). The winch integrated in the rear of the logbunk has a drum capacity of 250 m wire cable of 15 mm diameter. The winch offers a manual steering mode for rigging the cable and a synchronized mode during driving combined with continuous adjustment of pulling force up to a maximum of 100 kN on the inner layer. The Rottne F10^{b} 8-wheel forwarder was fitted with 710/40 x 22.5 Nokian Nordman Forest tires (Nokian Heavy Tires Ltd., Finland); no chains or bogie-tracks were mounted during the field trial. The tires had an average inflation of 0.4 MPa and an average tread depth of 25 mm. The forwarder was loaded with 5.2 Mg of logs, approximately 50% of its payload capacity, thus, totalling a loaded mass of 21.5 Mg. This load was kept constant throughout the experiment (Figure 6-1).

Figure 6-1. Loaded forwarder Rottne F10^{b} at the study site, driving on the machine operating trail.

6.2.2. *Experimental setup*

For the experiment, a previously used and permanently marked machine operating trail within the stand was selected. The loaded forwarder passed this machine operating trail six times (pass number = *PN*) with an average travel speed of 0.35 m s^{-1}. Within the machine operating trail, six test plots measuring

2 m in length and 4 m in width were laid out. The first three plots were passed without traction-assist and the rest with traction-assist, resulting in two treatment groups (*Winch* = 'no' or 'yes', respectively) (**Figure 6-2**).

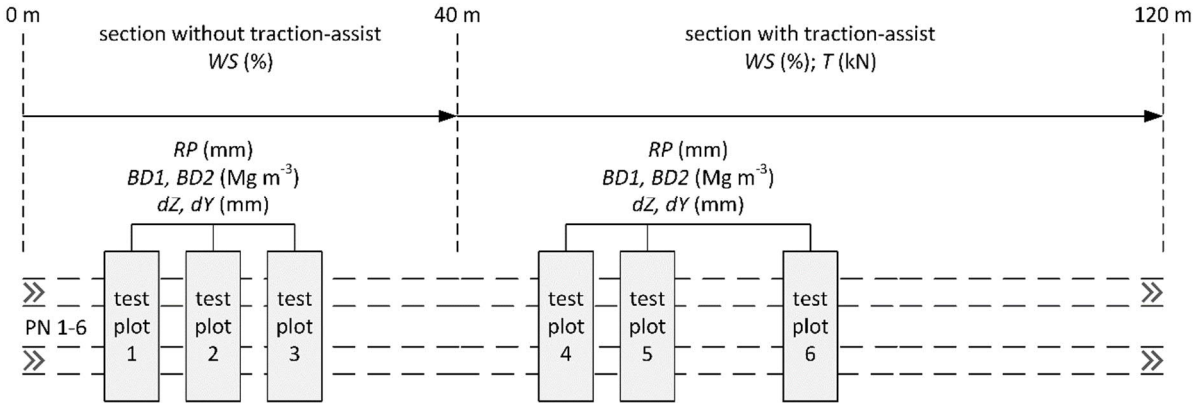

Figure 6-2. Scheme of the study site with marked test plots showing the driving direction of the forwarder, which crossed the plots six times (*PN* = 1 to 6). Wheel slippage (*WS*) was measured along the whole machine operating trail length, tensile force (*T*) along the traction-assist section. Rutting process (*RP*), pre- and post-operational soil bulk density (*BD1* and *BD2*, respectively) and vertical (*dZ*) and horizontal (*dY*) tracer movements were measured within the plots.

Two incremental rotary encoder sensors SENDIX 5000 from KÜBLER (Fritz Kübler GmbH, Germany), including the software from SEATEC (Seatec Software und Automatisierungstechnik GmbH, Germany), were used to measure wheel speed (*Vw*) and travel speed (*Vt*) of the forwarder over ground along the whole machine operating trail (**Figure 6-3**). One sensor was mounted on the second wheel of the front bogie-axle, the second on the front part of the machine for capturing travel speed. The measurement rate during the experiment was set to 15 Hz. Afterwards, both speeds were used to calculate the slippage of the wheels (*WS*) according to equation (10).

$$WS = (1 - \frac{Vt}{Vw}) * 100 \tag{10}$$

In addition, along the section with traction-assist, tensile force (*T*) in the cable was recorded using a flexible tensile force measurement kit, consisting of a load shackle (ALTHEN SHK-B-12-4202), analogue digital amplifier (HBM Quantum MX840), miniature lanless PC, GPS device, ruggedized notebook PC (Panasonic Toughbook) and two batteries, as described by Holzfeind *et al.* (2019). As accurate timestamps were necessary to merge tensile force data with wheel slippage data, the PC clock was synchronized with the attached GPS device.

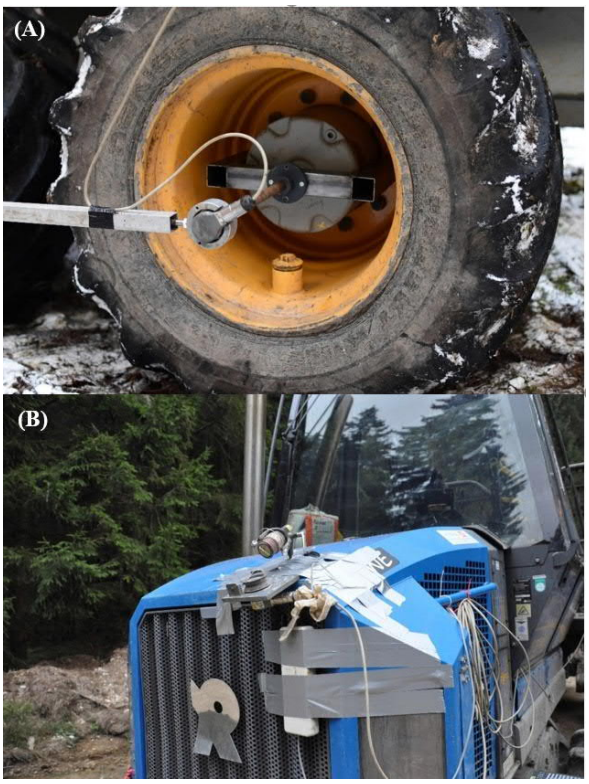

Figure 6-3. Installed incremental rotary encoder sensor to measure wheel speed, mounted on the second wheel of the front bogie-axle (A) and on the front part of the machine for capturing travel speed (B).

After each machine pass, the effect of rutting by the machine was captured at each plot with a laser scanning system (model: PS100-90, Triple-IN GmbH, Germany). The scanner was driven by an electric stepper motor, traveling on a rail across the plot, recording the cross profile (4.5 m x ~3.0 m). Based on the scanner position, a tailored software solution transferred the measured values into a digital elevation model afterwards. To avoid inaccuracies by loose material, only the values of the central section of both ruts (2 x 0.3 m x 3.0 m) were extracted and averaged. The difference to the previous measurement was giving the rutting process (*RP*). To ensure, that the scanner always had the same height at each plot, fixed tripods were used to hold the rail in position (**Figure 6-4**). Although the laser scans produce detailed information on rut formation after every passage, it was difficult to determine horizontal soil displacement below surface.

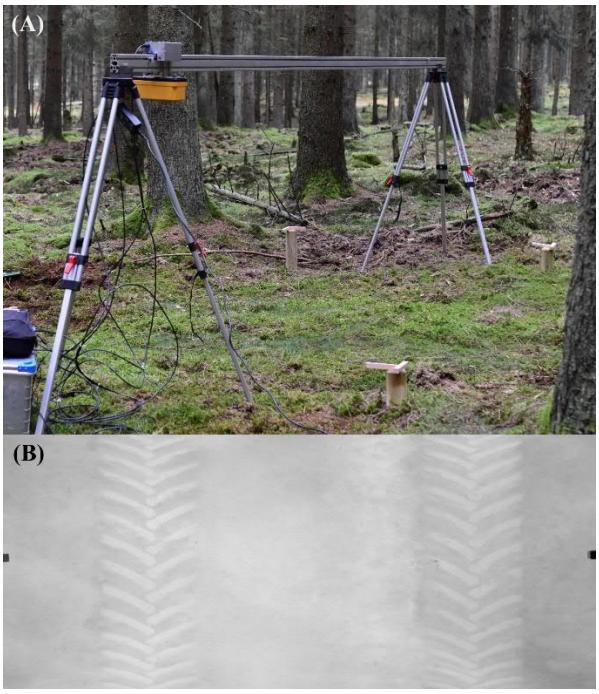

Figure 6-4. Set up of the terrestrial laser scanning system moving on a rail between two tripods above the test plots for scanning the surface after every pass (A), and an example of a processed digital terrain model of the tracks on a machine operating trail (B).

Therefore, soil displacement below surface was quantified by the use of corpuscular aluminium tracers, following the approach described by Haas *et al.* (2018). Consecutively numbered tracers were positioned in 100 mm surface depth and 200 mm spacing along a horizontal reference beam, levelled on wooden pegs, across the machine operating trail on each plot. After the last machine pass, the tracers were excavated. Their movements were determined through a yardstick with reference to the levelled beam. The lateral movement *dY*, and the vertical movement *dZ* were used to calculate the Euclidean distance (*eucl*).

In addition, two soil samples on each plot (left and right wheel track) were taken with 100 cm^3 sample rings, before the first and after the final machine pass, to determine pre- and post-operational soil bulk density at 0.10 m depth in the mineral soil through bulk density analysis following standard procedures (Blume *et al.* 2016). For the estimation of pre-operational soil bulk density, samples were taken 0.50 m in front of each plot, giving *BD1*, while post-operational soil bulk density was determined by samples taken within the plot, giving *BD2*. Soil compaction (*SC*) was estimated according to equation (11).

$$SC = \frac{BD2 - BD1}{BD1} * 100 \qquad (11)$$

Mixture probes from the sampled soil probes were created for the analysis of texture, according to Durner *et al.* (2017). Additionally, volumetric water content was measured using a moisture meter (ThetaProbe with HH2 Soil Moisture Meter, Delta-T Devices Ltd., England) at a depth of 0.10 m in the mineral soil, at each location of soil sampling at the same time.

Table 6-1. Table of abbreviations used.

Acronym	parameter	unit
PN	pass number	numeric
RP	rut depth increment per *PN*, rutting process	mm
Vt	travel speed	m s^{-1}
Vw	wheel speed	m s^{-1}
WS	wheel slippage	%
T	tensile force	kN
BD1	pre-operational soil bulk density	Mg m^{-3}
BD2	post-operational soil bulk density	Mg m^{-3}
SC	soil compaction	%
dZ	vertical tracer movement	mm
dY	lateral tracer movement	mm
eucl	Euclidean distance of tracer movements	mm

6.2.3. *Data analysis*

The data was analysed using R (R Core Team 2019), applied with Rstudio (RStudio Team 2016). For *WS* and *T* averaged values per second were used. The correlation between *WS* and *T* was estimated by the use of a linear model (*lm*). This was done for the traction-assist section only. The parameters *WS*, *RP*, *SC* and *eucl* were compared between treatments (*Winch*: x='yes', y='no') by means of unpaired unequal variances tests (Welch's t-tests). To assess an overall soil compaction by the conducted field trial, *SC* was tested against zero (one sample t-test). Inline values are given with two significant digits. Averaged values are given as mean±SD. Significance level for all statistical analysis was set at α=0.05.

6.3. Results

6.3.1. *Wheel slippage*

Overall, mean wheel slippage (*WS*) on the first section of the machine operating trail (40 m) without winch was 5.3±10.9%, whereas *WS* over all passes on the covered distance (80 m) with traction-assist technology was significantly lower (t-test, $p<0.001$, **Table 6-2**) with 0.37±10.19% (**Table 6-3** and **Figure 6-5**). Negative values indicate that the winch has pulled the forwarder over the ground due to excessive traction-assist, resulting in a negative slip. In total, 40% of values during the measurement were negative.

Table 6-2. One sample t-tests of soil compaction (SC=x) on six test plots with the alternative hypothesis: true mean is greater than zero.

Test statistic	df	P value	Alternative hypothesis	mean of x
0.78	4	0.24	greater	3.27

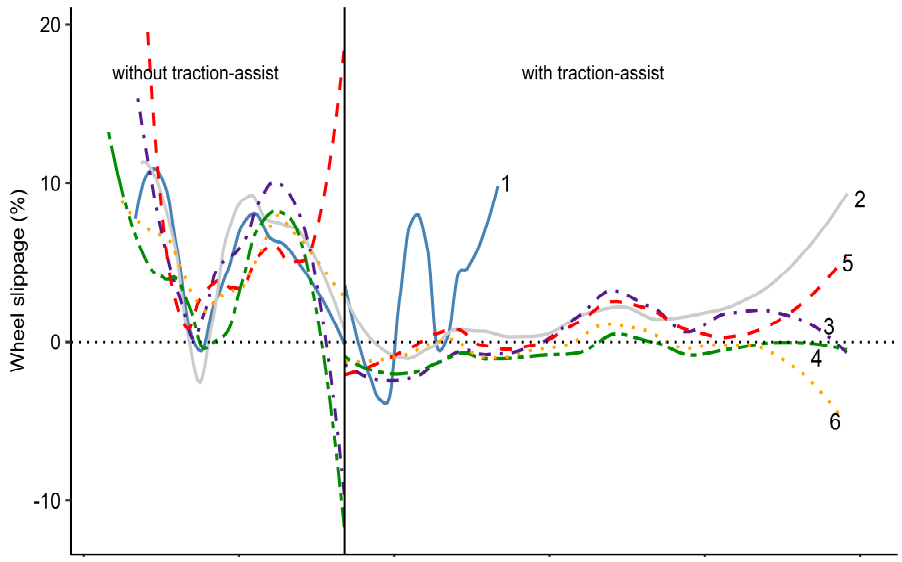

Figure 6-5. Smoothed lines of wheel slippage for the six machine passes (labelled with consecutive numbers) of the Rottne F10[b]. A manual adjustment by the forest machine operator was done after the first and second pass, increasing the basic traction effort. The first 40 m of machine operating trail were driven without traction-assist, the following 80 m using traction-assist technology during driving.

Table 6-3. Captured values of wheel slippage (%) for each machine pass (PN) without traction-assistance (Winch='no') and with traction-assistance (Winch='yes') over all passes based on averaged data per second. With number of observations (n), 5th percentile (0.05), mean value (mean), standard deviation (SD) and the 95th percentile (0.95).

Winch	PN	n	0.05	mean	SD	0.95
no	1	129	-12.90	5.47	11.18	23.34
	2	114	-10.30	6.12	12.60	21.10
	3	125	-8.87	5.44	9.46	23.36
	4	148	-13.74	4.11	10.69	17.83
	5	125	-8.33	6.11	13.06	23.13
	6	144	-10.34	4.99	8.41	16.61
	all	785	-11.30	5.32	10.92	20.30
yes	1	97	-10.52	2.87	11.49	17.22
	2	242	-14.34	1.57	10.66	17.70
	3	217	-15.06	0.13	10.17	15.31
	4	244	-14.91	-0.81	9.07	13.12
	5	248	-15.21	0.52	10.06	15.94
	6	241	-13.15	-0.57	10.18	15.43
	all	1289	-14.41	0.37	10.19	15.73

6.3.2. *Wheel slippage and tensile force*

Whereas slippage was higher along the unassisted section of the machine operating trail, it significantly decreased with increasing tensile force on the assisted section (*lm*, $p<0.001$, **Table 6-4** and **Figure 6-6**). The two adjustments of *T* in terms of traction assisting effort lead to three groups with an average *T* of 12±1 kN (*PN* = 1), 21±1 kN (*PN* = 2) and 31±2 kN for (*PN* = 3 to 6) (**Figure 6-6** and **Table 6-5**). After the final adjustment of the traction winch (*PN* = 3 to 6), *WS* was low with an average of -0.19±9.87% (**Table 6-3**).

Table 6-4. Coefficients of the fitted linear model to estimate the response between wheel slippage and tensile force (T).

Effect	Estimate	Std. Error	t value	Pr(>|t|)
(Intercept)	5.34	0.36	14.87	1.4e-47
T	-0.18	0.02	-11.19	2.8e-28

Table 6-5. Recorded values of tensile force (kN) for each machine pass (PN), based on averaged data per second. With number of observations (n), 5th percentile (0.05), mean value (mean), standard deviation (SD) and the 95th percentile (0.95).

PN	n	0.05	mean	SD	0.95
1	97	11.87	12.44	0.58	13.43
2	242	19.07	20.59	1.27	22.50
3	217	28.03	30.31	1.70	32.42
4	244	29.79	31.80	1.58	33.95
5	248	28.86	30.96	1.74	33.22
6	241	29.22	31.12	1.42	33.30
all	1289	12.48	27.70	6.15	33.26

The standardized values (z) of *WS* and *T* were calculated according to:

$$z = \frac{x - \mu}{\sigma} \tag{12}$$

with the specific value (x), mean value (μ) and the standard deviation (σ). This scaling reveals the interaction between both parameters. High rates in tensile force caused lower wheel slippage and vice versa. Except for the first pass, on the first half of the covered distance the tensile forces were higher than the mean, which lead to low slippage. In the second half, higher *WS* occurred due to lowered *T* (**Figure 6-7**).

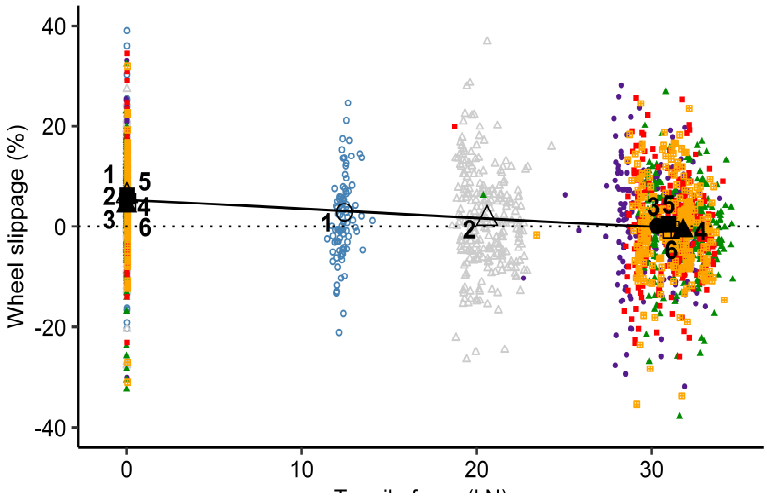

Figure 6-6. Slippage and tensile force data per second (small symbols) and mean values (large symbols) for each machine pass (indicated by shape and consecutive numbers). The line shows an inverse response between wheel slippage and tensile force, which was zero without traction-assist and was increased per machine pass.

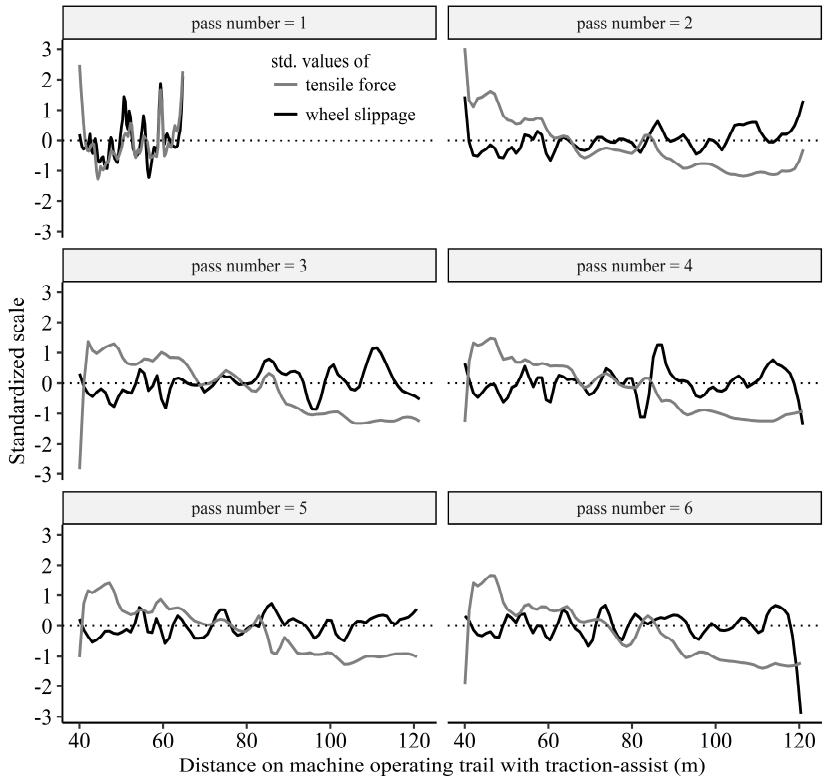

Figure 6-7. Standardized wheel slippage and tensile force values over the distance covered with traction-assist for each machine pass, based on mean values per second.

6.3.3. *Soil Impact*

The pre-operational bulk density (*BD1*) within plots was 0.74 Mg m^{-3}, and varied between the test plots by 13%. The movement of the aluminium tracers was marginal with an average value of -0.83±5.52 mm in lateral direction and 9.1±14.7 mm along the vertical axis. Both directional movements were converted to Euclidean distances, leading to mean displacements of 14±12 mm (**Table 6-6**). No movements could be detected in a rectangular direction to the machine operation trail (spacing of 200 mm).

Occurring vertical soil displacement resulted in an average rut depth increment per machine pass of 4.6±6.8 mm, ranging from -8.3 mm to 25 mm. This resulted in a rut depth of 24±5 mm after the six passes within the section of the machine operating trail without traction-assist, and 31±8 mm within the section where the machine was operating traction-assisted (t-test, ns, **Table 6-7**). In this study, driving on the machine operating trail did neither increase soil bulk density (t-test, ns, **Table 6-7**), nor did *SC* differ between the treatments (t-test, ns, **Table 6-2**). The movements of aluminium tracers did not follow expected directions (a horizontal movement opposite traffic direction) in general; the usage of the traction-assist technology had no influence on the movement of the tracers (t-test, ns, **Table 6-7**). The measured *RP* showed no difference between the treatments (t-test, ns, **Table 6-7**).

Table 6-6. Descriptive statistics of pre- and post-operational soil bulk density (BD1, BD2, respectively; Mg m^{-3}), soil compaction (SC, %), rut depth increment per machine pass (RP, mm) and movements of corpuscular tracers (dY, dZ and Euclidean distance of both, eucl, mm) when no winch is used (Winch='no') and when traction-assistance is used (Winch='yes'). With number of observations (n), 5th percentile (0.05), mean value (mean), standard deviation (SD) and the 95th percentile (0.95).

Acronym	*Winch*	n	0.05	mean	SD	0.95
BD1	*no*	12	0.71	0.71	0.00	0.71
	yes	18	0.61	0.75	0.11	0.87
	all	30	0.61	0.74	0.09	0.87
BD2	*no*	12	0.75	0.76	0.01	0.77
	yes	18	0.65	0.76	0.09	0.86
	all	30	0.65	0.76	0.07	0.86
SC	*no*	12	4.80	6.25	1.51	7.70
	yes	18	-13.18	1.28	10.61	10.11
	all	30	-13.18	3.27	8.54	10.11
RP	*no*	18	-2.45	4.04	5.15	13.63
	yes	18	-5.16	5.10	8.24	22.98
	all	36	-4.45	4.57	6.80	16.48
dY	*no*	57	-4.00	-1.67	7.75	0.00
	yes	57	0.00	0.00	0.00	0.00
	all	114	0.00	-0.83	5.52	0.00
dZ	*no*	57	-15.00	8.14	15.55	40.00
	yes	57	-11.00	10.13	13.84	35.00
	all	114	-15.00	9.14	14.69	36.75
eucl	*no*	57	0.00	14.71	12.33	41.00
	yes	57	0.00	13.29	10.79	35.00
	all	114	0.00	14.00	11.55	40.00

Table 6-7. Unpaired two-sample Welch t-tests of wheel slippage (WS, %), soil compaction (SC, %), tracer movements (eucl, mm) and rutting process (RP, mm) for both treatments (Winch: 'yes' or 'no') with the alternative hypothesis: true difference in means is not equal to zero.

Testing variable	Statistic	P value	Alternative hypothesis	mean of *yes*	mean of *no*
WS	-10.25	6.59e-24	two.sided	0.37	5.32
SC	-0.67	5.69e-01	two.sided	1.28	6.25
eucl	-0.65	5.15e-01	two.sided	13.29	14.71
RP	0.46	6.49e-01	two.sided	5.10	4.04

6.4. Discussion

6.4.1. *Wheel slippage and tensile force*

Studies on machines with assisting winches assume that using such technology decreases wheel slippage (e. g. Visser and Stampfer, 2015). Yet, to the authors' best knowledge, no field trials, directly comparing wheel slippage of traction-assisted and non-assisted wheel-based forestry machines, was conducted on flat terrain since the pilot trials of Salsbery and Hartsough (1993). This underlies the relevance of the present study, and further reveals the existing knowledge gap. This field trial was able to reduce this gap, with a special focus on flat terrain with limited trafficability.

In the present study, six machine passes with the loaded forwarder without traction-assist caused an average slippage of 5.3±10.9% over the observed 40 m of machine operating trail. Although the machine was driving on flat terrain, slip appeared since resisting forces to the vehicle reduce the effective energy expenditure (Saarilahti and Ala-Ilomäki, 1997). Using traction-assist technology over the following 80

m on the same machine operating trail, the six passes resulted in an average slippage of almost zero with 0.37±10.19%, as illustrated in **Figure 6-5**. Shown negative values might be caused by dragging the machine over the ground, inhomogeneous micro-topography, uncertainties of the sensors and steering activities of the machine. Wheel slippage was calculated according to equation (10). Thereto, wheel speed was measured on the second wheel of the front bogie-axle, whereas travel speed was measured at the front canter of the machine. Thus, steering the machine to the right might have caused lower values of slippage, steering the machine to the left probably resulted in higher values. Additionally, single negative slippage recordings might also be caused by uncertainty in capturing the data with the two rotary encoders. However, comparing both treatments in terms of wheel slippage is possible because mean values were used.

The measured slippage responded inversely to the tensile force exerted (**Figure 6-6**). Based on these results, the study confirms that using traction-assist technology generally decreases wheel-slippage of ground-based forest machinery in flat terrain. However, within a holistic view, when merging the tensile force measurements with the slippage data, results indicate that proper adjustment of the winch was an influencing factor, unneglectable for the actual extent of slippage. Setting the pulling force of the winch too low may not reduce slippage in the desired degree. On the other hand, setting the pulling force of the winch too high, may lead to negative slippage, which might induce an equivalent impact on the soil as positive slippage. During negative slippage, the machine is rather dragged over the ground, causing lateral soil displacement with bulge formation, and thus negatively affects soil physical properties, further cause root shear, and increases surface runoff and erosion potential (Horn et al., 2007; Haas et al., 2018; Poltorak et al., 2018). Results from Söhne (1952) indicate that the risk of serious harm done to the soil increases with increasing slip. High wheel spin leads to a complete shearing-off of the topmost soil structures. Consequently, loose soil material can get washed away with the next intense rain. Since soil is recognized as a fundamental factor for biological production and ecosystem functions, margins for acceptable wheel slippage might be beneficial to reduce soil disturbance by low traction.

The maximum tensile force of the winch depends on manual adjustments and in our case had a mean of 31±2 kN after the final adjustment. Considering the flat terrain of the study site, this seems high compared to an average of 31 kN during driving loaded in a slope as observed by Holzfeind et al. (2019) and 33 kN in uphill forwarding operations measured by Holzleitner et al. (2018). The correct adjustment of the basic tensile force was difficult and induced high values of slippage in the beginning of the field trial, when T was too low to compensate traction force. The partially insufficient synchronization between the movement of the machine and enforced tensile force led to an oscillating course of slippage with contrary values of tensile force and shifts between slippage and tensile force peaks, as shown in **Figure 6-7**. The authors of the present study assume, that inhomogeneous micro-topography along the machine travel might additionally induce small peaks in tensile force, resulting in a suboptimal synchronization between winch and machine during travel.

Technical solutions for appropriate synchronization of winch-technology, according to machine movement and tensile force, can reduce negative soil impact (e.g. Cavalli and Amishev, 2019). The correct winch settings according to the required forces is a fundamental challenge to overcome in order to enable full use of advantages of traction-assist technology. The individual settings and adjustments of basic tensile force according to operational conditions is essential for optimal machine support (Mologni et al., 2018). This underlies the additional need for operational tensile force monitoring and derived active winch adjustment on the fly. Yet, at present, adequate winch adjustment also highly depends on the experience of the operator, identifying specific operational conditions. Hence, although this technology has a great potential for reduction of soil disturbances, it is still in its infancy (Visser and Stampfer, 2015).

6.4.2. *Soil impact*

During the field trials, volumetric water content was relatively low resulting from the specific weather conditions of the previous growing season. On soils with low moisture content, the frictional resistance to deformation is high due to a high degree of particle-to-particle bonding and interlocking (Cambi et al., 2015). This might have been the main reason that soil displacement and soil compaction did only occur to a minor extent, despite the selection of a sensitive site. Additionally, the payload of the machine was only half of the capacity (Figure 6-1), since only short wood logs were available at the study site for use during the experiment, leading to a gross mass of 21.5 Mg, compared to the fully loaded machine of approximately 26 Mg. Although these two factors are limiting the validity and transferability of our results, considering the pilot character of our study, still, considerable findings with respect to soil impacts were revealed.

6.4.3. *Compaction*

Soil bulk density increased by 3.3±9.4% compared to the pre-operational density of 0.74±0.1 Mg m^{-3}. This increase is low, compared to other findings, even considering the fact, that sampling took place on a pre-existing machine operating trail where machine traffic had already occurred. For example, Jamshidi et al. (2008) estimated an increase of soil bulk density of up to 48%, after harvesting operations were conducted. Labelle and Jaeger (2011) reported an average increase of soil bulk density of 19% after operations on sites without previous machine traffic. According to Daddow and Warrington (1983), the growth limiting soil bulk density would amount approximately to 1.50 Mg m^{-3} for the texture analysed in the current study (sand: 36±3%, silt: 36±7%, clay: 28±8%), which was not reached by far on the machine operating trail of this study.

Soil moisture is a main factor affecting compressibility of the soil and thus the resulting increase in soil bulk density (Terzaghi et al., 1996). When forest soils are dry, soil moisture content is affecting the appearing compaction during skidding operations in a very low content (Froehlich et al., 1980). Machine traffic on soils with high moisture content is known from the literature to increases soil bulk density until a distinct compaction. These patterns are likely to appear when water potential is above field capacity, leading to a significant increase in soil bulk density. The results of the recent study show a negligible increase in soil bulk density, what can have two reasons in general; the low volumetric water content and a relatively high pre-operational soil bulk density driven by previous operations conducted on the machine operating trail (McNabb et al., 2001). These reasons might also explain a lack of treatment effects (Garren et al., 2019). It can be assumed, that the pre-compaction on the track of the permanent machine operating trails caused by preceding operations was high and hampered additional compaction at the surveyed machine operating trail (Ampoorter et al., 2009). Besides that, pre-compaction of the cohesive-frictional soil may additionally influence occurring soil displacement through heavy forest machines (e.g. McNabb et al., 2001).

6.4.4. *Rutting process*

Within this study, overall soil displacement was negligible and a difference between treatments could not be observed within measured displacement of the mineral soil. The aluminium tracers moved only a few millimetres, which is very low compared to the results of (Haas et al., 2018), who measured tracer movements up to a few meters on inclined terrain. Soil displacement takes place in lateral, upwards and frontal direction, possibly resulting in rutting and bulging adjacent to the tracks (Poltorak et al., 2018). The rut depth measured in this study averaged to 27±7 mm. Moderate rutting, as measured within this field trial, was observed in other studies during dry conditions, too: The winch-assisted forwarders used in the field trial of (Garren et al., 2019) lead to a low overall rut depth of 0 to 95 mm on different slope classes, ranging from 27 to 38 ° (51% to 78%). Eliasson (2005) determined rut depth from 60 to 92 mm

after five machine passes of a forwarder with a weight of 37.8 Mg on a gently downhill slope. Average rutting depths under dry conditions were generally less than 100 mm even with heavy traffic, as in the study of Rollerson (1990), and raised up to 450 mm under wet conditions. Owende et al. (2002) considered ruts with a depth of up to 100 mm as allowable for an eco-efficient timber harvesting on sensitive sites.

Poltorak et al. (2018) reported soil moisture as a main factor influencing rut depth. High values in soil moisture result in soil conditions which make it susceptible to soil displacement. Deep ruts occurred predominantly in soils with a volumetric soil moisture above 50% (Poltorak et al., 2018). This underlines the suitable traffic conditions on our site during the experiment, with rather dry conditions, caused by the dry summer, despite being a site of usually restricted trafficability. Additionally, roots in the forest soil could reduce the rutting process (Poltorak et al., 2018; Engell, 2019). The effect of low volumetric soil moisture and a high occurrence of coarse roots in the test plots (not measured) are assumed to overcome the mitigating potential of the traction-assist in the present trial. This endorses that besides appropriate technology, also situational evaluation of site conditions by an experienced operator, are crucial in facilitating low impact timber harvesting operations. However, in order to fully quantify the benefits of traction-assist technology and appropriate operational setting, up-scaled investigations, considering differing site conditions are required.

6.5. Conclusions

The current study was able to confirm that traction-assist reduced wheel slippage during the trial conducted on a sensitive site in flat terrain. The results indicate, that the application of relatively high tensile force decreases wheel slippage markedly. Still, it was not possible to approve a mitigating effect on soil impacts on a wider scope. Reasons for the limited effect of the applied traction-assist in the presented field trial may be given by: (a) The underutilized payload capacity of the used forwarder, reaching only 50%. (b) The pre-compaction of the machine operating trail, which has been traversed during earlier operations, (c) favourable operational conditions such as low soil moisture and (d) a strong network of coarse roots, stabilizing mineral topmost soil. Still, traction-assist technology seems to bear great potential to reduce machine induced soil impacts under more unfavourable conditions.

Acknowledgements

This research received funding from the Bio-Based Industries Joint Undertaking under the EU's H2020 research and innovation program for the TECH4EFFECT project (grant agreement no. 720757) and was financially supported by Eva Mayr-Stihl Stiftung. The authors further acknowledge the support of the "Landesforsten Rheinland-Pfalz", providing the research site and experimental machine, as well as technical support through the entire team of the "Kompetenzzentrum Waldtechnik Landesforsten (KWL)", in particular Christoph Jager and Jürgen Pink. Further, we would like to acknowledge the help of Stefan Lieven and David Pörtner during the field data collection, as well as Dr. Martin Jansen and his team, namely Sylvia Bondzio, from the soil lab, Soil Science of Temperate Ecosystems, Georg-August-Universität Göttingen, for supporting the soil sample analysis. Additionally, we acknowledge the contribution of Prof. Dr. Friederike Lang and the entire team of the Chair of Soil Ecology at the University of Freiburg for the technical support during the study design and the equipment lending. We further appreciate the valuable comments of two anonymous reviewers, improving the overall quality of the article.

7. General discussion

The work presented in this dissertation focussed on the prediction of traffic-induced rutting on forest soil, especially through the application of the topography-derived depth-to-water (DTW) index. To this end, multiple investigations were undertaken: (1) occurring rut depth was related to predictions based on DTW, the topographic wetness index (TWI) and retrievals from terramechanical test procedures (**Chapter 2**). It was subsequently demonstrated, that measurements with the dual-mass cone penetrometer, penetration depth as well as a modified Cone Index (handheld Penetrologger) could successfully predict occurring ruts. (2) We extensively validated the DTW-derived prediction of soil strength, quantified with the modified Cone Index, and soil moisture on six study sites across Europe (**Chapter 3**). The conjectured season-adapted representation of moisture levels by DTW map-scenarios was not confirmed. (3) To overcome this limitation, machine learning models were trained to predict soil moisture, based on data containing DTW, TWI, soil maps and daily retrievals of soil moisture captured by the SMAP mission (Reichle et al., 2020a) (**Chapter 5**). This procedure, based on DEMs which are available for large parts of Europe (**Chapter 4**), and incorporating openly accessible moisture estimates. By utilizing different data sources, and a fusion of grids of different resolutions, the accuracy of predictions was significantly improved, resulting in 74% of accurately predicted **wet** values, compared to 38% accurate **wet** values predicted by DTW. The improved trafficability prediction can enhance the application of mitigating measures and improve upon the scheduling of forest operations. With having accurate predictions of soil state at hand, soil impacts can be held at a minimum, as shown during our field trial conducted on relatively dry ground (**Chapter 6**).

DTW-derived predictions of rutting were reported by several studies, with contradicting results. Vega-Nieva et al. (2009) showed that 65% of ruts with a depth of more than 25 cm were located in areas with a vertical proximity to ground water of less than 1 m, while 93% of such ruts occurred on areas with DTW values of less than 10 m. A high frequency of severe rut depth on several study sites in Norway was observed within areas where the DTW index was less than 1 m (Heppelmann et al.). In contrast, Mohtashami et al. (2017) could not confirm such patterns in a field trial, where the inclusion of DTW values did not improve the accuracy of a linear model fitted to various parameters, to describe the occurring extents and degrees of rut depth on machine operating trails. Ågren et al. (2014) valued the utilization of DTW maps to predict rutting as critical. Similar to the latter mentioned findings, the predictability of rut depth by means of DTW could not be confirmed in our field trial conducted in a temperate broadleaved stand (**Chapter 2, Figure 2-9**).

The lacking response between rut depth and DTW-values might be reasoned by the omission of characteristics of machine traffic, such as the type of forest machines used, type of operation, number of machine passes (Eliasson and Wästerlund, 2007), and experience of the drivers (Suvinen, 2006; Prinz et al., 2018). Moreover local disturbances, soil organic matter, soil texture, coarse fraction, soil's permeability, root network (Gerasimov and Katarov, 2010), and terrain characteristics determine the soil's susceptibility to deformations and other detrimental impacts (Case et al., 2005; Vega-Nieva et al., 2009; Jutras and A., 2011; White et al., 2012; Ågren et al., 2014; Mohtashami et al., 2017), but are not considered by the DTW concept. Thus, the creation of deep ruts may be too complex of a process to be predicted by one index (e.g. DTW) alone. It seems unlikely to be able to predict rutting using static map-scenarios of DTW across diverse operational settings conducted on a variety of site conditions. Better performance regarding the prediction of rut depth was accordingly reached when data was separated by study sites in the work of Mohtashami et al. (2017).

Although deep soils with high moisture levels, less coarse fraction, higher organic matter content and increasing litter depth (Murphy et al., 2011) were detectable by DTW in the survey of Campbell et al. (2013), the concept lacks of an adequate consideration of overall levels of soil moisture caused by

varying weather conditions. Adaptations to seasonal effects are intended to be addressed by the setting of generalized flow initiation areas (FIA, **Appendix III, section 3.3.3**). For scientific purposes, FIA was usually selected after the field trial was performed, orientated towards the best correlation and performance of the maps used (e.g. **section 2.2.4,** Echiverri and Ellen Macdonald, 2020). Such post impact selection of the most appropriate map-scenarios is not feasible for practical purposes. Forestry stakeholders have to choose in advance which individual map-scenario to use for a given operation. The assignment of distinct map-scenarios to "wet", "moist", "dry" and "very dry or frozen" conditions, according to Jones and Arp (2019), is imprecise and requires an approximation by the user of DTW-maps (**Chapter 2**). Moreover, soils are a heterogeneous natural resource allocated on highly structured topography (Liakos et al., 2018), with complex mechanisms of water accumulation, making the selection of an appropriate FIA a challenging task (White et al., 2012; Leach et al., 2017; Lidberg et al., 2020). Although DTW maps are already used by forest practitioners (e.g. J.D. Irving, Limited, New Brunswick, Canada; similar maps are openly available in Finland, Sweden and parts of Norway), the before-mentioned aspects might both impede the effectiveness of DTW-maps due to potentially defective assessments of present levels of soil moisture, and interfere with the conjectured solution to capture overall levels of soil moisture by universally set FIAs.

Current research showed the enhanced possibilities to accurately include present moisture conditions, enabled through the use of machine learning approaches for trafficability predictions (Pohjankukka et al., 2016; Bont et al., 2020; Lidberg et al., 2020; Melander et al., 2020; Salmivaara et al., 2020). Tree-based machine learning algorithms are able to represent non-linear relationships between predictor and response variables, based on the hierarchical structure of the model (Heung et al., 2016). By the application of such a model, the accuracy of prediction of wet soils could clearly be improved, as demonstrated in **Chapter 5**. Recent retrievals of soil moisture were made openly accessible by NASA (2021). Although these estimates were provided at a course grid cell size (9 by 9 km), the correlation between them and means of in-situ measurements of soil moisture at a site (**Figure 5-1**) point out a promising usage for trafficability predictions. Since a cautious prediction system is vital for successfully avoiding severe soil disturbances, **Chapter 5** set out to reduce deviations in predictions of wet soils made by binary values of DTW. This was achieved by the parametrization of machine learners and conservatively selecting hyperparameters to enable appropriate predictions on unseen data.

The use of machine learning approaches to improve the predictability of soils prone to severe deformations is envisioned to contribute to eco-efficient forest management. Through the knowledge of temporarily unfavourable operating conditions on sites, such sites can be avoided in the first place (Mattila and Tokola, 2019), without starting an operation, until it has to be stopped owing to severe and unsightly soil damage (**Chapter 2**). In addition, sufficient prediction of trafficability enables the appropriate planning of operations (Murphy et al., 2008; Sirén et al., 2019b), the definition of instructions for machine operators (D'Acqui et al., 2020) and optimized routing within the stand (Flisberg et al., 2021). Through advanced planning of operations per se (**Chapter 5**), as well as implementing a set of available tools (**section 1.3**: i-v), occurring soil damage can be kept to acceptably low extents and degrees. Although the application of winch-assistance did not result in reduced soil impacts, it was shown, that multiple passes with a loaded forwarder can result in low degrees of rut depth, when driving on relatively dry soils (**Chapter 6**).

In large parts of Central Europe, where machine traffic in forests is restricted to forest roads and machine operating trails (Ampoorter et al., 2009), an improved prediction of trafficability can especially ensure and maintain the technical functionality of machine operating trails, which act as permanent infrastructure, planned for reuse during multi-entry silvicultural treatments. Only if already existing machine operating trails continue to be trafficable, can machine-traffic be confined to these areas. The

extensive time required for soil recovery after traffic-induced compaction has occurred (Rab, 2004; Ampoorter et al., 2010), highlights the restriction of machine traffic to machine operating trails, to avoid negative consequences for water and gas permeability (Frey et al., 2009; Ebeling et al., 2017) soil fauna and biota (Beylich et al., 2010), tree regeneration (Wästerlund, 1985; Williamson and Neilsen, 2000) particularly on silty soils (Ampoorter et al., 2011) and growth of vegetation (DeArmond et al., 2021), including trees (Kozlowski, 1999). As shown in **Chapter 6** (**Table 6-6**), the traffic-induced soil impacts causing rutting and compaction can be kept at a minimum if machines drive on permanent machine operating trails under favourable conditions (i.e. dry soils). A rut depth increment of merely 0.5 cm was measured per pass of a loaded forwarder with a total mass of 21.5 Mg.

Especially in countries where forest operations are conducted in an area-wise fashion, adequate predictions of trafficability can contribute to avoiding heavy machine traffic crossing perennial and intermittent streams. Machine traffic on streams are frequently associated with severe damages, which lead to deleterious sediment transports into adjacent streams (Wit et al., 2014; Ågren et al., 2015). Considering DTW maps, buffer zones around stream networks could be delineated (Echiverri and Ellen Macdonald, 2020; Lidberg et al., 2020), but its implementation is still pending due to inaccurate planning material (Kuglerová et al., 2014; 2017). In line with the intensified conservation of stream networks, the avoidance of such could lead to lower extents and degrees of rut depth and compaction. The area-wise traffic in forest stands seems to trust to a recovery of the disturbed soil, as driven by self-mulching due to swelling clay or freeze-thaw cycles (DeArmond et al., 2021), and plant-root penetration in the upper soil (Bottinelli et al., 2014). Yet, the negative consequences for soils trafficked are inevitable and irreversible (Klaes et al., 2016), promoting the rigid utilization of predictive systems and possibly the introduction of permanent machine operating trails for sustainable forest management in national forest management practices (Vossbrink and Horn, 2004; Ampoorter et al., 2009).

The low demand of input data to create DTW maps fosters a large-scaled application of related predictive systems, but required digital elevation models (DEM) are currently retailed as commercial products from federal organizations in Germany (**Chapter 4**). The provision of a state-wide DEM with a cell size of 200 m is contained within Germany's obligations under the INSPIRE legislation (European Commission - Joint Research Centre, 2021b), and therefore exempted of any fees. The coarse grid cell size makes this openly accessible data unsuitable for all intents and purposes of trafficability predictions (Ågren et al., 2014). However, local institutions freely provide regional high-resolution DEMs under the INSPIRE umbrella, available at the national geoinformation portals already (**Chapter 4**). Openly accessible or commercially purchased DEMs can be used by researchers and individual institutions to create DTW maps (**Appendix IV**), but a state-wide provision of DTW maps, as already achieved in e.g. Sweden, is pending (**Chapter 4**). In order to fulfil the goals stated in the European Green Deal (European Commission - Joint Research Centre, 2019), as well as in the Forest strategy (European Commission - Joint Research Centre, 2021a), scientific intentions and practical applications addressing an environmental conservation should be supported through making various geospatial data openly accessible. Melander et al. (2020) highlighted the advantages of the forest data platform, as continuously available for the entire forest in Finland. It can be assumed that intentions aiming towards improved trafficability prediction and its application into forest management would benefit from a similar data availability in Central Europe.

8. General conclusions

Establishing a common system of trafficability prediction to support sustainable forest management would be a worthwhile endeavour. In this work, the application of different measures to be used to assess soil's susceptibility to traffic-induced deformations was demonstrated. Although terramechanical test procedures resulted in successful predictions of occurring rut depth following a harvesting operation, practical utilization of such tools seems questionable, owing to extensive efforts necessary for implementing them. Therefore, emphasis should be given to cartographic predictive systems, based on readily available input data. The validation of DTW-derived predictions using time-series of soil moisture and strength revealed the key aspect for accurate trafficability predictions – an appropriate inclusion of current levels of soil moisture. Herein, daily moisture retrievals from the SMAP mission were used to represent overall moisture conditions. Tree-based machine learners were trained on these moisture estimates, fused with DTW-maps and proved powerful in the prediction of forest soil state und thus trafficability. To be fully functional though, machine learning approaches rely upon large data sets, which are currently associated with labour intensive post-harvest monitoring. Machine-mounted sensors and the utilization of fieldbus data, capturing occurring soil impacts, can and will remedy such constraints and deeply change forest management, towards environmentally sound and eco-efficient forest operations.

9. References

Abbas, D., Di Fulvio, F., and Spinelli, R. (2017). European and United States perspectives on forest operations in environmentally sensitive areas. *Scandinavian Journal of Forest Research* 35, 1–14. doi: 10.1080/02827581.2017.1338355

Adams, H. D., Macalady, A. K., Breshears, D. D., Allen, C. D., Stephenson, N. L., Saleska, S. R., et al. (2010). Climate-Induced Tree Mortality: Earth System Consequences. *Eos, Transactions American Geophysical Union* 91. doi: 10.1029/2010EO170003

Agherkakli, B., Najafi, A., and Sadeghi, S. H. (2010). Ground based operation effects on soil disturbance by steel tracked skidder in a steep slope of forest. *Journal of forest science* 56, 278–284. doi: 10.17221/93/2009-JFS

Ågren, A., Larson, J., Paul, S. S., Laudon, H., and Lidberg, W. (2021). Use of multiple LIDAR-derived digital terrain indices and machine learning for high-resolution national-scale soil moisture mapping of the Swedish forest landscape. *Geoderma* 404, 115280. doi: 10.1016/j.geoderma.2021.115280

Ågren, A., Lidberg, W., and Ring, E. (2015). Mapping Temporal Dynamics in a Forest Stream Network—Implications for Riparian Forest Management. *Forests* 6, 2982–3001. doi: 10.3390/f6092982

Ågren, A., Lidberg, W., Strömgren, M., Ogilvie, J., and Arp, P. (2014). Evaluating digital terrain indices for soil wetness mapping – a Swedish case study. *Hydrology and Earth System Sciences* 18, 3623–3634. doi: 10.5194/hess-18-3623-2014

Akumu, C. E., Baldwin, K., and Dennis, S. (2019). GIS-based modeling of forest soil moisture regime classes: Using Rinker Lake in northwestern Ontario, Canada as a case study. *Geoderma* 351, 25–35. doi: 10.1016/j.geoderma.2019.05.014

Ala-Ilomäki, J., Lindeman, H., Mola-Yudego, B., Prinz, R., Väätäinen, K., Talbot, B., et al. (2021). The effect of bogie track and forwarder design on rut formation in a peatland. *International Journal of Forest Engineering* 45, 1–8. doi: 10.1080/14942119.2021.1935167

Ala-Ilomäki, J., Salmivaara, A., Launiainen, S., Lindeman, H., Kulju, S., Finér, L., et al. (2020). Assessing extraction trail trafficability using harvester CAN-bus data. *International Journal of Forest Engineering* 31, 138–145. doi: 10.1080/14942119.2020.1748958

Alberdi, I., Bender, S., Riedel, T., Avitable, V., Boriaud, O., Bosela, M., et al. (2020). Assessing forest availability for wood supply in Europe. *Forest Policy and Economics* 111, 102032. doi: 10.1016/j.forpol.2019.102032

Albizu-Urionabarrenetxea, P., Tolosana-Esteban, E., and Roman-Jordan, E. (2013). Safety and health in forest harvesting operations. Diagnosis and preventive actions. A review. *The Forestry Chronicle* 22, 392. doi: 10.5424/fs/2013223-02714

Alpine convention (1995). *Übereinkommen zum Schutz der Alpen: Alpenkonvention*.

Alpine convention (1998). *Protocol on the implementation of the alpine convention of 1991 in the domain of soil conservation: Protocol on soil conservation*.

Ampoorter, E., Frenne, P. de, Hermy, M., and Verheyen, K. (2011). Effects of soil compaction on growth and survival of tree saplings: A meta-analysis. *Basic and Applied Ecology* 12, 394–402. doi: 10.1016/j.baae.2011.06.003

Ampoorter, E., Schrijver, A. de, van Nevel, L., Hermy, M., and Verheyen, K. (2012). Impact of mechanized harvesting on compaction of sandy and clayey forest soils: results of a meta-analysis. *Annals of forest science* 69, 533–542. doi: 10.1007/s13595-012-0199-y

Ampoorter, E., van Nevel, L., Vos, B. de, Hermy, M., and Verheyen, K. (2010). Assessing the effects of initial soil characteristics, machine mass and traffic intensity on forest soil compaction. *Forest Ecology and Management* 260, 1664–1676. doi: 10.1016/j.foreco.2010.08.002

Ampoorter, E., Verheyen, K., and Hermy, M. (2009). Soil damage after mechanized harvesting: Results of a meta-analysis. *Proceedings of the 2009 Council on Forest Engineering (COFE) Conference Proceedings:"Environmentally Sound Forest Operations", Lake Tahoe, CA, USA*. doi: 10.1007/s13595-012-0199-y

Andersson, J., Bodin, K., Lindmark, D., Servin, M., and Wallin, E. (2021). Reinforcement Learning Control of a Forestry Crane Manipulator. *arXiv:2103.02315v1*.

Arbeitsgemeinschaft der Vermessungsverwaltungen der Länder der Bundesrepublik Deutschland (2021). *ATKIS®-Digitale Geländemodelle [ATKIS-Digital elevation modells]*. Accessed November 08, 2021, http://www.adv-online.de/AdV-Produkte/Geotopographie/Digitale-Gelaendemodelle/

Arvidsson, J., and Keller, T. (2007). Soil stress as affected by wheel load and tyre inflation pressure. *Soil and Tillage Research* 96, 284–291. doi: 10.1016/j.still.2007.06.012

Arvidsson, J., Sjöberg, E., and van den Akker, J. J.H. (2003). Subsoil compaction by heavy sugarbeet harvesters in southern Sweden. *Soil and Tillage Research* 73, 77–87. doi: 10.1016/S0167-1987(03)00101-6

Awaida, A., and Westervelt, J. (2020). Geographic Resources Analysis Support System (GRASS GIS). USA: Geographic Resources Analysis Support System (GRASS GIS) Software, https://grass.osgeo.org

Baltensweiler, A., Walthert, L., Hanewinkel, M., Zimmermann, S., and Nussbaum, M. (2021). Machine learning based soil maps for a wide range of soil properties for the forested area of Switzerland. *Geoderma Regional* 27, e00437. doi: 10.1016/j.geodrs.2021.e00437

Bartels, S. F., Caners, R. T., Ogilvie, J., White, B., and Macdonald, S. E. (2018). Relating Bryophyte Assemblages to a Remotely Sensed Depth-to-Water Index in Boreal Forests. *Front Plant Sci* 9. doi: 10.3389/fpls.2018.00858

Bavarian State Institute of Forestry (2012). *Bodenschutz beim Forstmaschineneinsatz [Soil protection during forest operations]*. Freising.

Berendt, F., Fortin, M., Jaeger, D., and Schweier, J. (2017). How Climate Change Will Affect Forest Composition and Forest Operations in Baden-Württemberg—A GIS-Based Case Study Approach. *Forests* 8, 298. doi: 10.3390/f8080298

Bethmann, S., and Wurster, M. (2016). Zum Image der Forstwirtschaft [Image of forestry]. *AFZ-DerWald* 3, 38–42.

Beven, K. J., and Kirkby, M. J. (1979). A physically based, variable contributing area model of basin hydrology / Un modèle à base physique de zone d'appel variable de l'hydrologie du bassin versant. *Hydrological Sciences Bulletin* 24, 43–69. doi: 10.1080/02626667909491834

Beylich, A., Oberholzer, H.-R., Schrader, S., Höper, H., and Wilke, B.-M. (2010). Evaluation of soil compaction effects on soil biota and soil biological processes in soils. *Soil and Tillage Research* 109, 133–143. doi: 10.1016/j.still.2010.05.010

Bezirksregierung Köln (2020). *Digitales Geländemodell DGM1 [Digital elevation model]*. Accessed November 08, 2021, https://www.bezreg-koeln.nrw.de/brk_internet/geobasis/hoehenmodelle/digitale_gelaendemodelle/gelaendemodell/index.html

Bishop, K., Seibert, J., Nyberg, L., and Rodhe, A. (2011). Water storage in a till catchment. II: Implications of transmissivity feedback for flow paths and turnover times. *Hydrological Processes* 25, 3950–3959. doi: 10.1002/Hyp.8355

Bivand, R. S. (2021). rgrass7: Interface Between GRASS 7 Geographical Information System and R, https://CRAN.R-project.org/package=rgrass7

Bivand, R. S., Pebesma, E. J., and Virgilio Gomez-Rubio (2013). *Applied spatial data analysis with R, Second edition*. New York: Springer.

Bivand, R. S., Tim Keitt, and Barry Rowlingson (2021). rgdal: Bindings for the 'Geospatial' Data Abstraction Library, https://CRAN.R-project.org/package=rgdal

Bjelanovic, I., Comeau, P., and White, B. (2018). High Resolution Site Index Prediction in Boreal Forests Using Topographic and Wet Areas Mapping Attributes. *Forests* 9, 113. doi: 10.3390/f9030113

BMDW (2010). *Bundesministerium für Digitalisierung und Wirtschaftsstandort. Bundesgesetz über eine umweltrelevante Geodateninfrastruktur des Bundes (Geodateninfrastrukturgesetz – GeoDIG) StF: BGBl. I Nr. 14/2010 (NR: GP XXIV RV 400 AB 590 S. 53. BR: 8276 AB 8279 S. 781.) [CELEX-Nr. 32007L0002]: Gesamte Rechtsvorschrift für Geodateninfrastrukturgesetz.*

Bont, L. G., Fischer, C., and Fraefel, M., Baltensweiler, A. (2020). Mapping soil trafficability with statistical models and machine learning algorithms. *SNS CAR NB NORD Conference* 22.-24.09.2020.

Botta, G. F., Becerra, A. T., and Tourn, F. B. (2009). Effect of the number of tractor passes on soil rut depth and compaction in two tillage regimes. *Soil and Tillage Research* 103, 381–386. doi: 10.1016/j.still.2008.12.002

Bottinelli, N., Hallikainen, V., Goutal, N., Bonnaud, P., and Ranger, J. (2014). Impact of heavy traffic on soil macroporosity of two silty forest soils: Initial effect and short-term recovery. *Geoderma* 217-218, 10–17. doi: 10.1016/j.geoderma.2013.10.025

Breidenbach, J., McRoberts, R. E., Alberdi, I., Antón-Fernández, C., and Tomppo, E. (2021). A century of national forest inventories – informing past, present and future decisions. *Forest Ecosystems* 8. doi: 10.1186/s40663-021-00315-x

Breiman, L. (2001). Random forests. *Machine Learning* 45, 5–32. doi: 10.1023/A:1010933404324

Brown, M., Ghaffariyan, M. R., Berry, M., Acuna, M., Strandgard, M., and Mitchell, R. (2020). The progression of forest operations technology and innovation. *Australian Forestry* 83, 1–3. doi: 10.1080/00049158.2020.1723044

Bundesamt für Kartographie und Geodäsie (2017). *Tasks and Organization.* Accessed May 18, 2017, https://www.bkg.bund.de/EN/About-BKG/Tasks-and-Organization/tasks-and-organization.html

Bygdén, G., Eliasson, L., and Wästerlund, I. (2003). Rut depth, soil compaction and rolling resistance when using bogie tracks. *Journal of Terramechanics* 40, 179–190. doi: 10.1016/j.jterra.2003.12.001

Cambi, M., Certini, G., Neri, F., and Marchi, E. (2015). The impact of heavy traffic on forest soils: A review. *Forest Ecology and Management* 338, 124–138. doi: 10.1016/j.foreco.2014.11.022

Campbell, D. M.H., White, B., and Arp, P. (2013). Modeling and mapping soil resistance to penetration and rutting using LiDAR-derived digital elevation data. *Journal of Soil and Water Conservation* 68, 460–473. doi: 10.2489/jswc.68.6.460

Canillas, E. C., and Salokhe, V. M. (2002). A decision support system for compaction assessment in agricultural soils. *Soil and Tillage Research* 65, 221–230. doi: 10.1016/S0167-1987(02)00002-8

Case, B. S., Meng, F.-R., and Arp, P. (2005). Digital elevation modelling of soil type and drainage within small forested catchments. *Canadian Journal of Soil Science* 85, 127–137. doi: 10.4141/S04-008

Cavalli, R., and Amishev, D. (2019). Steep terrain forest operations – challenges, technology development, current implementation, and future opportunities. *International Journal of Forest Engineering* 21, 1–7. doi: 10.1080/14942119.2019.1603030

Chen, T., He, T., Benesty, M., Khotilovich, V., Tang, Y., Cho, H., et al. (2021). *xgboost: Extreme Gradient Boosting.* Accessed November 09, 2021, https://CRAN.R-project.org/package=xgboost

Coleman, T. L., Agbu, P. A., and Montgomery, O. L. (1993). Spectral differentiation of surface soils and soil properties: Is it possible from space platforms? *Soil Science* 155, 283–293.

Cooperation OGD Österreich (2021). *Open Data Österreich.* Accessed June 14, 2021, https://www.data.gv.at/

Crawford, L. J., Heinse, R., Kimsey, M. J., and Page-Dumroese, D. S. (2021). Soil Sustainability and Harvest Operations. *General Technical Report RMRS.* doi: 10.2737/RMRS-GTR-421

Creative Optimization AB (2021). *Timbertrail - A new road in the forest with Timbertrail*. Accessed November 08, 2021, https://creativeoptimization.se/en/solutions/timbertrail/#timbertrail

D'Acqui, L. P., Certini, G., Cambi, M., and Marchi, E. (2020). Machinery's impact on forest soil porosity. *Journal of Terramechanics* 91, 65–71. doi: 10.1016/j.jterra.2020.05.002

Daddow, R. L., and Warrington, G. (1983). *Growth-limiting soil bulk densities as influenced by soil texture*. Fort Collins, Colorado: USDA Forest Service.

Danielsson, S. "Mistra Digital Forest - Keynotes," in *Mistra Digital Forest 2021*.

David Suits, L., Sheahan, T. C., Chen, D.-H., Lin, D.-F., Liau, P.-H., and Bilyeu, J. (2005). A Correlation Between Dynamic Cone Penetrometer Values and Pavement Layer Moduli. *Geotechnical Testing Journal* 28, 42–49. doi: 10.1520/GTJ12312

DeArmond, D., Ferraz, J., and Higuchi, N. (2021). Natural Recovery of Skid Trails. A Review. *Canadian Journal of Forest Research*. doi: 10.1139/cjfr-2020-0419

Dobos, E., Montanarella, L., Nègre, T., and Micheli, E. (2001). A regional scale soil mapping approach using integrated AVHRR and DEM data. *International Journal of Applied Earth Observation and Geoinformation* 3, 30–42. doi: 10.1016/S0303-2434(01)85019-4

Durner, W., Iden, S. C., and Unold, G. von (2017). The integral suspension pressure method (ISP) for precise particle-size analysis by gravitational sedimentation. *Water Resources Research* 53, 33–48. doi: 10.1002/2016WR019830

DWD (2019a). *Deutscher Klimaatlas*. Accessed July 24, 2019, https://www.dwd.de/DE/klimaumwelt/klimaatlas/klimaatlas_node.html

DWD (2019b). *Niederschlag: vieljährige Mittelwerte 1981 - 2010*. Accessed September 23, 2020, https://www.dwd.de/DE/leistungen/klimadatendeutschland/mittelwerte/nieder_8110_fest_html.html?view=nasPublication&nn=16102

Ebeling, C., Fründ, H.-C., Lang, F., and Gaertig, T. (2017). Evidence for increased P availability on wheel tracks 10 to 40 years after forest machinery traffic. *Geoderma* 297, 61–69. doi: 10.1016/j.geoderma.2017.03.003

Echiverri, L. F.I., and Ellen Macdonald, S. (2020). A topographic moisture index explains understory vegetation response to retention harvesting. *Forest Ecology and Management* 474, 118358. doi: 10.1016/j.foreco.2020.118358

Edlund, J., Keramati, E., and Servin, M. (2013). A long-tracked bogie design for forestry machines on soft and rough terrain. *Journal of Terramechanics* 50, 73–83. doi: 10.1016/j.jterra.2013.02.001

EFFORTE (2018). *Efficient forestry for sustainable and cost-competitive bio-based industry*. Accessed May 10, 2021, https://www.luke.fi/efforte/partners/

Eijkelkamp Agrisearch Equipment (2013). *User Manual for the Moisture Meter type HH2*. Accessed August 07, 2020, https://www.eijkelkamp.com/download.php?file=M1142602e_Soil_moisture_meter_f1ab.pdf

Eijkelkamp Agrisearch Equipment (2020). *Field inspection Vane tester*. Accessed September 29, 2020, https://en.eijkelkamp.com/products/field-measurement-equipment/field-inspection-vane-tester.html

Eklöf, K., Schelker, J., Sørensen, R., Meili, M., Laudon, H., Brömssen, C. von, et al. (2014). Impact of forestry on total and methyl-mercury in surface waters: distinguishing effects of logging and site preparation. *Environmental science & technology* 48, 4690–4698. doi: 10.1021/es404879p

Eliasson, L. (2005). Effects of forwarder tyre pressure on rut formation and soil compaction. *Silva Fennica* 39, 549–557. doi: 10.14214/sf.366

Eliasson, L., and Wästerlund, I. (2007). Effects of slash reinforcement of strip roads on rutting and soil compaction on a moist fine-grained soil. *Forest Ecology and Management* 252, 118–123. doi: 10.1016/j.foreco.2007.06.037

Engell, H.-M. (2019). *Untersuchung der armierenden Wirkung von Wurzelsystemen in der Humusauflage von Fichtenwäldern auf Mineralböden aus Löss [Investigation of the reinforcing effect*

of root systems in the humus layer of spruce forests on mineral soils from loess]. Master thesis. Göttingen: University of Göttingen.

Engler, B., Hoffmann, S., and Zscheile, M. (2021). Rubber tracked bogie-axles with supportive rollers – a new undercarriage concept for log extraction on sensitive soils. *International Journal of Forest Engineering* 32, 43–56. doi: 10.1080/14942119.2021.1834814

Entekhabi, D., Yueh, S., and Lannoy, G. de (2014). *SMAP handbook: Soil Moisture Active Passive*. Accessed November 08, 2021, https://lirias.kuleuven.be/retrieve/526486

European Commission - Joint Research Centre (2004). *European Soil Data Centre (ESDAC)*. Accessed November 09, 2021, https://esdac.jrc.ec.europa.eu

European Commission - Joint Research Centre (2019). *A European Green Deal.* Accessed November 09, 2021, https://ec.europa.eu/info/strategy/priorities-2019-2024/european-green-deal_de

European Commission - Joint Research Centre (2021a). *EU-Forststrategie: Hochwertige Bewirtschaftung der EU-Wälder und Waldgebiete [Future EU Forest strategy: High-quality management of EU forests and woodlands]*. Accessed November 09, 2021, https://www.europarl.europa.eu/news/de/press-room/20201002IPR88442/eu-forststrategie-hochwertige-bewirtschaftung-der-eu-walder-und-waldgebiete

European Commission - Joint Research Centre (2021b). *INSPIRE*. Accessed November 09, 2021, https://inspire.ec.europa.eu/about-inspire/563

European Commission and the European Soil Bureau Network (2004). *The European Soil Database distribution version V2.0: Attributes of the SGDBE version 4 beta.* Accessed November 09, 2021, https://esdac.jrc.ec.europa.eu/ESDB_Archive/ESDBv2/popup/sg_attr.htm

Farzaneh, B., Almassi, M., Sadeghi, M., and Minaei, S. (2012). Assessment of Soil Compaction Bulk Density Indices and Cone Index in Different Moistures and Depths for Application in Precise Tillage. *World Applied Sciences Journal* 20, 1704–1712. doi: 10.5829/idosi.wasj

Fassnacht, F. E., Latifi, H., Stereńczak, K., Modzelewska, A., Lefsky, M., Waser, L. T., et al. (2016). Review of studies on tree species classification from remotely sensed data. *Remote Sensing of Environment* 186, 64–87. doi: 10.1016/j.rse.2016.08.013

Feldwisch, N., and Friedrich, C. (2016). *Schädliche Bodenverdichtug vermeiden [Avoiding soil damages]*, https://publikationen.sachsen.de/bdb/artikel/26307

Finnish Meteorological Institute (2021). *Observation stations*. Accessed May 05, 2021, https://en.ilmatieteenlaitos.fi/observation-stations?filterKey=groups&filterQuery=precipitation

Fjeld, D., and Østby-Berntsen, Ø. (2020). The effects of an auxiliary axle on forwarder rut development – a Norwegian field study. *International Journal of Forest Engineering* 31, 192–196. doi: 10.1080/14942119.2020.1765645

Flisberg, P., Rönnqvist, M., Willén, E., Frisk, M., and Friberg, G. (2021). Spatial optimization of ground-based primary extraction routes using the BestWay decision support system. *Canadian Journal of Forest Research* 51, 675–691. doi: 10.1139/cjfr-2020-0238

Fox, J., and Weisberg, S. (2019). *An R Companion to Applied Regression*, https://socialsciences.mcmaster.ca/jfox/Books/Companion/

Frey, B., Kremer, J., Rüdt, A., Sciacca, S., Matthies, D., and Lüscher, P. (2009). Compaction of forest soils with heavy logging machinery affects soil bacterial community structure. *European Journal of Soil Biology* 45, 312–320. doi: 10.1016/j.ejsobi.2009.05.006

Froehlich, H. A., Azevedo, J., Cafferata, P., and Lysne, D. (1980). *Predicting soil compaction on forested land: Final Project Report to U.S. Forest Service.* Corvallis, Oregon.

Gabbert, C. C., Gazal, K., and McNeel, J. (2020). Economic Contributions of West Virginia's Forest Products Industry Over Time: A Look at 2006, 2010, 2015, and 2017 Data. *Forest Products Journal* 70, 200–212. doi: 10.13073/FPJ-D-19-00052

Garren, A. M., Bolding, M. C., Aust, W. M., Moura, A. C., and Barrett, S. M. (2019). Soil Disturbance Effects from Tethered Forwarding on Steep Slopes in Brazilian Eucalyptus Plantations. *Forests* 10, 721. doi: 10.3390/f10090721

Gelin, O., and Björheden, R. (2020). Concept evaluations of three novel forwarders for gentler forest operations. *Journal of Terramechanics* 90, 49–57. doi: 10.1016/j.jterra.2020.04.002

Geologian tutkimuskeskus luo geologisella osaamisella ratkaisuja (2019). *Maankamara [Soil mappings]*. Accessed November 08, 2021, https://gtkdata.gtk.fi/Maankamara/index.html

Geologischer Dienst NRW (2019). *Die Erdgeschichte unseres Landes [Earth history Germany]*. Accessed August 27, 2019, https://www.gd.nrw.de/ge_ev_stratigraphie.htm

Gerasimov, Y., and Katarov, V. (2010). Effect of bogie track and slash reinforcement on sinkage and soil compaction in soft terrains. *Croatian journal of forest engineering* 31, 35–45.

Goutal, N., Renault, P., and Ranger, J. (2013). Forwarder traffic impacted over at least four years soil air composition of two forest soils in northeast France. *Geoderma* 193-194, 29–40. doi: 10.1016/j.geoderma.2012.10.012

Goutal-Pousse, N., Bonnaud, P., Demaison, J., Nourrisson, G., George, P., and Ranger, J. “Soil compaction on two sensitive sites in north-eastern France and natural or assisted recovery processes,” in *Forest Engineering Conference 2014*.

Grabs, T., Seibert, J., Bishop, K., and Laudon, H. (2009). Modeling spatial patterns of saturated areas: A comparison of the topographic wetness index and a dynamic distributed model. *Journal of Hydrology* 373, 15–23. doi: 10.1016/j.jhydrol.2009.03.031

Grüll, M. (2011). Den Waldboden schonen–Vorsorgender Bodenschutz beim Einsatz von Holzerntetechnik [Soil protection in forest operations]. *Eberswalder Forstliche Schriftenreihe* 47, 37–44.

GSM Association (2021). *Mobile Network Coverage Maps*. Accessed June 15, 2021, https://www.gsma.com/coverage/#463

Haas, J., Fenner, P. T., Schack-Kirchner, H., and Lang, F. (2018). Quantifying soil movement by forest vehicles with corpuscular metal tracers. *Soil and Tillage Research* 181, 19–28. doi: 10.1016/j.still.2018.03.012

Haas, J., Hagge Ellhöft, K., Schack-Kirchner, H., and Lang, F. (2016). Using photogrammetry to assess rutting caused by a forwarder—A comparison of different tires and bogie tracks. *Soil and Tillage Research* 163, 14–20. doi: 10.1016/j.still.2016.04.008

Han, H.-S., Page-Dumroese, D. S., Han, S.-K., and Tirocke, J. (2006). Effects of Slash, Machine Passes, and Soil Moisture on Penetration Resistance in a Cut-to-length Harvesting. *International Journal of Forest Engineering* 17, 11–24. doi: 10.1080/14942119.2006.10702532

Hastie, T. (2020). *gam: Generalized Additive Models*. Accessed November 09, 2021, https://CRAN.R-project.org/package=gam

Heiskanen, J., Hallikainen, V., Salmivaara, A., Uusitalo, J., and Ilvesniemi, H. (2020). Predictive models to determine fine soil fractions and organic matter from readily available soil and terrain data of soils under boreal forest. *Geoderma Regional* 20, e00251. doi: 10.1016/j.geodrs.2019.e00251

Hengl, T., Nussbaum, M., Wright, M. N., Heuvelink, G. B. M., and Gräler, B. (2018). Random forest as a generic framework for predictive modeling of spatial and spatio-temporal variables. *PeerJ* 6, e5518. doi: 10.7717/peerj.5518

Heppelmann, J. B., Talbot, B., and Astrup, R. “Assessing the relationship between depth-to-water mapping and rut formation, following fully mechanized harvesting operations in Norway,” in *NB NORD 2020*.

Heubaum, F. (2015a). Bodenscherfestigkeit auf Rückegassen [Shear strength of forest soils on machine operating trails]. *Forst & Technik* 8, 18–22.

Heubaum, F. (2015b). *Bodenschutz im Staatsbetrieb Sachsenforst [Soil protection]: Projekte zur Technologieerprobung*. Accessed November 05, 2021, https://www.sbs.sachsen.de/download/Bodenschutz_Projekte_2015_09_30.pdf

Heung, B., Ho, H. C., Zhang, J., Knudby, A., Bulmer, C. E., and Schmidt, M. G. (2016). An overview and comparison of machine-learning techniques for classification purposes in digital soil mapping. *Geoderma* 265, 62–77. doi: 10.1016/j.geoderma.2015.11.014

Hijmans, R. J. (2020). raster: Geographic Data Analysis and Modeling, https://CRAN.R-project.org/package=raster

Hillel, D. (1998). *Environmental soil physics: Fundamentals, applications, and environmental considerations*. San Diego, California: Elsevier.

Holzfeind, T., Kanzian, C., Stampfer, K., and Holzleitner, F. (2019). Assessing Cable Tensile Forces and Machine Tilt of Winch-Assisted Forwarders on Steep Terrain under Real Working Conditions. *Croatian journal of forest engineering* 40, 281–296. doi: 10.5552/crojfe.2019.621

Holzfeind, T., Visser, R., Chung, W., Holzleitner, F., and Erber, G. (2020). Development and Benefits of Winch-Assist Harvesting. *Current Forestry Reports* 6, 201–209. doi: 10.1007/s40725-020-00121-8

Holzleitner, F., Kastner, M., Stampfer, K., Höller, N., and Kanzian, C. (2018). Monitoring Cable Tensile Forces of Winch-Assist Harvester and Forwarder Operations in Steep Terrain. *Forests* 9, 53. doi: 10.3390/f9020053

Horn, R., Vossbrink, J., Peth, S., and Becker, S. (2007). Impact of modern forest vehicles on soil physical properties. *Forest Ecology and Management* 248, 56–63. doi: 10.1016/j.foreco.2007.02.037

Hu, Z., Islam, S., and Cheng, Y. (1997). Statistical characterization of remotely sensed soil moisture images. *Remote Sensing of Environment* 61, 310–318. doi: 10.1016/S0034-4257(97)89498-9

IMGW-PIB (2021). *Observation stations*. Accessed May 05, 2021, https://www.imgw.pl/en/institute/imgw-pib

IUSS Working Group WRB (2015). World reference base for soil resources 2014, update 2015: International soil classification system for naming soils and creating legends for soil maps. *World Soil Resources Reports* 106.

Ivanovs, J., and Lupikis, A. (2018). Identification of wet areas in forest using remote sensing data. *Agronomy Research* 16, 2049–2055. doi: 10.15159/AR.18.192

Jacke, H., Brokmeier, H., and Hittenbeck, J. (2015). Bogiebänder:(Be-) Drückende Probleme [Bogie tracks: drawbacks]. *Forsttechnische Informationen* 67, 4–7.

Jacke, H., Hittenbeck, J., and Stiehm, C. (2011). Spuren im Wald - Zur Spurrillen-Diskussion um und auf Rückegassen [Discussion about rutting]. *ifa Schriftenreihe* 9.

Jamshidi, R., Jaeger, D., Raafatnia, N., and Tabari, M. (2008). Influence of Two Ground-Based Skidding Systems on Soil Compaction Under Different Slope and Gradient Conditions. *International Journal of Forest Engineering* 19, 9–16. doi: 10.1080/14942119.2008.10702554

Jenkins, M. J., Hebertson, E., Page, W., and Jorgensen, C. A. (2008). Bark beetles, fuels, fires and implications for forest management in the Intermountain West. *Forest Ecology and Management* 254, 16–34. doi: 10.1016/j.foreco.2007.09.045

Jones, M.-F. *Mapping soil trafficability by way of temporal hydrology modeling and spatial Wet-Areas-Mapping*. Dissertation. Fredericton, Canada: University of New Brunswick, Forestry and Environmental Management.

Jones, M.-F., and Arp, P. (2017). Relating Cone Penetration and Rutting Resistance to Variations in Forest Soil Properties and Daily Moisture Fluctuations. *Open Journal of Soil Science* 07, 149–171. doi: 10.4236/ojss.2017.77012

Jones, M.-F., and Arp, P. (2019). Soil Trafficability Forecasting. *Open Journal of Forestry* 9, 296–322. doi: 10.4236/ojf.2019.94017

Jourgholami, M., and Labelle, E. R. (2020). Effects of plot length and soil texture on runoff and sediment yield occurring on machine-trafficked soils in a mixed deciduous forest. *Annals of forest science* 77, 1734. doi: 10.1007/s13595-020-00938-0

Jutras, M.-F., and A., P. (2011). Determining Hydraulic Conductivity from Soil Characteristics with Applications for Modelling Stream Discharge in Forest Catchments. *Hydraulic Conductivity - Issues, Determination and Applications*, 189–202. doi: 10.5772/20309

Kankare, V., Luoma, V., Saarinen, N., Peuhkurinen, J., Holopainen, M., and Vastaranta, M. (2019). Assessing feasibility of the forest trafficability map for avoiding rutting – a case study. *Silva Fennica* 53. doi: 10.14214/sf.10197

Kartverket (2021). *Program for omløpsfotografering [Orbital Photography Program]*. Accessed November 08, 2021, https://kartverket.no/geodataarbeid/program-for-omlopsfotografering

Keller, T., Défossez, P., Weisskopf, P., Arvidsson, J., and Richard, G. (2007). SoilFlex: A model for prediction of soil stresses and soil compaction due to agricultural field traffic including a synthesis of analytical approaches. *Soil and Tillage Research* 93, 391–411. doi: 10.1016/j.still.2006.05.012

Keskin, H., Grunwald, S., and Harris, W. G. (2019). Digital mapping of soil carbon fractions with machine learning. *Geoderma* 339, 40–58. doi: 10.1016/j.geoderma.2018.12.037

Kirilenko, A. P., and Sedjo, R. A. (2007). Climate change impacts on forestry. *Proceedings of the National Academy of Sciences of the United States of America* 104, 19697–19702. doi: 10.1073/pnas.0701424104

Klaes, B., Struck, J., Schneider, R., and Schüler, G. (2016). Middle-term effects after timber harvesting with heavy machinery on a fine-textured forest soil. *European Journal of Forest Research* 135, 1083–1095. doi: 10.1007/s10342-016-0995-2

Kozlowski, T. T. (1999). Soil Compaction and Growth of Woody Plants. *Scandinavian Journal of Forest Research* 14, 596–619. doi: 10.1080/02827589908540825

Kristensen, J. A., Balstrøm, T., Jones, R. J. A., Jones, A., Montanarella, L., Panagos, P., et al. (2019). Development of a harmonised soil profile analytical database for Europe: a resource for supporting regional soil management. *SOIL* 5, 289–301. doi: 10.5194/soil-5-289-2019

Krumsteds, L. L., Ivanovs, J., Jansons, J., and Lazdins, A. (2019). Development of Latvian land use and land use change matrix using geospatial data of National forest inventory. 741.3Kb. *EMU DSpace* 17, 2295–2305. doi: 10.15159/AR.19.195

Kuglerová, L., Ågren, A., Jansson, R., and Laudon, H. (2014). Towards optimizing riparian buffer zones: Ecological and biogeochemical implications for forest management. *Forest Ecology and Management* 334, 74–84. doi: 10.1016/j.foreco.2014.08.033

Kuglerová, L., Hasselquist, E. M., Richardson, J. S., Sponseller, R. A., Kreutzweiser, D. P., and Laudon, H. (2017). Management perspectives on Aqua incognita : Connectivity and cumulative effects of small natural and artificial streams in boreal forests. *Hydrological Processes* 31, 4238–4244. doi: 10.1002/hyp.11281

Kuhn, M. (2020). *caret: Classification and Regression Training*. Accessed November 09, 2021, https://CRAN.R-project.org/package=caret

Kumar, A., Chen, Y., Sadek, A., and Rahman, S. (2012). Soil cone index in relation to soil texture, moisture content, and bulk density for no-tillage and conventional tillage. *CIGR Journal* 14, 26–37.

Kuratorium für Waldarbeit und Forsttechnik e.V. “Umweltgerechte Bewirtschaftung nasser Waldstandorte [Environmentally sound forestry on wet sites],” in *KWF-Thementage 2013*.

Kurczyński, Z., and Bakuła, K. (2013). “The selection of aerial laser scanning parameters for countrywide digital elevation model creation,” in *13th SGEM GeoConference on Informatics, Geoinformatics and Remote Sensing. SGEM2013 Conference Proceedings*, 695–702.

Labelle, E. R., and Jaeger, D. (2011). Soil Compaction Caused by Cut-to-Length Forest Operations and Possible Short-Term Natural Rehabilitation of Soil Density. *Soil Science Society of America Journal* 75, 2314–2329. doi: 10.2136/sssaj2011.0109

Labelle, E. R., and Jaeger, D. (2018). Management Implications of Using Brush Mats for Soil Protection on Machine Operating Trails during Mechanized Cut-to-Length Forest Operations. *Forests* 10, 19. doi: 10.3390/f10010019

Labelle, E. R., and Jaeger, D. (2019). Effects of steel flexible tracks on forwarder peak load distribution: Results from a prototype load test platform. *Croatian journal of forest engineering* 40, 1–23.

Labelle, E. R., Jaeger, D., and Poltorak, B. J. (2015). Assessing the Ability of Hardwood and Softwood Brush Mats to Distribute Applied Loads. *Croatian journal of forest engineering* 36, 227–242.

Labelle, E. R., and Kammermeier, M. (2019). Above- and belowground growth response of Picea abies seedlings exposed to varying levels of soil relative bulk density. *European Journal of Forest Research* 138, 705–722. doi: 10.1007/s10342-019-01201-6

Labelle, E. R., Poltorak, B. J., and Jaeger, D. (2019). The role of brush mats in mitigating machine-induced soil disturbances: An assessment using absolute and relative soil bulk density and penetration resistance. *Canadian Journal of Forest Research* 49, 164–178. doi: 10.1139/cjfr-2018-0324

Lacey, S. T., and Ryan, P. J. (2000). Cumulative management impacts on soil physical properties and early growth of Pinus radiata. *Forest Ecology and Management* 138, 321–333. doi: 10.1016/S0378-1127(00)00422-9

Land Oberösterreich (2021). *Land Oberösterreich - Digitales Geländemodell 50 cm / 1 m (XYZ) [Digital elevation model]*. Accessed June 14, 2021, https://www.land-oberoesterreich.gv.at/211787.htm

Landesamt für Geoinformationen und Landesvermessung Niedersachsen (2020). *Digitale Geländemodelle (DGM)*, https://www.lgln.niedersachsen.de/startseite/geodaten_karten/3d_geobasisdaten/dgm/digitale-gelaendemodelle-dgm-143150.html

Lantmäteriet (2020). *Produktbesriving GSD-Höjddata, grid 2+ [Digital elevation model]*, https://www.lantmateriet.se/globalassets/kartor-och-geografisk-information/hojddata/hojd2_plus_2.8.pdf

Launiainen, S., Guan, M., Salmivaara, A., and Kieloaho, A.-J. (2019). Modeling boreal forest evapotranspiration and water balance at stand and catchment scales: a spatial approach. *Hydrology and Earth System Sciences* 23, 3457–3480. doi: 10.5194/hess-23-3457-2019

Leach, J. A., Lidberg, W., Kuglerová, L., Peralta-Tapia, A., Ågren, A., and Laudon, H. (2017). Evaluating topography-based predictions of shallow lateral groundwater discharge zones for a boreal lake-stream system. *Water Resources Research* 53, 5420–5437. doi: 10.1002/2016WR019804

Lenth, R. V., Buerkner, P., Herve, M., Love, J., Riebl, H., and Singmann, H. (2019). emmeans: Estimated Marginal Means aka Least-Squares Means, https://CRAN.R-project.org/package=emmeans

LGLN (2020). *Landesamt für Geoinformation und Landesvermessung Niedersachsen: Digitale Geländemodelle (DGM) [Digital elevation model]*. Accessed September 24, 2020, https://www.lgln.niedersachsen.de/startseite/geodaten_karten/3d_geobasisdaten/dgm/digitale-gelaendemodelle-dgm-143150.html

Li, W., and Kang, F. (2020). Design and Analysis of Steering and Lifting Mechanisms for Forestry Vehicle Chassis. *Mathematical Problems in Engineering* 2020, 1–16. doi: 10.1155/2020/5971746

Li, Z.-L., Leng, P., Zhou, C., Chen, K.-S., Zhou, F.-C., and Shang, G.-F. (2021). Soil moisture retrieval from remote sensing measurements: Current knowledge and directions for the future. *Earth-Science Reviews* 218, 103673. doi: 10.1016/j.earscirev.2021.103673

Liakos, K. G., Busato, P., Moshou, D., Pearson, S., and Bochtis, D. (2018). Machine Learning in Agriculture: A Review. *Sensors* 18. doi: 10.3390/s18082674

Lidberg, W., Nilsson, M., and Ågren, A. (2020). Using machine learning to generate high-resolution wet area maps for planning forest management: A study in a boreal forest landscape. *Ambio* 49, 475–486. doi: 10.1007/s13280-019-01196-9

Lüscher, P., Frutig, F., Sciacca, S., Spjevak, S., and Thees, O. (2019). Physikalischer Bodenschutz im Wald [Soil protection in forests]. *WSL Merkblatt für die Praxis* 45.

Maracchi, G., Sirotenko, O., and Bindi, M. (2005). Impacts of Present and Future Climate Variability on Agriculture and Forestry in the Temperate Regions: Europe. *Climatic Change* 70, 117–135. doi: 10.1007/s10584-005-5939-7

Marchi, E., Chung, W., Visser, R., Abbas, D., Nordfjell, T., Mederski, P. S., et al. (2018). Sustainable Forest Operations (SFO): A new paradigm in a changing world and climate. *The Science of the total environment* 634, 1385–1397. doi: 10.1016/j.scitotenv.2018.04.084

Mariotti, B., Hoshika, Y., Cambi, M., Marra, E., Feng, Z., Paoletti, E., et al. (2020). Vehicle-induced compaction of forest soil affects plant morphological and physiological attributes: A meta-analysis. *Forest Ecology and Management* 462, 118004. doi: 10.1016/j.foreco.2020.118004

Matthews, B. W. (1975). Comparison of the predicted and observed secondary structure of T4 phage lysozyme. *Biochimica et Biophysica Acta (BBA) - Protein Structure* 405, 442–451. doi: 10.1016/0005-2795(75)90109-9

Mattila, U., and Tokola, T. (2019). Terrain mobility estimation using TWI and airborne gamma-ray data. *Journal of environmental management* 232, 531–536. doi: 10.1016/j.jenvman.2018.11.081

Max-Planck-Institute for Meteorology (2009). *REMO UBA: Regionale Klimasimulationen für Deutschland, Österreich und die Schweiz*. Accessed November 08, 2021, https://www.remo-rcm.de/060012/index.php.en

McNabb, D. H., Startsev, A. D., and Nguyen, H. (2001). Soil Wetness and Traffic Level Effects on Bulk Density and Air-Filled Porosity of Compacted Boreal Forest Soils. *Soil Science Society of America Journal* 65, 1238–1247. doi: 10.2136/sssaj2001.6541238x

Melander, L., Einola, K., and Ritala, R. (2020). Fusion of open forest data and machine fieldbus data for performance analysis of forest machines. *European Journal of Forest Research* 139, 213–227. doi: 10.1007/s10342-019-01237-8

Meyer, H., Reudenbach, C., Wöllauer, S., and Nauss, T. (2019). Importance of spatial predictor variable selection in machine learning applications – Moving from data reproduction to spatial prediction. *Ecological Modelling* 411, 108815. doi: 10.1016/j.ecolmodel.2019.108815

Mohtashami, S., Eliasson, L., Jansson, G., and Sonesson, J. (2017). Influence of soil type, cartographic depth-to-water, road reinforcement and traffic intensity on rut formation in logging operations: a survey study in Sweden. *Silva Fennica* 51. doi: 10.14214/sf.2018

Mologni, O., Dyson, P., Amishev, D., Proto, A. R., Zimbalatti, G., Cavalli, R., et al. (2018). Tensile force monitoring on large winch-assist forwarders operating in British Columbia. *Croatian journal of forest engineering* 39, 193–204.

Müller, F., Jaeger, D., and Hanewinkel, M. (2019). Digitization in wood supply – A review on how Industry 4.0 will change the forest value chain. *Computers and Electronics in Agriculture* 162, 206–218. doi: 10.1016/j.compag.2019.04.002

Murphy, P. N. C., Ogilvie, J., and Arp, P. (2009). Topographic modelling of soil moisture conditions: A comparison and verification of two models. *European Journal of Soil Science* 60, 94–109. doi: 10.1111/j.1365-2389.2008.01094.x

Murphy, P. N. C., Ogilvie, J., Castonguay, M., Zhang, C.-f., Meng, F.-R., and Arp, P. (2008). Improving forest operations planning through high-resolution flow-channel and wet-areas mapping. *The Forestry Chronicle* 84, 568–574. doi: 10.5558/tfc84568-4

Murphy, P. N. C., Ogilvie, J., Connor, K., and Arp, P. (2007). Mapping wetlands: A comparison of two different approaches for New Brunswick, Canada. *WETLANDS* 27, 846–854. doi: 10.1672/0277-5212(2007)27[846:MWACOT]2.0.CO;2

Murphy, P. N. C., Ogilvie, J., Meng, F.-R., White, B., Bhatti, J. S., and Arp, P. (2011). Modelling and mapping topographic variations in forest soils at high resolution: A case study. *Ecological Modelling* 222, 2314–2332. doi: 10.1016/j.ecolmodel.2011.01.003

Naghdi, R., Bagheri, I., Lotfalian, M., and Setodeh, B. (2009). Rutting and soil displacement caused by 450C Timber Jack wheeled skidder (Asalem forest northern Iran). *Journal of forest science* 55, 177–183. doi: 10.17221/102/2008-JFS

NASA (2021). *NASA-USDA SMAP Global Soil Moisture Data*. Accessed November 08, 2021, https://earth.gsfc.nasa.gov/hydro/data/nasa-usda-global-soil-moisture-data

National Land Survey of Finland (2019). *Open data file download service*. Accessed August 29, 2019, https://www.maanmittauslaitos.fi/en/e-services/open-data-file-download-service

Natural Resources Institute Finland (2019). *internal documents*. Accessed August 19, 2019, https://lukenet.fi/display/TUTI/Hila-aineistot

Natural Resources Institute Finland (2020). *Trafficability Prediction and Route Planning for Forest Machines - Luonnonvarakeskus*. Accessed May 10, 2021, https://www.luke.fi/en/projektit/tram/

NIBIO (2021). *SFI SmartForest: Bringing Industry 4.0 to the Norwegian forest sector*. Accessed May 20, 2021, https://www.nibio.no/en/projects/sfi-smartforest-bringing-industry-4.0-to-the-norwegian-forest-sector

Niedersächsische Landesforsten (2017). *Bodenschutz bei der Holzernte in den Niedersächsischen Landesforsten [Soil protection in forest operations]*. Accessed November 08, 2021, https://www.landesforsten.de/wp-content/uploads/2018/06/merkblatt_bodenschutz_apr_2017.pdf

Niemi, M. T., Vastaranta, M., Vauhkonen, J., Melkas, T., and Holopainen, M. (2017). Airborne LiDAR-derived elevation data in terrain trafficability mapping. *Scandinavian Journal of Forest Research* 32, 762–773. doi: 10.1080/02827581.2017.1296181

Noordermeer, L., Sørngård, E., Astrup, R., Næsset, E., and Gobakken, T. (2021). Coupling a differential global navigation satellite system to a cut-to-length harvester operating system enables precise positioning of harvested trees. *International Journal of Forest Engineering* 32, 119–127. doi: 10.1080/14942119.2021.1899686

Nordfjell, T., Björheden, R., Thor, M., and Wästerlund, I. (2010). Changes in technical performance, mechanical availability and prices of machines used in forest operations in Sweden from 1985 to 2010. *Scandinavian Journal of Forest Research* 25, 382–389. doi: 10.1080/02827581.2010.498385

Nordfjell, T., Öhman, E., Lindroos, O., and Ager, B. (2019). The technical development of forwarders in Sweden between 1962 and 2012 and of sales between 1975 and 2017. *International Journal of Forest Engineering* 30, 1–13. doi: 10.1080/14942119.2019.1591074

Nussbaum, M., Spiess, K., Baltensweiler, A., Grob, U., Keller, A., Greiner, L., et al. (2018). Evaluation of digital soil mapping approaches with large sets of environmental covariates. *SOIL* 4, 1–22. doi: 10.5194/soil-4-1-2018

O'Callaghan, J. F., and Mark, D. M. (1984). The extraction of drainage networks from digital elevation data. *Computer vision, graphics, and image processing* 28, 323–344. doi: 10.1016/S0734-189X(84)80011-0

Oltean, G. S., Comeau, P., and White, B. (2016a). Carbon isotope discrimination by Picea glauca and Populus tremuloides is related to the topographic depth to water index and rainfall. *Canadian Journal of Forest Research* 46, 1225–1233. doi: 10.1139/cjfr-2015-0491

Oltean, G. S., Comeau, P., and White, B. (2016b). Linking the Depth-to-Water Topographic Index to Soil Moisture on Boreal Forest Sites in Alberta. *Forest Science* 62, 154–165. doi: 10.5849/forsci.15-054

O'Sullivan, M.F., Henshall, J.K., and Dickson, J.W. (1999). A simplified method for estimating soil compaction. *Soil and Tillage Research* 49, 325–335. doi: 10.1016/S0167-1987(98)00187-1

Overpeck, J. T., Rind, D., and Goldberg, R. (1990). Climate-induced changes in forest disturbance and vegetation. *Nature* 343, 51–53. doi: 10.1038/343051a0

Owende, P. M. O., Lyons, J., Haarlaa, R., Peltola, A., Spinelli, R., Molano, J., et al. (2002). Operations protocol for eco-efficient wood harvesting on sensitive sites. ECOWOOD Partnership.

Pebesma, E. J. (2018). Simple Features for R: Standardized Support for Spatial Vector Data. *The R Journal* 10, 439–446. doi: 10.32614/RJ-2018-009

Pebesma, E. J., and Bivand, R. S. (2005). *Classes and methods for spatial data in R*, https://CRAN.R-project.org/doc/Rnews/

Pei, T., Qin, C.-Z., Zhu, A.-X., Yang, L., Luo, M., Li, B., et al. (2010). Mapping soil organic matter using the topographic wetness index: A comparative study based on different flow-direction algorithms and kriging methods. *Ecological Indicators* 10, 610–619. doi: 10.1016/j.ecolind.2009.10.005

Peterson, B. G., and Carl, P. (2020). PerformanceAnalytics: Econometric Tools for Performance and Risk Analysis, https://CRAN.R-project.org/package=PerformanceAnalytics

Pfeifer, S., Rechid, D., and Bathiany, S. (2021). *Klimaausblick Deutschland.* Accessed November 15, 2021, https://www.gerics.de/imperia/md/content/csc/projekte/klimasignalkarten/gerics_klimaausblick_germany_version1.2_deutsch.pdf

Picchio, R., Jourgholami, M., and Zenner, E. K. (2021). Effects of Forest Harvesting on Water and Sediment Yields: a Review Toward Better Mitigation and Rehabilitation Strategies. *Curr Forestry Rep* 55, 3. doi: 10.1007/s40725-021-00146-7

Picchio, R., Latterini, F., Mederski, P. S., Tocci, D., Venanzi, R., Stefanoni, W., et al. (2020). Applications of GIS-Based Software to Improve the Sustainability of a Forwarding Operation in Central Italy. *Sustainability* 12, 5716. doi: 10.3390/su12145716

Pohjankukka, J., Riihimäki, H., Nevalainen, P., Pahikkala, T., Ala-Ilomäki, J., Hyvönen, E., et al. (2016). Predictability of boreal forest soil bearing capacity by machine learning. *Journal of Terramechanics* 68, 1–8. doi: 10.1016/j.jterra.2016.09.001

Poltorak, B. J., Labelle, E. R., and Jaeger, D. (2018). Soil displacement during ground-based mechanized forest operations using mixed-wood brush mats. *Soil and Tillage Research* 179, 96–104. doi: 10.1016/j.still.2018.02.005

Powers, D. M. W. (2011). Evaluation: from precision, recall and F-measure to ROC, informedness, markedness and correlation. *arXiv:2010.1061.*

Prinz, R., Spinelli, R., Magagnotti, N., Routa, J., and Asikainen, A. (2018). Modifying the settings of CTL timber harvesting machines to reduce fuel consumption and CO2 emissions. *Journal of Cleaner Production* 197, 208–217. doi: 10.1016/j.jclepro.2018.06.210

QGIS.org (2020). *QGIS Geographic Information System.* Open Source Geospatial Foundation Project.

R Core Team (2020). *R: A Language and Environment for Statistical Computing.* Vienna, Austria: The R Foundation for Statistical Computing.

Rab, M. A. (2004). Recovery of soil physical properties from compaction and soil profile disturbance caused by logging of native forest in Victorian Central Highlands, Australia. *Forest Ecology and Management* 191, 329–340. doi: 10.1016/j.foreco.2003.12.010

Reichle, R., Lannoy, G. de, Koster, R., Crow, W., Kimball, J., and Liu, Q. (2020a). *SMAP L4 Global 3-hourly 9 km EASE-Grid Surface and Root Zone Soil Moisture Geophysical Data, Version 5.* Accessed November 11, 2021, https://nsidc.org/data/SPL4SMGP/versions/3

Reichle, R., Lannoy, G. de, Koster, R., Crow, W., Kimball, J., and Liu, Q. (2020b). *SMAP L4 Global 9 km EASE-Grid Surface and Root Zone Soil Moisture Land Model Constants, Version 5*. Accessed November 11, 2021, https://nsidc.org/data/SPL4SMLM/versions/5

Reyer, C. P. O., Bathgate, S., Blennow, K., Borges, J. G., Bugmann, H., Delzon, S., et al. (2017). Are forest disturbances amplifying or canceling out climate change-induced productivity changes in European forests? *Environmental Research Letters* 12, 34027. doi: 10.1088/1748-9326/aa5ef1

Rickenbach, M., and Steele, T. W. (2005). Comparing mechanized and non-mechanized logging firms in Wisconsin: Implications for a dynamic ownership and policy environment. *Forest Products Journal* 55, 21.

Ringdahl, O., Hellström, T., Wästerlund, I., and Lindroos, O. (2012). Estimating wheel slip for a forest machine using RTK-DGPS. *Journal of Terramechanics* 49, 271–279. doi: 10.1016/j.jterra.2012.08.003

Rollerson, T. P. (1990). Influence of Wide-Tire Skidder Operations on Soils. *Journal of Forest Engineering* 2, 23–30. doi: 10.1080/08435243.1990.10702620

Saarilahti, M., and Ala-Ilomäki, J. (1997). Measurement and modelling of wheel slip in forwarding on moraine forest floor. *Scandinavian Journal of Forest Research* 12, 316–319. doi: 10.1080/02827589709355416

Sakai, H., Nordfjell, T., Suadicani, K., Talbot, B., and Bøllehuus, E. (2008). Soil compaction on forest soils from different kinds of tires and tracks and possibility of accurate estimate. *Croatian journal of forest engineering* 29, 15–27.

Salmivaara, A., Launiainen, S., Perttunen, J., Nevalainen, P., Pohjankukka, J., Ala-Ilomäki, J., et al. (2020). Towards dynamic forest trafficability prediction using open spatial data, hydrological modelling and sensor technology. *Forestry* 93, 662–674. doi: 10.1093/forestry/cpaa010

Salmivaara, A., Miettinen, M., Finér, L., Launiainen, S., Korpunen, H., Tuominen, S., et al. (2018). Wheel rut measurements by forest machine-mounted LiDAR sensors – accuracy and potential for operational applications? *International Journal of Forest Engineering* 29, 41–52. doi: 10.1080/14942119.2018.1419677

Salsbery, B. P., and Hartsough, B. R. (1993). Control of a cable-towed vehicle to minimize slip. *Journal of Terramechanics* 30, 325–335. doi: 10.1016/0022-4898(93)90009-M

Samaniego, L., Kumar, R., and Attinger, S. (2010). Multiscale parameter regionalization of a grid-based hydrologic model at the mesoscale. *Water Resources Research* 46, 230. doi: 10.1029/2008WR007327

Schelhaas, M.-J., Nabuurs, G.-J., and Schuck, A. (2003). Natural disturbances in the European forests in the 19th and 20th centuries. *Global change biology* 9, 1620–1633. doi: 10.1046/j.1365-2486.2003.00684.x

Schönauer, M. (2019). *Mapping App - Minimize site impact through improved planning and operations. TECH4EFFECT. Deliverable 4.3*, http://www.tech4effect.eu/wp-content/uploads/2020/02/d43-open-source-mapping-application-for-smartphone-and-tablet.pdf

Schönauer, M. (2020). Supplementary data for: Comparison of selected terramechanical test procedures and cartographic indices to predict rutting caused by machine traffic during a cut-to-length thinning-operation. Göttingen Research Online / Data, 2020. doi: 10.25625/LQJBML

Schönauer, M., Hoffmann, S., Maack, J., Jansen, M., and Jaeger, D. (2021a). Comparison of Selected Terramechanical Test Procedures and Cartographic Indices to Predict Rutting Caused by Machine Traffic during a Cut-to-Length Thinning Operation. *Forests* 12, 113. doi: 10.3390/f12020113

Schönauer, M., Holzfeind, T., Hoffmann, S., Holzleitner, F., Hinte, B., and Jaeger, D. (2020). Effect of a traction-assist winch on wheel slippage and machine induced soil disturbance in flat terrain. *International Journal of Forest Engineering* 39, 1–11. doi: 10.1080/14942119.2021.1832816

Schönauer, M., and Maack, J. (2021). R-code for calculating depth-to-water (DTW) maps using GRASS GIS (Version v1). *Zenodo*. doi: 10.5281/zenodo.5638518

Schönauer, M., Prinz, R., Väätäinen, K., Astrup, R., Pszenny, D., Lindeman, H., et al. (2021b). Spatio-temporal prediction of soil moisture using soil maps, topographic indices and NASA Earthdata. *Zenodo*. doi: 10.5281/zenodo.5691527

Schönauer, M., Talbot, B., and Jaeger, D. (2019). *Terrain accessibility maps for 4 case study areas. TECH4EFFECT. Deliverable 4.1*. Accessed March 30, 2021, http://www.tech4effect.eu/media-corner/public-deliverables/

Schönauer, M., Väätäinen, K., Prinz, R., Lindeman, H., Pszenny, D., Jansen, M., et al. (2021c). Spatio-temporal prediction of soil moisture and soil strength by depth-to-water maps. *International Journal of Applied Earth Observation and Geoinformation* 105, 102614. doi: 10.1016/j.jag.2021.102614

Seibert, J., Bishop, K., and Nyberg, L. (1997). A test of TOPMODEL'a ability to predict spatially distributed groundwater levels. *Hydrological Processes* 11, 1131–1144. doi: 10.1002/(SICI)1099-1085(199707)11:9<1131:AID-HYP549>3.0.CO;2-%23

Seidl, R., Schelhaas, M.-J., and Lexer, M. J. (2011). Unraveling the drivers of intensifying forest disturbance regimes in Europe. *Global change biology* 17, 2842–2852. doi: 10.1111/j.1365-2486.2011.02452.x

Seixas, F., and McDonald, T. (1997). Soil compaction effects of forwarding and its relationship with 6- and 8-wheel drive machines. *Forest Products Journal* 47, 46–52.

Seki, K. (2007). SWRC fit – a nonlinear fitting program with a water retention curve for soils having unimodal and bimodal pore structure. *Hydrology and Earth System Sciences Discussions* 4, 407–437.

Siekmeier, J. A., Young, D., and Beberg, D. (2000). "Comparison of the Dynamic Cone Penetrometer with Other Tests During Subgrade and Granular Base Characterization in Minnesota," in *Nondestructive testing of pavements and backcalculation of moduli: third volume* (ASTM International), 175-175-14.

Simard, M., Romme, W. H., Griffin, J. M., and Turner, M. G. (2011). Do mountain pine beetle outbreaks change the probability of active crown fire in lodgepole pine forests? *Ecological Monographs* 81, 3–24. doi: 10.1890/10-1176.1

Singh, V. K., Kumar, D., Kashyap, P. S., Singh, P. K., Kumar, A., and Singh, S. K. (2020). Modelling of soil permeability using different data driven algorithms based on physical properties of soil. *Journal of Hydrology* 580, 124223. doi: 10.1016/j.jhydrol.2019.124223

Sirén, M., Ala-Ilomäki, J., Lindeman, H., Uusitalo, J., Kiilo, K. E. K., Salmivaara, A., et al. (2019a). Soil disturbance by cut-to-length machinery on mid-grained soils. *Silva Fennica* 53. doi: 10.14214/sf.10134

Sirén, M., Ala-Ilomäki, J., Mäkinen, H., Lamminen, S., and Mikkola, T. (2013). Harvesting damage caused by thinning of Norway spruce in unfrozen soil. *International Journal of Forest Engineering* 24, 60–75. doi: 10.1080/19132220.2013.792155

Sirén, M., Salmivaara, A., Ala-Ilomäki, J., Launiainen, S., Lindeman, H., Uusitalo, J., et al. (2019b). Predicting forwarder rut formation on fine-grained mineral soils. *Scandinavian Journal of Forest Research* 34, 145–154. doi: 10.1080/02827581.2018.1562567

Söhne, W. (1952). Die Kraftübertragung zwischen Schlepperreifen und Ackerboden [Force transmission between tire and soil]. *Grundlagen der Landtechnik-Konstrukteurhefte* 7, 75–87.

Sohrabi, H., Jourgholami, M., Jafari, M., Tavankar, F., Venanzi, R., and Picchio, R. (2021). Earthworms as an Ecological Indicator of Soil Recovery after Mechanized Logging Operations in Mixed Beech Forests. *Forests* 12, 18. doi: 10.3390/f12010018

Sørensen, R., and Seibert, J. (2007). Effects of DEM resolution on the calculation of topographical indices: TWI and its components. *Journal of Hydrology* 347, 79–89. doi: 10.1016/j.jhydrol.2007.09.001

Sørensen, R., Zinko, U., and Seibert, J. (2006). On the calculation of the topographic wetness index: evaluation of different methods based on field observations. *Hydrology and Earth System Sciences* 10, 101–112. doi: 10.5194/hess-10-101-2006

Southee, F. M., Treitz, P. M., and Scott, N. A. (2012). Application of Lidar Terrain Surfaces for Soil Moisture Modeling. *photogramm eng remote sensing* 78, 1241–1251. doi: 10.14358/PERS.78.11.1241

Starke, M., Derron, C., Heubaum, F., and Ziesak, M. (2020). Rut Depth Evaluation of a Triple-Bogie System for Forwarders—Field Trials with TLS Data Support. *Sustainability* 12. doi: 10.3390/su12166412

Startsev, A. D., and McNabb, D. H. (2000). Effects of skidding on forest soil infiltration in west-central Alberta. *Canadian Journal of Soil Science* 80, 617–624. doi: 10.4141/S99-092

Startsev, A. D., and McNabb, D. H. (2009). Effects of compaction on aeration and morphology of boreal forest soils in Alberta, Canada. *Canadian Journal of Soil Science* 89, 45–56. doi: 10.4141/CJSS06037

Šušnjar, M., Horvat, D., and Šešelj, J. (2006). Soil compaction in timber skidding in winter conditions. *Croatian journal of forest engineering* 27, 3–15.

Suvinen, A. (2006). Economic Comparison of the Use of Tyres, Wheel Chains and Bogie Tracks for Timber Extraction. *Croatian journal of forest engineering* 27, 81–102.

Suvinen, A., and Saarilahti, M. (2006). Measuring the mobility parameters of forwarders using GPS and CAN bus techniques. *Journal of Terramechanics* 43, 237–252. doi: 10.1016/j.jterra.2005.12.005

Suvinen, A., Tokola, T., and Saarilahti, M. (2009). Terrain trafficability prediction with GIS analysis. *Forest Science* 55, 433–442. doi: 10.1093/forestscience/55.5.433

Talbot, B., Pierzchała, M., and Astrup, R. (2017). Applications of remote and proximal sensing for improved precision in forest operations. *Croatian journal of forest engineering* 38, 327–336.

Tarboton, D. G. (1997). A new method for the determination of flow directions and upslope areas in grid digital elevation models. *Water Resources Research* 33, 309–319. doi: 10.1029/96WR03137

Tarboton, D. G. (2004). *Terrain Analysis Using Digital Elevation Models (TauDEM)*. Accessed February 15, 2021, https://hydrology.usu.edu/taudem/taudem3.1/

TECH4EFFECT (2020). *Knowledge and technologies for effective wood procurement*. Accessed May 10, 2021, http://www.tech4effect.eu/

Terzaghi, K., Peck, R. B., and Mesri, G. (1996). *Soil mechanics in engineering practice*. Hoboken, New Jersey: John Wiley & Sons.

Thünen-Institut (2012). *Dritte Bundeswaldinventur [National forest inventory]*. Accessed January 18, 2022, https://bwi.info

Tuomasjukka, D., Herder, M. D., Wallius, V., Rois, M., Kunttu, J., Korhonen, M., et al. (2020). *TECH4EFFECT. 2020. Knowledge and technologies for our forests of the future*. Accessed November 05, 2021, http://www.tech4effect.eu/wp-content/uploads/2020/09/policy-brief-web.pdf

UNFCCC (2015). *The Paris Agreement*. Accessed May 10, 2021, https://unfccc.int/sites/default/files/english_paris_agreement.pdf

University of Göttingen (2021). *Current projects*. Accessed November 08, 2021, https://www.uni-goettingen.de/de/laufende+projekte/525928.html

Ustin, S. L., and Gamon, J. A. (2010). Remote sensing of plant functional types. *The New phytologist* 186, 795–816. doi: 10.1111/j.1469-8137.2010.03284.x

Uusitalo, J., Ala-Ilomäki, J., Lindeman, H., Toivio, J., and Sirén, M. (2019). Modelling soil moisture – soil strength relationship of fine-grained upland forest soils. *Silva Fennica* 53. doi: 10.14214/sf.10050

Uusitalo, J., Ala-Ilomäki, J., Lindeman, H., Toivio, J., and Sirén, M. (2020). Predicting rut depth induced by an 8-wheeled forwarder in fine-grained boreal forest soils. *Annals of forest science* 77. doi: 10.1007/s13595-020-00948-y

Uusitalo, J., Salomäki, M., and Ala-Ilomäki, J. (2015). Variation of the factors affecting soil bearing capacity of ditched pine bogs in Southern Finland. *Scandinavian Journal of Forest Research* 30, 1–11. doi: 10.1080/02827581.2015.1012110

Väätäinen, K., Uusitalo, J., Launiainen, S., Peuhkurinen, J., Berqkvist, I., Ala-Ilomäki, J., et al. (2019). *EFFORTE D4.5. Validation of developed tools for operational planning*. Accessed November 05, 2021, https://www.luke.fi/efforte/wp-content/uploads/sites/14/2019/06/EFFORTE-D4.5-Validation-of-developed-tools-for-operational-planning.pdf

Vega-Nieva, D. J., Murphy, P. N. C., Castonguay, M., Ogilvie, J., and Arp, P. (2009). A modular terrain model for daily variations in machine-specific forest soil trafficability. *Canadian Journal of Soil Science* 89, 93–109. doi: 10.4141/CJSS06033

Venables, W. N., and Ripley, B. D. (2002). *Modern Applied Statistics with S*. New York: Springer.

Visser, R., and Stampfer, K. (2015). Expanding ground-based harvesting onto steep terrain: A review. *Croatian journal of forest engineering* 36, 321–331.

Vossbrink, J., and Horn, R. (2004). Modern forestry vehicles and their impact on soil physical properties. *European Journal of Forest Research* 123, 259–267. doi: 10.1007/s10342-004-0040-8

Waga, K., Malinen, J., and Tokola, T. (2020). A Topographic Wetness Index for Forest Road Quality Assessment: An Application in the Lakeland Region of Finland. *Forests* 11. doi: 10.3390/f11111165

Wästerlund, I. (1985). Compaction of till soils and growth tests with Norway spruce and scots pine. *Forest Ecology and Management* 11, 171–189. doi: 10.1016/0378-1127(85)90025-8

Webster, S. L., Grau, R. H., and Williams, T. P. (1992). *Description and application of dual mass dynamic cone penetrometer*. Vicksburg, Mississippi, US.

WetterKontor GmbH (2020). *Rückblick für Uslar (N) [Weather data]*. Accessed November 08, 2021, https://www.wetterkontor.de/de/wetter/deutschland/rueckblick.asp?id=R666&datum0=01.07.2020&datum1=31.08.2020&jr=2020&mo=9&datum=22.09.2020&t=8&part=0

Wężyk, P. (2015). *Podręcznik dla uczestników szkoleń z wykorzystaniem produktów LiDAR [Manual for participants in training with LiDAR products]*. Warszawa: Główny Urząd Geodezji i Kartografii.

Wheeler, B., Torchiano, M., and Torchiano, M. M. (2016). *Package 'lmPerm'*, https://github.com/mtorchiano/lmPerm

White, B., Ogilvie, J., Campbell, D. M.H., Hiltz, D., Gauthier, B., Chisholm, H. K., et al. (2012). Using the Cartographic Depth-to-Water Index to Locate Small Streams and Associated Wet Areas across Landscapes. *Canadian Water Resources Journal* 37, 333–347. doi: 10.4296/cwrj2011-909

Wickham, H., François, R., Henry, L., and Müller, K. (2020). dplyr: A Grammar of Data Manipulation, https://CRAN.R-project.org/package=dplyr

Willén, E., and Hannson, L. "Optimisation in operational forestry planning and operations," in *Mistra Digital Forest 2021*.

Williamson, J. R., and Neilsen, W. A. (2000). The influence of forest site on rate and extent of soil compaction and profile disturbance of skid trails during ground-based harvesting. *Canadian Journal of Forest Research* 30, 1196–1205.

Wit, H. A. de, Granhus, A., Lindholm, M., Kainz, M. J., Lin, Y., Braaten, H. F. V., et al. (2014). Forest harvest effects on mercury in streams and biota in Norwegian boreal catchments. *Forest Ecology and Management* 324, 52–63. doi: 10.1016/j.foreco.2014.03.044

Wright, M. N., and Ziegler, A. (2017). ranger: A Fast Implementation of Random Forests for High Dimensional Data in C++ and R. *J. Stat. Soft.* 77. doi: 10.18637/jss.v077.i01

Zanella, A., Jabiol, B., Ponge, J. F., Sartori, G., Waal, R. de, van Delft, B., et al. (2011). A European morpho-functional classification of humus forms. *Geoderma* 164, 138–145. doi: 10.1016/j.geoderma.2011.05.016

Zeng, L., Hu, S., Xiang, D., Zhang, X., Li, D., Li, L., et al. (2019). Multilayer Soil Moisture Mapping at a Regional Scale from Multisource Data via a Machine Learning Method. *Remote Sensing* 11, 284. doi: 10.3390/rs11030284

Ziesak, M. (2004). *Entwicklung eines Informationssystems zum bodenschonenden Forstmaschineneinsatz [Development of a system for low impact forerst operations]*. Dissertation. München, Germany: Technischen Universität München, Lehrstuhl für Forstliche Arbeitswissenschaft und Angewandte Informatik.

Zimbelman, E. G., and Keefe, R. F. (2018). Real-time positioning in logging: Effects of forest stand characteristics, topography, and line-of-sight obstructions on GNSS-RF transponder accuracy and radio signal propagation. *PLoS One* 13, e0191017. doi: 10.1371/journal.pone.0191017

10. Appendix

Appendix I. Example of a measured transect, used to calculate rut_H, rut_F and rut_T (**section 2.2.3**), by means of the code shown in **Appendix II**. Respectively to Dz_H and Dz_F, t_H and t_F were noted, to capture the position of visible machine tracks across the measuring transect.

transect	tr.length	Dz_{INIT}	Dz_H	Dz_F	t_H	t_F
41	-200	36	34	34	0	0
41	-180	32	33	33	0	0
41	-160	32	32	32	0	0
41	-140	32	32	31	0	0
41	-120	30	32	31	L	0
41	-100	31	33	33	L	L
41	-80	31	32	33	L	L
41	-60	29	30	35	L	L
41	-40	30	29	32	0	L
41	-20	27	28	29	0	L
41	0	29	29	28	0	0
41	20	29	30	29	0	0
41	40	30	29	30	0	0
41	60	29	30	29	0	0
41	80	31	32	31	0	0
41	100	29	32	31	R	0
41	120	32	33	34	R	R
41	140	33	34	36	R	R
41	160	35	36	37	R	R
41	180	37	37	37	0	R
41	200	38	39	38	0	R

Appendix II. R-grammar used to calculate rut_H, rut_F and rut_T.

```
library(dplyr) #package: {dplyr} (Wickham et al., 2020)


  Mean <- function(x) round(mean(x, na.rm=T), digits = 2)
  Max <- function(x) ifelse( !all(is.na(x)), max(x, na.rm=T), NA)

  data.frame %>% group_by(transect) %>%
    summarise(rutH = Mean(c(Max(DzH[tH == 'L'] - Dzinit[tH == 'L']),
                            Max(DzH[tH == 'R'] - Dzinit[tH == 'R']))),
              rutF = Mean(c(Max(DzF[tF == 'L'] - DzH[tF == 'L']),
                            Max(DzF[tF == 'R'] - DzH[tF == 'R']))),
              rutT = Mean(c(Max(DzF[tH != 0 | tF != 0] - Dzinit[tH != 0 | tF != 0]),
                            Max(DzF[tH != 0 | tF != 0] - Dzinit[tH != 0 | tF != 0]))))
```

Appendix III. Terrain accessibility maps for 4 case study areas.

This chapter contains parts of a TECH4EFFECT deliverable report and was made accessible via DOI:10.13140/RG.2.2.20707.17444 or http://www.tech4effect.eu/media-corner/public-deliverables/, on September 2019.

Full author list: Marian Schönauer [1], Bruce Talbot [2] and Dirk Jaeger [1]

1 Department of Forest Engineering and Work Science, Georg-August-Universität Göttingen, Büsgenweg 4, 37077 Göttingen, Germany

2 Forest Operations, Stellenbosch University, 7602 Stellenbosch, South Africa

Author's contributions: M.S., B.T., D.J. conceived and designed the experiments; M.S. performed the spatial analysis, data preparation and analysis; data interpretation, M.S., B.T. and D.J.; writing – original draft preparation, M.S., B.T.; writing – review and editing, M.S., B.T. and D.J.; supervision, D.J.

Appendix III.I Study areas selected for later validations

Four study areas have been selected in the partner countries Finland, Germany, Norway and Poland. Each study area has an approximate size of 50 km², where field trials can be conducted in the near future. These field trials will analyse the local risks of soil disturbance due to machine traffic and, as such, allow for validation of predictability of soil disturbances, in particular rut depth, by means of DTW-maps. Therefore, simulated and real operations will be performed and measurements of soil penetration resistance and shear strength, and soil moisture content will be conducted in conjunction with pedological analyses.

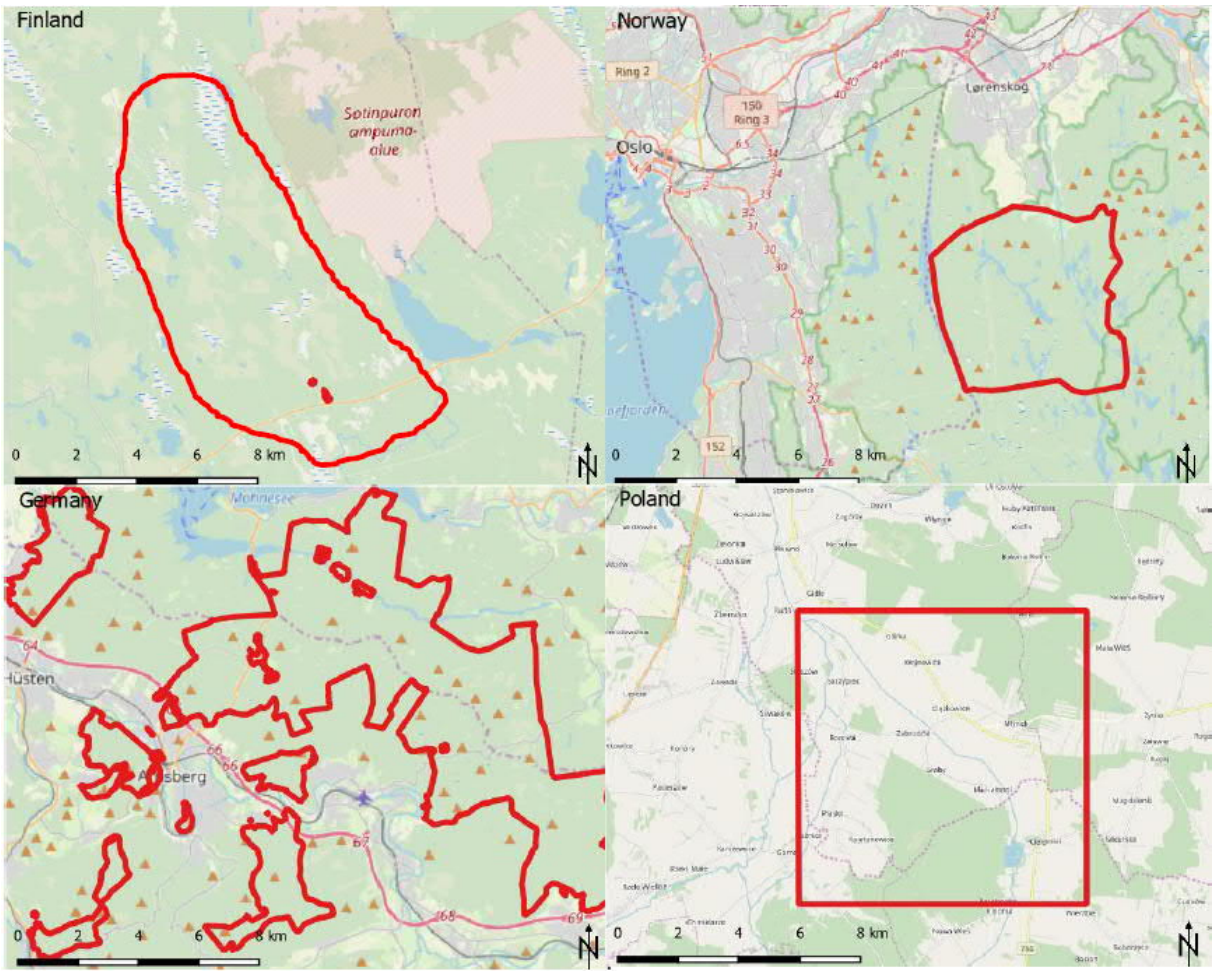

Figure 10-1. The location of the four study areas in Finland, Germany, Norway and Poland, indicated by a black triangle (top right) and a red outline (source: OpenStreetMap).

Table 10-1. Site characteristics and long-year means for temperature and annual precipitation of the study areas of the participating countries.

	Finland [9, 10, 11]	Germany [12, 13]	Norway [14, 15]	Poland [16]
Terrain	Flat, slightly hilly	Predominantly hilly, mountainous	Steep hills of exposed or lightly covered bedrock interspersed with low wet areas	mostly flat, varied by river valleys, and upland terrain in the eastern part
Elevation	140 to 250 m, mean 175 m	160 to 550 m, mean = 320 m	150 to 360 m, mean =217 m	188 to 270m, mean = 229 m
Location	Pohjois-Savo	Sauerland, North-Rhine-Westphalia	Losby Estsate, Lørenskog, Akershus County	South Poland, Border of Silesian and Lodz Voivodeship
Geomorphology	Karelids 3	the north-western foothills of the Rothaargebirge	South-eastern offshoots of Scandinavian Mountains	Contact of the Silesian-Krakow Upland, Kielce Upland and the Nidziańska Basin
Bedrock	Migmatitic tonalite, biotite paragneiss and granite	Claystone and Sandstone from Devon and Karbon	Gabbro, diorite, tonalite, partially converted Granite-biotite-gneis, biotite-muscovite gneiss	Sandr sands and gravels and tills as well as glacial sands and gravels
Soil types	Podzol and peat	Brown soils to Pseudogleys	Morainic till between rocky outcrops, some marine shale in low areas	13 types of soils, mainly brown and fawn soils
Mean Temp.	3.0 °C	8.9 °C	4.1 °C	7.9 °C
Mean annual precipitation	665 mm	790 mm	860 mm	582 mm
Typical tree species	Scots pine, Norway spruce and downy birch	Beech, spruce, pine	Norway spruce, Scots pine, birch	Pine, larch, spruce

Appendix III.II Description of the depth-to-water algorithm

According to our current state of knowledge, the DTW concept developed by Murphy et al. (2009) is the least data demanding approach for mapping wet areas and, hereby, identifying zones of low soil bearing capacity or trafficability. The presented method for the creation of a depth-to-water maps is based on geomorphological assessments and does not consider soil type, its variation and texture as a direct input parameter in the calculation. Consequently, the concept is not able to cover the special situations in peats or rocky overlays, and caution at the everyday use is necessary. Still, the advantages of being independent of high-resolution soil mapping overcome the disadvantages of partial inaccuracy

[9] National Land Survey of Finland (2019).
[10] Geologian tutkimuskeskus luo geologisella osaamisella ratkaisuja (2019).
[11] Natural Resources Institute Finland (2019).
[12] Geologischer Dienst NRW (2019).
[13] DWD (2019b).
[14] Geological Survey of Norway.
[15] Norwegian Meteorological Institute.
[16] Biuro Urządzania Lasu i Geodezji Leśnej 2017.

and inapplicability. In order to conduct the mapping approach in four European countries, this aspect even gets more evident.

The weaknesses of previous, topographically derived soil wetness indices, which are built on digital elevation models only, are in their inability to model spatial patterns of soil moisture or drainage conditions and the over-dependence on convergent flow accumulation (Murphy et al., 2009). UNB developed a new concept that is able to skirt these weaknesses. The combined information of hydrographic data and topographically derived flow accumulation are used to define a surface water feature layer in the first step. The required DEM is provided by governmental institutions.

Table 10-2. Provider and spatial resolution of the digital elevation model, used for the calculation of the DTW-index.

Country	Data provider	Resolution DEM [m]
Finland	National Land Survey of Finland	2.0
Germany	Bezirksregierung Köln	1.0
Norway	The Norwegian Mapping Authority	1.0
Poland	Polish Main Office of Geodesy and Cartography	1.0

In turn we created a 1.0 to 2.0 m resolution raster DEM using the exact height values of the LiDAR data sampled with a nearest neighbour function. In a first step we used the LiDAR-derived bare-earth DEM for finding and removing local depressions using the FILL function (Tarboton, 1997). The pit-free DEM was then used to delineate the shortest (least cumulative slope) flow path of each surface water cell by flow direction and slope. This process ensures the assignment of each cell to the downslope surface water cell with the most likely hydrological connection. Thereby, each cell within the DEM represents its real area of a landscape (e.g. 1 raster cell with a side length of 2 m is representing 4 m^2).

To allow the estimation of the predicted flow direction of these flow paths, two requirements are necessary: (1) the processing of the DEM, which is done by a “fill”-function, since artificial point depressions of the D8 flow accumulation algorithm would occur otherwise and (2) a mapping of culvert crossings (or expert appraisal instead) followed by manual breaching. After this preparation of the DEM, the surface flow accumulation, using the D8 algorithm to create unidirectional flow lines, is processed. In order to produce a surface flow network, upon which later calculations of the DTW-index are based, a threshold of 2.500 to 100.000 raster cells (representing 0.25 ha or 10 ha, respectively) is used. When this certain threshold is reached in a flow path, a flow line can be delineated in a grid of flow accumulation. A threshold of 4 ha is used as a standard value, since this value has been shown to work well across varying terrains.

The created grid of flow accumulation in conjunction with a grid of slope values is sufficient for the calculation of the DTW-index, which approximates the elevation difference between the cell in the landscape and the assigned surface water cell (grid of flow accumulation). The path of the least cumulative slope will be identified by a least-cost function, which is minimizing the distance and the slope from each landscape cell to the closest flow line. The distance is given by the cell size or its diagonal length, if the cell is draining into a cell on the edge (in this case a multiplier α is used). This path of least slope gradients is estimated for each cell and giving the DTW grid, which is formally defined by equation (9):

$$\text{DTW [m]} = \left[\sum \frac{dz_i}{dx_i}\, a\right] x_c \qquad (9)$$

Where $\frac{dz_i}{dx_i}$ is the slope of a cell i and a, the multiplier, is 1 in case of parallel drainage and $\sqrt{2}$ in case of diagonally drainage. x_c is the grid cell size [m].

Appendix III.III The application of the DTW-index

The DTW scale is metric and can be interpreted as a relative measure of soil drainage condition, which approximates the tendency of a point in the landscape to be saturated. Cells with a small value of DTW show a high tendency of surface water or water containing layers in the soil (Murphy et al., 2009). In practice, it can be referred to it as a metric index of likely end-of summer soil drainage conditions and soil bearing capacity, classified as follows:

0	<	DTW	<	10	cm	Very poor
10	<	DTW	<	25	cm	Poor
25	<	DTW	<	50	cm	Imperfect
50	<	DTW	<	100	cm	Moderate
100	<	DTW	<	1500	cm	Well
		DTW	>	1500	cm	excessive

Areas of lakes, streams and flow lines in the flow accumulation grid are set with a DTW-index of 0. Low values indicate wet soils, whereas the values of the DTW-index tend to increase with the distance to delineated flow lines in the landscape. The higher the value, the drier the soil is supposed to be. This nearly empirical approach is supported by the likely situation, that distinct points in a landscape are wetter, if located next to a delineated flow line or wet area and vice versa.

The reputed Topographic Wetness Index, which combines local upslope contributing area and slope (Sørensen et al., 2006), and the cartographic Depth-To-Water-index are the best performing soil wetness predictors, whereas the DTW-index has the advantage to be scale-independent for the most part and showed a higher accuracy of 80% in a Swedish case study (Ågren et al., 2014). Ågren et al. concluded, that the DTW may form the next generation of high-resolution wet-area maps, which will be applied in forestry and elsewhere.

Appendix IV. R-code for calculating depth-to-water (DTW) maps using GRASS GIS

Marian Schönauer [1,*], Joachim Maack [1]
[1] Department of Forest Work Science and Engineering, University of Göttingen, Göttingen
* corresponding author. E-mail address: marian.schoenauer@uni-goettingen.de

The depth-to-water (DTW) concept was conceived, developed and tested at the University of New Brunswick (Faculty of Forestry and Environmental Management), by Fan-Rui Meng, Jae Ogilvie and Paul Arp, as described by, e.g., Murphy et al. (2007; 2009). This R-code was developed by Marian Schönauer and Joachim Maack, during the work for Schönauer et al. (2021c). It is free for use, and can be cited as:

Schönauer, M., Maack, J., 2021. R-code for calculating depth-to-water (DTW) maps using GRASS GIS. Zenodo. doi: 10.5281/zenodo.5638517

```
lapply(c("rgdal", "raster", "rgrass7", "sf", "sp"), require, character.only = TRUE)
# (Pebesma and Bivand, 2005; Bivand et al., 2013; Pebesma, 2018; Hijmans, 2020; Bivand et al., 2021;
Bivand, 2021)
use_sp()
```

start GRASS GIS 7.6 (Awaida and Westervelt, 2020) --> crs downloaded already --> select a fully downloaded location and mapset 'PERMANENT' --> **start R** version 4.0.5 and RStudio **in the GRASS cmd shell** via 'rstudio'

```
Country <- "FIN" # define string for country, in example "FIN" for "Finland"
dem <- file.path(.) # define file name of the digital elevation model (raster format, *.tif), for example:
"D:/DEM_FIN.tif"

execGRASS("g.proj", # actualize projection, the one from the file is used
        georef = file.path(dem),
        flags = c('t','c'))

execGRASS('r.in.gdal', # insert the DEM to GDAL
        input  = file.path(dem),
        output = 'DEM',
        flags  = c('overwrite','o', 'e'))

execGRASS("g.region", # Align region to resolution (could be benefitial for calculating slopes)
        align = 'DEM')
```

The function ‘r.hydrodem’ removes all depressions (flags = ‘a’) from the DEM which is nesseray for calculating interruption-free flow channels which later represent the surface water. One could also set max size (e.g. size = 5000, but then flags ‘a’ has to be eliminated).

```
execGRASS('r.hydrodem',
        input = 'DEM',
        output = 'filledHydroDem',
        flags = c('a','overwrite'))
```

D8 Flow Directions (flags = ‘s’) are calculated, resulting in a flow-direction layer showing into which neighbouring cell the water will flow. Additionally, the flow accumulation (accumulation = <name>) using the created D8 flow directions is created.

```
execGRASS('r.watershed',
        elevation = 'filledHydroDem',
        accumulation = 'accum',
        flags = c('s', 'a', 'overwrite'))
```

A grid of terrain slope is calculated on the original (not-filled) DEM. Later, a cost-function will be applied to these values, why units are set to [percent].

```
execGRASS('r.slope.aspect',
        elevation ='DEM',
        slope = 'slope',
        format = 'percent',
        flags = c('a','overwrite'))
```

A function is defined for efficient calculations:

```
calcDTW <- function(fia) {
```

For calculating the flow paths, it is necessary to define a threshold (t) for the minimal flow initiation area (FIA), meaning how much area needs to accumulate downward the slope for resulting in a channel with simulated surface water. Commonly, t is set between 0.25 ha and 16 ha (32 ha).

```
  t = fia * 10000/res(raster(dem))[1]^2 # flow accumulation is based on number of cells. We need upstream contributing area [m^2], why the FIA is corrected by the spatial resolution of the DEM.
```

The layer of flow paths needs to be converted into a binary format (0 = no channel, 1 = channel), as start points for the cost function.

```
  execGRASS('r.mapcalc', # select channels (above threshold) and transform them into binary variables
          expression = paste0('flowLines = if(accum >= ', t, ', 1, null())'),
          flags = c('overwrite'))
```

Finally, the DTW can be calculated as the minimum height difference (slope in percent scaled by the spatial resolution of the layer) between each cell and the flow path (surface water) layer using a cost function. The cost function (Awaida and Westervelt, 2020) starts at each point of the plot paths and sums up the height difference to each raster cell.

```
  execGRASS('r.cost', # calculate the least-cost of slope [%], starting from the channels
          input = 'slope',
          start_raster = 'flowLines',
          output = 'cost',
          null_cost = 0,
          flags = c('overwrite','k')) #'k' for with Knight's move for more accurate results - but longer computations

  DTWxha<-raster(readRAST('cost')) # read raster from gdal and save it as object

  DTWxha1<- DTWxha*res(raster(dem))[1]/100 # since GRASS r.slope.aspect gives a measure in percent, the cost-grid needs to be corrected by resolution and divided by 100 to achieve [m]

  writeRaster(DTWxha1, paste0('D:/DTW_', Country,'_FIA_',fia,'_ha.tif'),
            overwrite = T)} # write and save the raster, an exemplatory file path is given

lapply(c(0.25,1,2,4,10,16), calcDTW) # and finally run the function for the the desired FIAs.
```

#NOTE: As an alternative, DTW can be calculated using functions of the free toolbox TauDEM (Tarboton, 2004). The DTW map-scenarios investigated by Schönauer et al. (2021c) were created using TauDEM, but for some reason the code does not execute on all tested systems. That is why we changed it to a platform independent version using GRASS GIS. Resultant predictions of DTW map-scenarios, either created using TauDEM or GRASS GIS were equivalent, with negligible location differences of the flow paths. The alternating commands were:

```
#system("mpiexec -n 8 pitremove -z raster2_scale.tif -fel raster2_pitremove.tif")# Pitremove
#system("mpiexec -n 8 D8Flowdir -p raster2_anp.tif -sd8 raster2_sd8.tif -fel raster2_pitremove.tif", show.output.on.console=F, invisible=F)# D8 flow directions
#system("mpiexec -n 8 AreaD8 -p raster2_anp.tif -ad8 raster2_ad8.tif")# Contributing area
```

Appendix V. R-grammar used to transform global hdf5-grid files, as available from the Soil Moisture Active and Passive mission, run by NASA, to spatial rasters.

```
#install.packages("BiocManager")
#BiocManager::install("rhdf5")
library("rhdf5")
library("raster")
library("rgdal")
library("gdalUtils")
library("smapr")
library("dplyr")


rm(list=ls())

path <- paste("D:/Brendan/SMAP_L4/")

# list of h5 files
files <- list.files(path,
                    pattern = "\\.h5$",
                    recursive = TRUE)

# overview of the hdf5 file
rhdf5::h5ls(paste0(path, files[1]))

# select long-lat values
latitude <- values(raster(rhdf5::h5read(paste0(path, files[1]), name = "/cell_lat")))
longitude <- values(raster(rhdf5::h5read(paste0(path, files[1]), name = "/cell_lon")))
dat<-data.frame(lon = c(min(longitude, na.rm=T),max(longitude, na.rm=T)), # upper left extent
          lat = c(max(latitude, na.rm=T),min(latitude, na.rm=T))) # lower right extent
cord.dec = SpatialPoints(cbind(dat$lon, dat$lat), proj4string = CRS("+proj=longlat"))
cord<-spTransform(cord.dec, CRS("+init=epsg:6933"))

# x<-files[1]
doit<-function(x) {
f <- paste0(path, x)
  v1<-rhdf5::h5read(f, name = "/Analysis_Data/sm_surface_analysis")
  #v2<-rhdf5::h5read(f, name = "/Soil_Moisture_Retrieval_Data_PM/soil_moisture_pm")
  out1 <- t(v1)
  outr <- raster(out1)
  crs(outr) <- "+proj=longlat"
  values(outr) <- ifelse(values(outr)<0, NA, values(outr))

  pathTiff<-file.path(paste0(path, "0tiff/sm_surface_", substr(f, 45, 55)))
  writeRaster(outr, pathTiff, overwrite = T, format = "GTiff")
  gdal_translate(src_dataset = paste0(pathTiff, ".tif"),
              dst_dataset = file.path(paste0(pathTiff, "_ref.tif")), # set filename here, (1) _am.tif (2) _pm.tif
              of = "GTiff",
              a_ullr = c(xmin(cord), ymax(cord), xmax(cord), ymin(cord)),
              a_srs = "+proj=cea +lon_0=0 +lat_ts=30 +ellps=WGS84 +units=m",
              co="TILED=YES",
              verbose=TRUE)
  file.remove(paste0(pathTiff, ".tif"))
}

# apply the function to the list of input files
sapply(files, doit)
```

Appendix VI. Fifteen land mass constants, available from Reichle, R., Lannoy, G. de, Koster, R., Crow, W., Kimball, J. & Liu, Q. (2020) *SMAP L4 Global 9 km EASE-Grid Surface and Root Zone Soil Moisture Land Model Constants, Version 5*. Available from: https://doi.org/10.5067/5C36BVQZW28K, were considered for modelling soil moisture content. * indicates variables which were kept as input after checking for reduncancy and co-variation.

Data field name	Unit	Description
*clsm_cdcr1	kg m^{-2}	Catchment deficit at which baseflow ceases
*clsm_cdcr2	kg m^{-2}	Maximum water holding capacity of land field
clsm_dzgt1	m	Thickness of soil heat diffusion model layer 1
clsm_dzgt2	m	Thickness of soil heat diffusion model layer 2
clsm_dzgt3	m	Thickness of soil heat diffusion model layer 3
clsm_dzgt4	m	Thickness of soil heat diffusion model layer 4
clsm_dzgt5	m	Thickness of soil heat diffusion model layer 5
clsm_dzgt6	m	Thickness of soil heat diffusion model layer 6
*clsm_dzpr	m	Thickness of profile soil moisture layer (“depth-to-bedrock” in the Catchment model)
clsm_dzrz	m	Thickness of root zone soil moisture layer
clsm_dzsf	m	Thickness of surface soil moisture layer
clsm_dztsurf	m	Thickness of soil layer associated with surface_temp
*clsm_poros	m^3 m^{-3}	Soil porosity
*clsm_veghght	m	Vegetation canopy height
clsm_wp	m^3 m^{-3}	Soil wilting point

Appendix VII. Several variables, as available from European Commission - Joint Research Centre (2004) *European Soil Data Centre (ESDAC).* Available from: https://esdac.jrc.ec.europa.eu/ [Accessed 19 August 2021], were considered for modelling of soil moisture content. * indicates variables which were kept as input after checking for reduncancy and co-variation.

Data field name	Description
*AGLIM1	Code of the most important limitation to agricultural use of the STU
*AGLIM1NNI	Dominant limitation to agricultural use (without no information)
*AGLIM2	Code of a secondary limitation to agricultural use of the STU
*AGLIM2NNI	Secondary limitation to agricultural use (without no information)
*ALT	ELEVATION
ALT_MAX	100 m class maximum altitudes
ALT_MIN	100 m class minimum altitudes
*ATC	Accumulated temperature class
*AWC_SUB	Subsoil available water capacity
*AWC_TOP	Topsoil available water capacity
*BS_SUB	Base saturation of the subsoil
*BS_TOP	Base saturation of the topsoil
*CEC_SUB	Subsoil cation exchange capacity
*CEC_TOP	Topsoil cation exchange capacity
*CRUST	Soil crusting class
DGH	Depth to a gleyed horizon
DIFF	Soil profile differentiation
DIMP	Depth to an impermeable layer
*DR	Depth to rock
*EAWCSUB	Subsoil easily available water capacity
*EAWCTOP	Topsoil easily available water capacity
*ERODIBI	Soil erodibility class
FAO85FU	Full soil code of the STU from the 1974 (modified CEC 1985) FAO-UNESCO Soil Legend
FAO85FU_CL	Confidence level for FAO85FU
FAO90FU	Full soil code of the STU from the 1990 FAO-UNESCO Soil Legend
FAO90FU_CL	Confidence level for FAO90FU
*HG	Hydrogeological class
*IL	Code for the presence of an impermeable layer within the soil profile of the STU
*MIN	Profile mineralogy
*MIN_SUB	Subsoil mineralogy
*MIN_TOP	Topsoil mineralogy
*OC_TOP	Topsoil organic carbon content
*PARMADO	Code for dominant parent material of the STU
PARMADO_CL	Confidence level for PARMADO
*PARMASE	Code for secondary parent material of the STU
PARMASE_CL	Confidence level for PARMASE
PD_SUB	Subsoil packing density
*PD_TOP	Topsoil packing density
PEAT	Peat
*PHYSCHI	Physi-chemical factor of soil crusting & erodibility

*PMH	Parent material hydrogeological type
ROO	Depth class of an obstacle to roots within the STU
*SLOPE_DOM	Dominant slope class of the STU
*SLOPE_SEC	Secondary slope class of the STU
STR_SUB	Subsoil structure
*STR_TOP	Topsoil structure
*TD	Rule infered subsoil texture
*TEXT	Dominant surface textural class (completed from dominant STU)
*TEXTCRU	Textural factor of soil crusting
TEXTDEPCHG	Depth class to a textural change of the dominant and/or secondary surface texture of the STU
*TEXTERO	Textural factor of soil erodibility
TEXTSRFDOM	Dominant surface textural class of the STU
*TEXTSRFSEC	Secondary surface textural class of the STU
*TEXTSUBDOM	Dominant sub-surface textural class of the STU
*TEXTSUBSEC	Secondary sub-surface textural class of the STU
USE	Regrouped land use class
*USE_DOM	Code for dominant land use of the STU
USE_SEC	Code for secondary land use of the STU
*VS	Volume of stones
*WM1	Code for normal presence and purpose of an existing water management system in agricultural land on more than 50% of the STU
*WM2	Code for the type of an existing water management system
*WR	Dominant annual average soil water regime class of the soil profile of the STU
*WRBFU	Full soil code of the STU from the World Reference Base (WRB) for Soil Resources
*ZMAX	Maximum elevation above sea level of the STU (in metres)
ZMIN	Minimum elevation above sea level of the STU (in metres)

Acknowledgements

I would like to thank several people who substantially contributed to the successful outcome of this work. First of all, I thank Prof. Dr. Dirk Jaeger for providing the infrastructure and funds to conduct this project and research. I am grateful for his scientific advice and his ideas and input regarding my work. I thank Dr. Martin Jansen for the great cooperation and supervision, especially for enriching this work by soil-related aspects. I want to thank for the administrative support by Tanja Kern and the whole team of the Department of Forest Engineering and Work Science, including Dr. Stephan Hoffmann who edited the thesis. I want to thank the TECH4EFFECT family, for bidding me welcome into the scientific world of forestry and for our joint research. Last but not least, I would like to direct the acknowledgements to my parents, Anni and Johann, to my sibling Carina and niece Claudia.